

ISSN 1307-3729

REHVA
3E

Federation of
European Heating,
Ventilation and
Air Conditioning
Associations

The **REHVA** European HVAC Journal

Volume: 59

Issue: 5

October 2022

www.rehva.eu



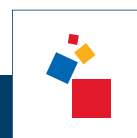
CLIMA 2022 papers on
Health & Comfort
with focus on aerosols, IAQ and comfort



Get in touch with
our **sustainable**
future at
ISH 2023

World's leading trade fair for
HVAC + Water

Save
the
Date!



ISH

13.–17. 3. 2023
Frankfurt am Main

Editor-in-Chief:

Jaap Hogeling
jh@rehva.eu

Editorial Assistant:

Marie Joannes
mj@rehva.eu

General Executive:

Ismail Ceyhan, Turkey

REHVA BOARD

President:

Cătălin Lungu

Vice Presidents:

Lada Hensen Centnerová

Livio Mazzarella

Pedro Vicente-Quiles

Johann Zirngibl

Ivo Martinac

Kemal Gani Bayraktar

EDITORIAL BOARD

Murat Cakan, Turkey

Guangyu Cao, Norway

Tiberiu Catalina, Romania

Francesca R. d'Ambrosio, Italy

Ioan Silviu Dobosi, Romania

Lada Hensen, The Netherlands

Karel Kabele, Czech Republic

Risto Kosonen, Finland

Jarek Kurnitski, Estonia

Livio Mazzarella, Italy

Dejan Mumovic, United Kingdom

Ilinca Nastase, Romania

Natasa Nord, Norway

Dusan Petras, Slovakia

Olli Seppänen, Finland

Branislav Todorovic, Serbia

Peter Wouters, Belgium

CREATIVE DESIGN AND LAYOUT

Jarkko Narvanne, jarkko.narvanne@gmail.com

ADVERTISEMENTS

Nicoll Marucciová, nm@rehva.eu

SUBSCRIPTIONS AND

CHANGES OF ADDRESSES

REHVA OFFICE:

Washington Street 40

1050 Brussels, Belgium

Tel: +32-2-5141171

info@rehva.eu, www.rehva.eu

PUBLISHER

TEKNİK SEKTÖR YAYINCILIĞI A.Ş.

Fikirtepe Mah., Rüzgar Sk. No: 44C

A3 Blok, Kat:11 D:124 Kadıköy/Istanbul, Turkey

REHVA Journal is distributed in over 50 countries through the Member Associations and other institutions. The views expressed in the Journal are not necessarily those of REHVA or its members. REHVA will not be under any liability whatsoever in respect of contributed articles.

Cover photo: ColorMaker / shutterstock.com

Contents

Download the articles from www.rehva.eu -> REHVA Journal

EDITORIAL

- 4 Health & Comfort**
Jaap Hogeling

CLIMA 2022 TOP PAPERS

- 5 CLIMA 2022 conference papers on the theme HEALTH & COMFORT**
- 7 Evaluation of preventive measures in mitigating the risk of airborne infection of COVID-19**
Yunus Emre Cetin & Martin Kriegel
- 12 Aerosol transmission in rotary wheel heat exchangers**
Heinrich Huber, Thomas Richter, Florian Brzezinski & Michael Riediker
- 18 Development of a non-contact modular screening clinic (NCMSC) for COVID-19**
Jinkyun Cho, Jinho Kim, Jongwoon Song & Seungmin Jang
- 24 Thermal inactivation of the corona virus (SARS-CoV-2) in air volumes**
André Schlott, Thomas Hutsch, Eileen Sauer, Jens Wetschky, Jana Hessel, Susanne Bailer, John Laubert & Stefan Lösch
- 31 Health and energy assessment of a demand controlled mechanical extraction ventilation system**
Janneke Ghijsels, Klaas De Jonge & Jelle Laverge
- 40 Low-temperature radiant cooling panel for hot and humid climate**
Gongsheng Huang, Nan Zhang & Yuying Liang
- 46 Impact of future climate on the performances of ground-source cooling system**
Abantika Sengupta, Pieter Proot, Tom Trioen, Hilde Breesch & Marijke Steeman
- 56 A Multi-Domain Approach to Explanatory and Predictive Thermal Comfort Modelling in Offices**
Eugene Mamulova, Henk W. Brink, Marcel G.L.C. Loomans, Roel C.G.M. Loonen & Helianthe S.M. Kort
- 63 Exploring futures of summer comfort in Dutch households**
Lenneke Kuijer & Lada Hensen Centnerová

- 69 Correlation of subjective and objective air quality data in shopping centres as a function of air temperature and relative humidity**
Mahmoud El-Mokadem, Kai Rewitz & Dirk Müller

ARTICLES

- 75 Cross-infection risk between two people standing close to each other at different room temperatures**
Peter V. Nielsen
- 76 Smart air quality control in residences for optimised energy use and improved health of occupants**
Elizabeth Cooper & Yan Wang
- 81 Why a unified IAQ approach is critical to securing public health**
Morten Schmelzer
- 84 Next-Generation Energy Performance Certificates. What novel implementation do we need?**
Lina Seduikyte, Phoebe-Zoe Morsink-Georgali, Christiana Panteli, Panagiota Chatzipanagiotidou, Koltsios Stavros, Dimosthenis Ioannidis, Laura Stasiulienė, Paulius Spūdys, Darius Pupeikis, Andrius Jurelionis & Paris Fokaides
- 89 Healthy Homes Design Competition: "reTHINK living"**
Caroline Reich & Amelie Reiser
- 94 Tiny Homes – A Tiny solution to a big problem**
Laura Denoyelle

REHVA WORLD

- 98 Meet the BIM-SPEED Competition Winners & Finalists**
Jasper Vermaut

INDUSTRY EXPERTISE

- 102 Smart Industrial Thermal Imaging Device PX1 by iRay**

EVENTS & FAIRS

- 105 Exhibitions, Conferences and Seminars in 2022 & 2023**

Advertisers

- | | | | |
|-------------------------------|----|---------------------------------------|-----|
| ✓ LIGHT + BUILDING | 2 | ✓ WORLD SUSTAINABLE ENERGY DAYS 2023. | 62 |
| ✓ SWEGON | 6 | ✓ INFIRAY | 103 |
| ✓ UPONOR | 17 | ✓ PURMO | 104 |
| ✓ BELIMO | 23 | ✓ REHVA MEMBERS | 106 |
| ✓ REHVA BRUSSELS SUMMIT | 30 | ✓ REHVA SUPPORTERS | 107 |
| ✓ ACREX INDIA 2023 | 55 | ✓ REHVA BRUSSELS SUMMIT | 108 |

Next issue of REHVA Journal

Instructions for authors are available at www.rehva.eu (> Publications & Resources > Journal Information). Send the manuscripts of articles for the journal to Jaap Hogeling jh@rehva.eu.

Health & Comfort

With focus on aerosols, IAQ and comfort. At the same time, we are aware of EU policy actions like the Green Deal, Renovation Wave, Fit for 55 by 2030 and Repower EU plan which are the drivers for the ongoing EPBD (2018) revision expected to be published beginning 2023. The updated draft EPBD provides more attention to health and comfort. In the renovation wave program, there is a focus on tackling energy poverty and worst-energy performing buildings towards healthy housing.

By referring in EPBD Annex 1 to EN16798-1 there is an incentive to include an IEQ performance indicator in the EP Certificate and by doing so, include the energy use of absent or underperforming building systems in the EP. In the expected EPBD this is still softly addressed in art.4 (related to MEPS), and in art.6 (New Buildings) IEQ issues shall be addressed. Annex 1 art.2 says: ... indoor, conditions, and in order to optimise health, indoor air quality and comfort levels defined by MS's. We hope that this language will stay, or even better, become stronger. We all know that the health costs due to poor IEQ in buildings is much higher than the energy use possibly related to a better IEQ!

The current situation in Europe, the high fuel prices and shortages due to Europe's dependency on Russian fuel supply and the war in Ukraine requires many people to accept lower thermal comfort levels during this winter season. In many countries the government advises or requires lower temperatures in buildings during the winter. This will lead to thermal discomfort at workplaces and in houses where people cannot

afford the high fuel prices. This will affect productivity at workplaces and may cause health issues in residential buildings. Compensation with higher activity levels (think of the elderly) and more clothing is not always possible. Working behind the computer keyboard as many persons do, will be hindered by lower temperatures of the hands and fingers.

Saving on fuel cost and at the same time ask for better ventilation to avoid high COVID-19 infection risk levels is also a challenge. In many existing situations like in schools heat recovery systems are not present or designed for higher ventilation rates. At the same time school building management is confronted with high energy costs and the requirement to install CO₂ sensors in classrooms to stimulate better (often natural) ventilation. These are challenges which are easier to cope with if during the last 10–20 years school building operators had been more responsive on the widely reported poor IEQ in school buildings.

But we have to be realistic, these reduced comfort levels and higher costs are small offerings compared to the suffering of the people of Ukraine. ■



JAAP HOGELING

Editor-in-Chief
REHVA Journal



CLIMA 2022 conference papers on the theme HEALTH & COMFORT

Twenty CLIMA 2022 papers have been acknowledged as high ranking on the theme HEALTH & COMFORT.

Ten are included in this issue:

Evaluation of preventive measures in mitigating the risk of airborne infection of COVID-19

Yunus Emre Cetin, Martin Kriegel

Aerosol transmission in rotary wheel heat exchangers

Heinrich Huber, Thomas Richter, Florian Brzezinski, Michael Riediker

Development of a non-contact modular screening clinic (NCMSC) for COVID-19

Jinkyun Cho, Jinho Kim, Jongwoon Song, Seungmin Jang

Thermal inactivation of the corona virus (SARS-CoV-2) in air volumes

André Schlott, Thomas Hutsch, Eileen Sauer, Jens Wetschky, Jana Hessel, Susanne Bailer, John Laubert, Stefan Lösch

Health and energy assessment of a demand controlled mechanical extraction ventilation system

Janneke Ghijsels, Klaas De Jonge, Jelle Laverge

Low-temperature radiant cooling panel for hot and humid climate

Gongsheng Huang, Nan Zhang, Yuying Liang

Impact of future climate on the performances of ground-source cooling system

Abantika Sengupta, Pieter Proot, Tom Trioen, Hilde Breesch, Marijke Steeman.

A Multi-Domain Approach to Explanatory and Predictive Thermal Comfort Modelling in Offices

Eugene Mamulova, Henk W. Brink, Marcel G.L.C. Loomans, Roel C.G.M. Loonen, Helianthe S.M. Kort

Exploring futures of summer comfort in Dutch households

Lenneke Kuijter, Lada Hensen Centnerová

Correlation of subjective and objective air quality data in shopping centers as a function of air temperature and relative humidity

Mahmoud El-Mokadem, Kai Rewitz, Dirk Müller

The other ten papers can be accessed on-line::

[Droplet Concentration Produced during Expiratory Activities and Evaluation of Relative Infection Risk](#)

Arisu Furusawa, Takashi Kurabuchi, Jeongil Kim, Masaki Shimizu, Haruki Taguchi

(Best paper award for the theme Health and Comfort)

[Control of the bed thermal environment by a ventilated mattress](#)

Ge Song, Mariya Petrova Bivolarova, Guoqiang Zhang, Arsen Krikor Melikov

[Cooling effects on fatigue recovery during summer sleep](#)

Noriko Umemiya, Mitsunori Suzuki

[Dynamics of metabolic rate in male individuals due to the meal and regular office activities](#)

Dolaana Khovalyg, Jiyoun Kwak

[Estimating Long-Term Indoor PM2.5 of Outdoor and Indoor Origin using Low-Cost Sensors](#)

Tongling Xia, Yue Qi, Xilei Dai, Ruoyu You, Junjie Liu, Chun Chen

[Investigation of PECS on the basis of a virtual building controller](#)

Katharina Boudier, Sabine Hoffmann

[Investigation of the group differences in indoor environmental quality](#)

Zheng Li, Ongun Berk Kazanci, Qingwen Zhang Bjarne W. Olesen

[Self-reported health and comfort of outpatient workers in six hospitals](#)

AnneMarie Eijkelenboom, Philomena M. Bluysen

[Temperature calibration and Annual performance of cooling for ceiling panels](#)

Seyed Shahabaldin Seyed Salehib, Karl-Villem Vösab, Jarek Kurnitskia, Martin Thalfeldt

[Thermal comfort perception and indoor climate: Results from the OPSCHALER project](#)

Arjen Meijer, Anastasia Petropoulou, Andrea Joseph Thaddeus, Laure Itard



Our need for knowledge is greater than ever

To meet the challenges of our business, we at Swegon believe in constantly upgrading our knowledge and going beyond our traditional engineering skills. Whether it's about decreasing the carbon footprint or improving the indoor environments of our buildings, we are happy to share what we have learnt during 90 years in the business. But we also provide the award-winning platform Swegon Air Academy, connecting experts from across the field of indoor climate to share knowledge with a wider audience.

We believe this is more important than ever, and so we have just launched a new Swegon Air Academy website – have a look and get inspired.

swegonairacademy.com.



Swegon Air Academy



Evaluation of preventive measures in mitigating the risk of airborne infection of COVID-19



YUNUS EMRE CETIN

Hermann-Riestchel-Institut,
Chair of Energy, Comfort
and Health in Buildings,
Technische Universitaet
Berlin, Berlin, Germany,
y.cetin@tu-berlin.de



MARTIN KRIEDEL

Hermann-Riestchel-Institut,
Chair of Energy, Comfort
and Health in Buildings,
Technische Universitaet
Berlin, Berlin, Germany

Abstract: In this study, a systematic approach for estimating the infection probability under different infection control strategies is presented for several indoor cases. Increased airflow rates, ventilation schemes, air cleaning equipment, disinfection systems, and face masks are considered according to existing guidelines and standards. These strategies are implemented to care facilities, schools, and offices with varying scenarios. Infection probability calculations are conducted based on the widely used Wells-Riley model. The possible variation of the input parameters is evaluated by employing the Monte Carlo approach to increase the representativeness of the findings. Results show that the infection risk reduction of 15 to 99% is possible depending on the measure preferred.

Keywords: Indoor air quality, COVID-19, preventive measures, Wells-Riley model.

1. Introduction

The novel coronavirus COVID-19 pandemic impinged millions of people [1]. Overwhelming numbers of reported cases brought into attention the importance of preventive strategies to alleviate the propagation of extremely infectious diseases. Multiple guidelines have raised the concern on the indoor airborne transmission of COVID-19 and many recommendations have been released by organizations [2–4]. These recommendations and strategies in terms of building, room, and personal scale have been reviewed and discussed from different perspectives [5–7]. In this context, infection risk assessment is considered a useful tool that may help to quantify and compare the effectiveness of corresponding infection control measures.

Wells-Riley [8,9] and dose-response models are known as two fundamental approaches in infection

risk modelling for ventilated indoor enclosures. In general, the infection risk is characterized by a probability between 0 to 1. Models preferred can provide a quantitative risk assessment to deal with the ongoing epidemic and help to comprehend possible results of varying circumstances. The Wells-Riley model is a simple and quick approach based on the quantum concept, which also considers infectivity and source strength. The infection risk prediction with the Wells Riley assumes that the pathogens are homogeneously distributed in a room. The dose-response model on the other hand can provide more precise and realistic outputs than the Wells-Riley model. Nevertheless, this model is less handy since it requires infectious dose data to construct the dose-response relationship [10,11].

The Wells–Riley model and its modifications have been extensively used for the investigation and evaluation of

the infection risk of numerous ventilated environments from different perspectives [12–17]. In corresponding studies, key parameters of the Wells-Riley model like quantum generation and breathing rate are evaluated mostly as a constant. In fact, these fundamental parameters have a varying character and considering them as a constant may result in misleading conclusions. Also, the effect of preventive measures on infection risk mitigation was rarely inspected and compared in a quantitative way. Hence, the motivation of this study is to evaluate the effect of different infection preventive strategies by employing the Wells-Riley model in which the probability distributions of unknown parameters are considered. For this purpose, the stochastic Monte Carlo approach is used to broaden the representativeness of the results. The effect of displacement ventilation, standalone air cleaners, installing partition, upper room UVGI systems, and wearing N95 masks are evaluated. The findings can be used in the ongoing struggle against COVID-19 by helping to understand effective countermeasures in infection.

2. Methods

2.1 Infection risk model

The Wells-Riley equation is mainly described as follows:

$$P_0 = \frac{D}{S} = 1 - e^{-IqQ_b t/Q} \quad (1)$$

where P_0 is the probability of infection, D is the number of cases, S is the number of susceptible, I is the number of infectors, q is the quanta emission rate by one infector (*quanta/h*), Q_b is the breathing rate of the susceptible person (m^3/h), and Q is the volume flow rate of pathogen free air (m^3/h). In this study, the above version of the Wells-Riley equation is modified to include the use of N95 masks, air cleaners, displacement ventilation, partition, and UVGI system. The modified equation is given as follows:

$$P = 1 - e^{-(1-\eta_s)(1-\eta_I) \frac{IqQ_b t}{V\alpha}} \quad (2)$$

In this equation, η_s and η_I represents the mask filtration efficiency of the susceptible and infected persons respectively. V is the volume of the room (m^3) and α expresses the equivalent air change rate (given in Eq.3) which depends equivalent ventilation air change rate (λ_{vent}), inactivation rate of ultraviolet germicidal irradiation (k_{UV}), and natural inactivation (k_{inact}).

$$\alpha = \lambda_{vent} + k_{UV} + k_{inact} \quad (3)$$

The equivalent ventilation rate (λ_{vent}) includes the air supply rate of the HVAC system (λ_{HVAC}) and portable air cleaners (λ_{PAC}). Here, in order to reflect the imperfect mixing case in different ventilation concepts like displacement ventilation an additional ventilation parameter (ϵ_{HVAC}) is also included to this equation as seen below. This additional ventilation parameter is equal to one for a perfect mixing situation which is one of the main assumptions in Wells-Riley consideration. A similar factor is also employed in another modification of Wells-Riley by Sun and Zhai [14].

$$\lambda_{vent} = \lambda_{HVAC} \epsilon_{HVAC} + \lambda_{PAC} \quad (4)$$

Air supply rate of the HVAC system (λ_{HVAC}) is composed of supplied air flow rate of outdoor air ($\lambda_{outdoor}$) and recirculated air ($\lambda_{recirculated}$). It is given in the following form:

$$\lambda_{HVAC} = \lambda_{outdoor} + \lambda_{recirculated} \quad (5)$$

where η_{filter} is the filtration efficiency of the filters.

2.2 Cases considered

Three different base cases namely an elderly nursing home, a waiting area at the doctor's office, and a classroom are evaluated. Layouts, occupancy levels, duration of stay, ventilation configurations are assigned based on literature and the most typical real practices. Definitions and details regarding corresponding cases are given in **Table 1**.

Table 1. Settings of the studied cases.

Space	Elderly nursing home	Waiting area at doctor's office	Music lesson in a classroom	Corridor in a school	Gym in a school
Duration of stay (min)	60	60	60	15	90
Number of total people	2	10	25	40	25
Volume of space (m^3)	3x4x2.7	4x5x2.7	5x8x3.2	30x1.25x3.2	15x27x5.5
Outdoor ventilation rate (l/s)	8.6	44	137		452.5
Quanta generation (h^{-1})	58±31	58 ± 31	970±390	251±134	492±270
Breathing rate (m^3/h)	0.3±0.2	0.3± 0.2	1.3±0.85	1.3±0.85	2.5±1.75

2.3 Model parameters

Two critical parameters in the Wells-Riley equation are quanta generation rate (q) and breathing rate (p). The quantum generation rate depends on disease type, infector activity, etc., and varies significantly [18]. In this study, the quantum generation rate is adapted from the studies of Shen et al. [19], Millet et al. [20], and Hartmann et al. [21]. Breathing rates are assigned up to the activity levels. In each scenario, only one infectious pathogen emitter exists. It is also assumed that the infectious aerosols become evenly distributed throughout the space promptly. Quantum generation and breathing rates are assumed to follow the normal distribution. Variations of these inputs are applied by using the stochastic Monte Carlo approach on the calculations. In every setup, 50,000 trials are simulated.

Minimum outdoor ventilation rates are calculated in accordance with Ashrae Standard 62.1 [22]. In these calculations space area and occupant number are taken into account as seen in the following form:

$$\lambda_{outdoor} = R_p P_z + R_a A_z \quad (6)$$

where R_p is the outdoor airflow rate required per person (L/s), P_z is the occupant number, R_a is the outdoor airflow rate required per unit area (L/s), and A_z is the net floor area (m²). Required airflow rates are determined by the minimum ventilation rates presented in Ashrae Standard 62.1 [22].

For the base cases mixing ventilation ($\epsilon_{HVAC} = 1$) is applied. The fraction of outdoor ventilation on the air supply rate of the HVAC system is specified as 25% [23]. The filtration efficiency of the filters (η_{filter}) in recirculation is considered as 70% [22]. Natural inactivation is assumed to have a uniform distribution between 0 and 1 h⁻¹.

For the base cases mixing ventilation ($\epsilon_{HVAC} = 1$) is applied. The fraction of outdoor ventilation on the air supply rate of the HVAC system is specified as 25% [23]. The filtration efficiency of the filters (η_{filter}) in recirculation is considered as 70% [22]. Natural inactivation is assumed to have a uniform distribution between 0 and 1 h⁻¹.

At first, infection probability is calculated for the base cases. Then, six different mitigation strategy is applied, and the effect of these strategies is evaluated individually. Proposed strategies are as follows:

- Increased outdoor ventilation rate is analysed by employing 100% outdoor air.
- Air distribution patterns affect the ventilation factor (ϵ_{HVAC}) considerably. Displacement ventilation has the potential to reduce the exposure in the breathing region so it is considered with a factor of 1.2 to 2 [24].
- Installing partition is considered by a factor of 1.1 – 3 [24].
- Portable air cleaners are becoming popular recently. The use of such air cleaners is assumed to supply clean air with a rate of 12 m³/h per square meter, which is suitable with the current EPA guide [25].
- Proper use of an upper room UVGI system is assumed to provide an air change rate of 2 to 6 h⁻¹ [26].
- N95 masks can filter the droplets significantly. Filtration efficiency for both susceptible and infected persons is assumed as between 70% to 95% [27,28].

3. Results and discussion

The calculated infection rates for the base cases are shown in **Table 2**. The infection probabilities over 10% are considered as high risky spaces and these values are bolded. As it is observed, infection rates indicate a large variation in considered cases. The least risky space is found as the waiting area at the doctor's

Table 2. Infection probabilities for base cases.

Space	Infection probability (%)	
	Mean	SD
Elderly nursing home	14	11
Waiting area at doctor's office	3.4	2.8
Music lesson in a classroom	40	23
Corridor in a school	32	22.6
Gym in a school	24	18.4

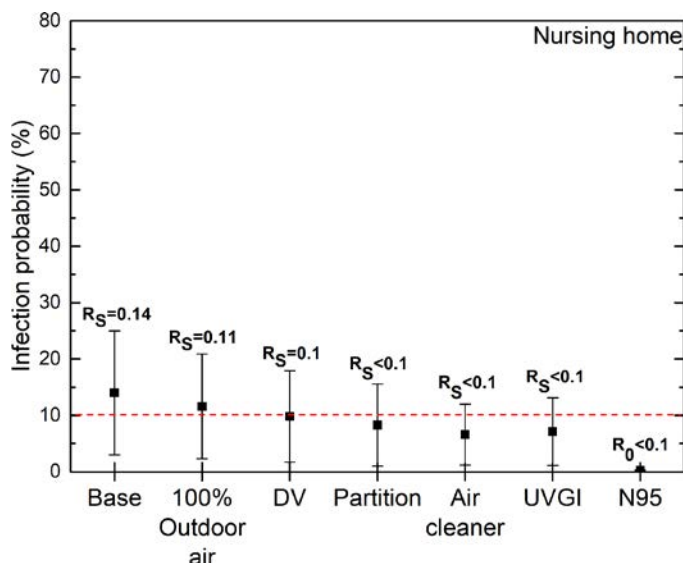


Figure 1. Infection risk predictions for the nursing home.

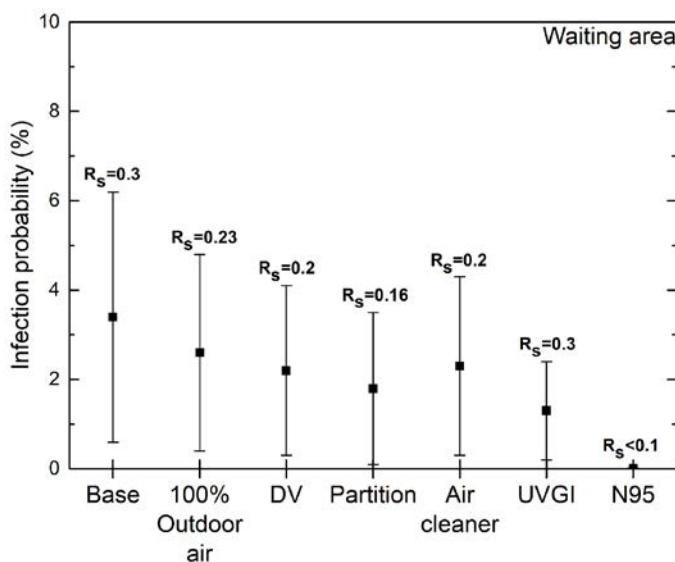


Figure 2. Infection risk predictions for the waiting area.

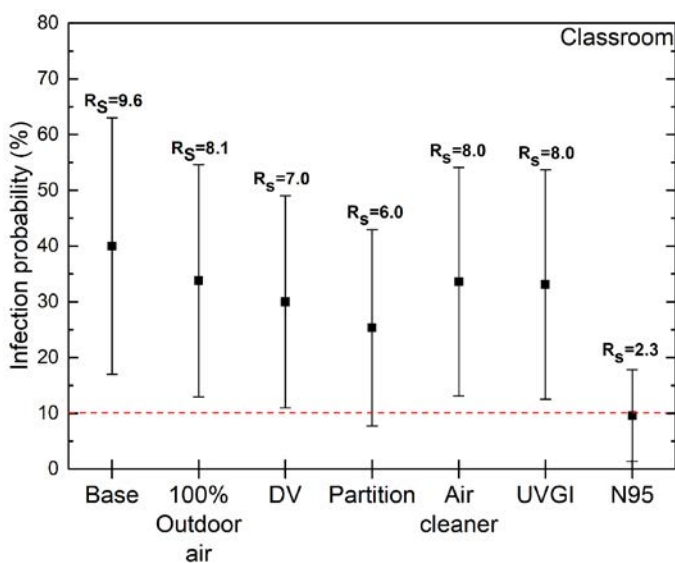


Figure 3. Infection risk predictions for the classroom.

office. As a result of the excessive quanta generation rate the music class configuration shows the highest infection risk potential (40%) among evaluated scenarios. As a result, it can be said that without any mitigation strategy all the cases apart from the waiting area show a considerable risk in terms of infection probability.

Infection risk probabilities under different mitigation measures for the nursing home, waiting area, classroom, corridor, and gym are depicted in **Figure 1**, **Figure 2**, **Figure 3**, **Figure 4**, and **Figure 5** respectively. Mean value of the situational reproduction number ($R_S = P \cdot S$) [28] in each case is also given in these figures. R_S points out the infection spreading in community. If $R_S > 1$ it is considered that an epidemic occurred.

In general, it is seen that all the measures help to decrease the infection probability to some extent. For the nursing home shown in **Figure 1**, the average infection probability decreases about 17% when the supply air is 100% outdoor originated. Nevertheless, in this case, the average infection risk is still higher than the threshold level with an 11.6% infection probability. All the other measures help to reduce the infection risk between 30% to 98%. In all these cases average infection risk is reduced to below 10% and the limit is met. Also, since the $R_S > 1$ in all cases the spread of the disease is unlikely for the nursing home.

As seen in **Figure 2**, in the case of the waiting area considered measures alleviated the infection probability in the range of 23-99%. In this case, the lowest risk reduction is obtained with the use of 100% outdoor air, and the highest reduction is with the N95 face masking as expected. Both the values of infection probability and R_S point out that the lowest risk is obtained for the waiting area at doctor's office.

Infection risk predictions for the classroom, corridor and the gym are given in **Figure 3**, **Figure 4** and **Figure 5** respectively. It is deduced from the findings that the evaluated measures are not adequate in terms of attaining the threshold limit mostly. In all three cases high reproduction number ($R_S > 1$) points a risk of serious outbreak. In every evaluated configuration, the use of N95 masks meets the threshold value and stands as the only solution for the lowest infection probability. Still, it should be noted that it might not

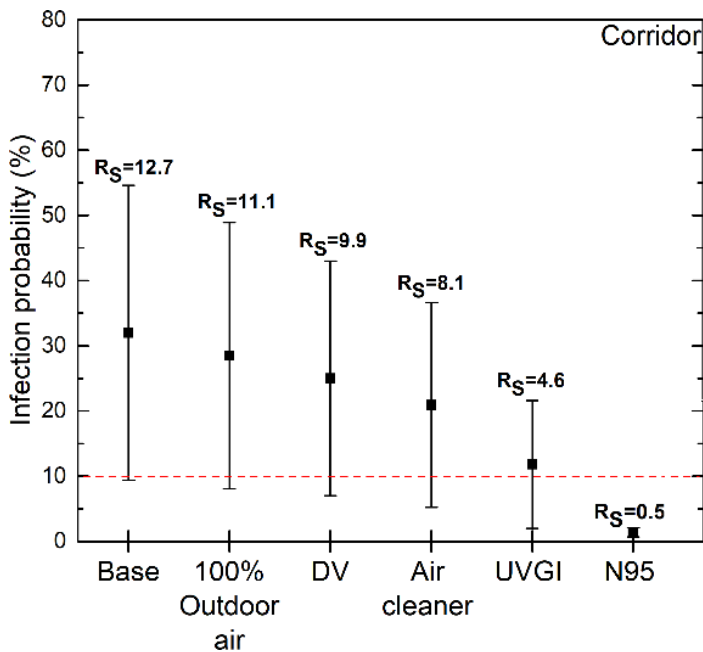


Figure 4. Infection risk predictions for the corridor.

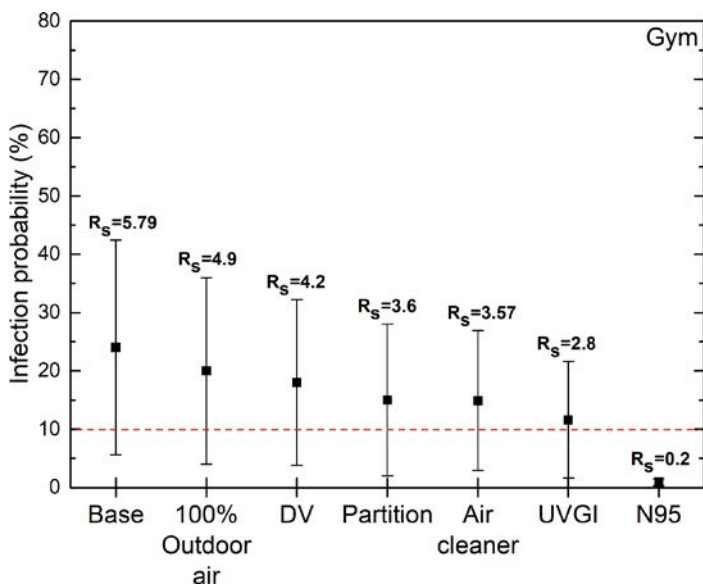


Figure 5. Infection risk predictions for the gym.

be a feasible solution in a music class. Also, for a deeper analysis of the mask efficiency leakage during inhalation and exhalation can be considered in terms of personal protection related factor [28]. For an efficient reduction of the infection risk, the combined effect of the multiple measures can also be evaluated with including feasibility and cost considerations.

4. Conclusions

In the present paper, possible infection preventive measures were analysed for five different settings by employing the well-known Wells-Riley model. Increased outdoor ventilation rate, displacement ventilation, installing partition, portable air cleaners, UVGI systems, and N95 face masks were evaluated. Related model parameters were determined based on the literature and practices. The stochastic Monte Carlo approach was used in calculations in order to include the variations of the input parameters. Future studies can evaluate the combined effect of different risk-mitigating factors from a feasibility and cost standpoint.

Important outcomes are summarized below:

- Predicted infection risk values show a deviating figure depending on the boundary conditions of the cases.
- Based on the evaluated measures risk reduction is possible between 15.5 to 99%.
- Infection risk-mitigating measures lower the probability although this may not be sufficient to achieve the predetermined limit for some cases.
- The use of N95 masks may reduce the infection risk remarkably. This potential can be considered as an easy option for complicated cases at first instance. ■

5. Acknowledgement

This study is supported by The Federal Institute for Research on Building, Urban Affairs and Spatial Development with funding code of SWD-10.08.18.7-20.02.

6. References

Please find the full list of references in the original article at <https://proceedings.open.tudelft.nl/clima2022/article/view/299>

Aerosol transmission in rotary wheel heat exchangers



HEINRICH HUBER
Institute of Building
Technology and Energy,
Lucerne University of
Applied Sciences and
Arts, Horw, Switzerland
heinrich.huber@hslu.ch



THOMAS RICHTER
Hoval Aktiengesellschaft,
Vaduz, Lichtenstein



FLORIAN BRZEZINSKI
Institute of Building
Technology and Energy,
Lucerne University of
Applied Sciences and
Arts, Horw, Switzerland



MICHAEL RIEDIKER
SCOEH: Swiss Centre
for Occupational and
Environmental Health,
Winterthur, Switzerland

Abstract: Transmission by aerosols is considered the main route of COVID-19 infections indoors. Therefore, limiting air transfer between supply and extract air in ventilation systems is critical. Rotary wheels are very efficient heat recovery devices, but have a higher exhaust air transfer ratio (EATR) compared to other types. This raises the question whether a relevant transfer of aerosols can take place and whether this is different from the EATR. Experimental investigations were carried out with an aerosol whose properties are well comparable to human lung aerosols. In parallel, the EATR was determined with tracer gas. For Rotary wheels without purge sector the aerosol transfer ratio was typically 1 to 2 percentage points below the EATR. The results allow the conclusion that rotary wheels designed and operated according to current standards transfer only a non-relevant small amount of aerosols and thus do not pose an infection risk for COVID-19 in applications such as offices where the frequency of highly infectious individuals is low to moderate. However, aerosol transmission in hygienically relevant quantities is conceivable in poorly designed systems, but this does not only affect rotary wheels.

Keywords: Ventilation, aerosol transmission, heat recovery, rotary wheel

1. Introduction

Aerosols are considered a main cause of COVID-19 infections indoors. Therefore, limiting air transfer between supply and extract air in ventilation systems is critical.

In bidirectional ventilations systems, heat recovery is state of the art and is even required in the European regulation for ecodesign requirements for ventilation units. Rotary heat exchangers (RHE) are an efficient and economically interesting solution and are therefore widely used. A disadvantage of RHE is that due to the physical principle and the mechanical implementation

a higher exhaust air transfer ratio (EATR) can occur than with other common heat recovery categories such as plate heat exchangers or run around coil systems. Measures to minimise and evaluate the EATR of RHEs are well known and recommended e.g. in the REHVA COVID-19 Guide [1]. Special attention must be paid to the correct pressure ratios and purge sector. However, RHEs are not generally equipped with purge sectors. Another aspect is the fact that the surface of an RHE is touched by both supply and extract air. Although this enables humidity recovery, it also carries the risk of transferring undesirable substances.

The characteristics of RHEs raise the question of whether relevant aerosol transfer can take place and whether this differs from EATR. For hygienically demanding applications of RHEs, it is crucial to have more knowledge about the phenomenon of aerosol transfer. On the initiative of a company, the University of Applied Sciences and Arts Lucerne (HSLU) together with the Swiss Centre for Occupational and Environmental Health (SCOEH) carried out experimental investigations [2].

2. Research methods

2.1. Principle and test rig

The Building Technology Laboratory of the HSLU operates a test rig for heat recovery devices. In **Figure 1** the scheme of the test rig is shown. In all four air streams temperature, humidity, air flow rate and tracer gas concentration can be measured. For the aerosol measurements, a particle generator was installed in the exhaust air inlet duct and additional measuring devices in all four air streams.

Test objects were two RHEs without purge sector and with a free diameter of 1 000 mm: a condensation rotor (aluminium) and a sorption rotor (aluminium with molecular sieve coating). The nominal airflow is between 1 400 to 4 199 m³/h for a face velocity of

1 – 3 m/s. On both sides air inlet temperatures were 20°C ± 1K and air inlet humidity 40% RH ± 10% RH.

In order to make a conclusion of the aerosol transmission, the EATR and the aerosol transfer ratio (ASTR) were determined and compared.

2.2. Exhaust Air Transfer Ratio (EATR)

The EATR was measured based on EN 308:2022 [3] by injecting Sulphur Hexafluoride (SF₆) tracer gas in the duct of the exhaust inlet. The EATR is calculated with the following formula:

$$EATR = \frac{a_{22} - a_{21}}{a_{11} - a_{21}} \times 100 \text{ [%]} \quad (1)$$

where

a_{11} is SF₆ concentration exhaust inlet [ppm],

a_{21} is SF₆ concentration supply inlet [ppm],

a_{22} is SF₆ concentration supply outlet [ppm].

2.3. Aerosol Transfer Ratio (ASTR)

The test setup for the ASTR measurements was done in the same way as for the EATR. Aerosol measuring devices (Sensirion SPS30) were installed in pairs in each of the four air streams. The sensors count the particulate

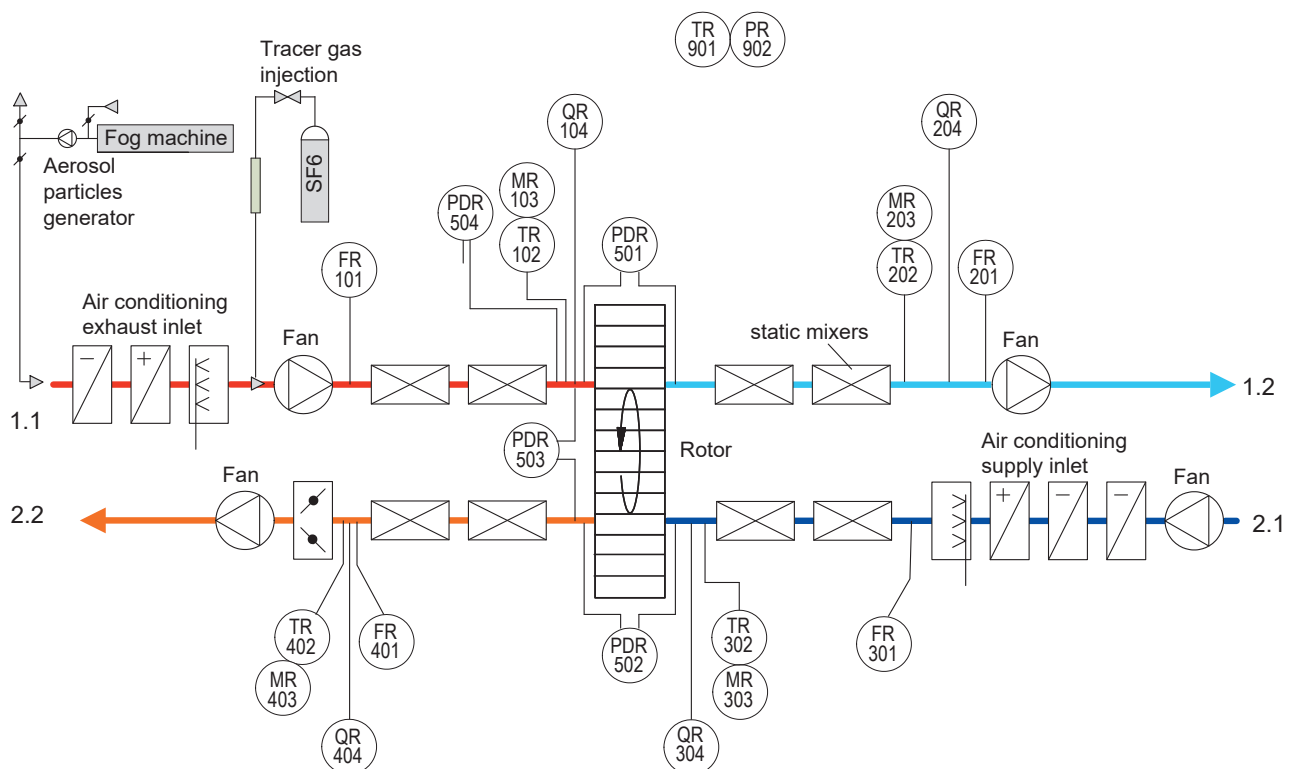


Figure 1. Scheme of the test rig for heat recovery devices. Symbols: **first letter** F air flow rate, P pressure, T temperature, M humidity, Q concentration; **subsequent letter** D difference; **auxiliary letter** R registration; **air flow type** 1.1 exhaust inlet, 1.2 exhaust outlet; 2.1 supply inlet, 2.2 supply outlet.

matter based on laser scattering in a size of 0.3 to 10 μm and provide a good assessment of concentrations over a wide range [4]. To keep the aerosol concentration in the supply inlet air as low as possible, the installed filters of the class ISO ePM1 50% (F7) were replaced with HEPA filters H14. During the measurement, aerosol was applied in pulses in the duct of the exhaust inlet air. The aerosol used has an average diameter of just over one micrometer and is therefore comparable in size to exhaled aerosol [5]. Like human exhaled aerosol, the used aerosol is liquid at normal ambient temperatures, hygroscopic and moderately viscous. It is produced by evaporation and condensation of a water-glycol mixture by a fog machine and is stable in air for a longer time [6].

The maximum peak heights at exhaust air inlet, supply air inlet and outlet were used for evaluation the ASTR according following formula:

$$ASTR = \frac{b_{22} - b_{21}}{b_{11} - b_{21}} \times 100 \quad [\%] \quad (2)$$

where

b_{11} is peak PM10 exhaust inlet [P/cm³],

b_{21} is peak PM10 supply inlet [P/cm³],

b_{22} is peak PM10 supply outlet [P/cm³].

2.4. Measurement uncertainty

For both EATR and ASTR, the measurement uncertainty was determined by repeating each test point usually five times. Since linearity is given for both measurement equipment, the measurement uncertainty can be determined by the standard deviation of EATR and ASTR and a coverage factor to reach a confidence level of 95%.

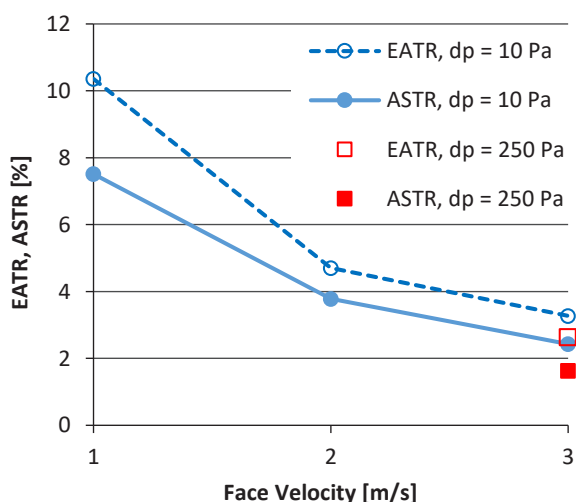


Figure 2. EATR and ASTR of the condensation rotor as function of the face velocity at isothermal conditions 20°C, 40% RH.

3. Results

3.1. Condensation rotary heat exchanger

Table 1 shows the results of the condensation RHE. The measurements were conducted with three different air face velocities (v) of 1, 2 and 3 m/s. Rotor speed (n) was 20 rpm and pressure difference between supply outlet and exhaust inlet (Δp_{22-11}) 10 Pa. One additional measuring point (MP) with a difference of 250 Pa between supply outlet and exhaust inlet was conducted.

Figure 2 shows the EATR and ASTR as function of the face velocity. Even if the ASTR plus the upper measurement uncertainty range partly exceeds the EATR, there is a clear tendency for the ASTR to be smaller than the EATR.

3.2. Sorption rotary heat exchanger

As with the condensation RHE, measurements with the sorption RHE were carried out at three different face velocities and a pressure difference of 10 Pa. Additional to the measurements with 20 rpm, measurements with 10 rpm rotor speed were conducted. **Table 2** shows the results of the sorption RHE.

Analogous to the results of the condensation RHE **Figure 3** shows that also with the sorption RHE the ASTR is below the EATR.

4. Discussion

4.1. Significance of the results

AHUs that comply with the European Ecodesign Regulation are typically designed for a face velocity (related to the inner cross-sectional area of the casing) of about 1.6 to 1.8 m/s. Since the face area of the of

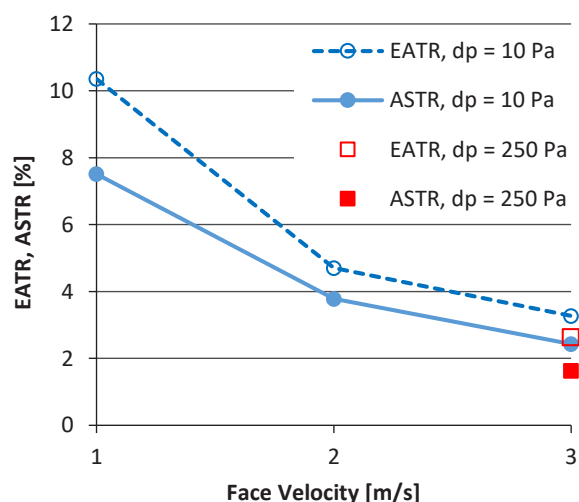


Figure 3. EATR and ASTR of the sorption rotor as function of the face velocity at isothermal conditions 20°C, 40% RH.

the RHE is about 10 to 20% smaller than the cross-sectional area of the AHU, the nominal face velocity of a RHE is typical approx. 2 m/s. In applications such as office buildings and schools, face velocities in the range of about 1 m/s often occur in partial load operation mode. On the other hand, the REHVA COVID-19 guideline recommends not using partial load operation in pandemic situations. Therefore, the measured EATR and ASTR at 2 m/s are considered for the infection risk assessment.

For condensation RHEs the rotor speed is in a range of 10 to 20 rpm, depending on design characteristics, e.g. foil thickness. For sorption RHEs 20 rpm can be seen as typical speed. Therefore, for the contamination risk assessment for both RHE types the measured values at 20 rpm are chosen. For the calculation of the contamination risk an ASTR of 4% is used, which is to understand as conservative value.

It goes without saying that these data are valid only for the tested RHE when using this specific fog aerosol. Nevertheless, the RHEs examined are real products that are judged to be typical in a market comparison.

The draft revision of the European Ecodesign Regulation from [7] serves as a comparison. In this draft a maximum EATR at nominal flow and nominal pressure of 5% is required. With reference to this source, a maximum EATR of 5% can be considered state of the art.

However, for hygienically sensitive applications, such as public buildings, the authors recommend taking measures to achieve a lower EATR. For RHE with a purge sector, an EATR below 0.5% can be achieved.

4.2. State of the art in filters

In German speaking countries the VDI 6022-1 [8] is considered reflecting the state of the art. The minimum filter class for supply air is ISO ePM1 50%. The extract air before entering a RHE shall pass a filter of class ISO ePM10 50%. As an estimate for the separation efficiency of lung aerosols the gravimetric arrestance of the filters up to a particle size of PM10 can be assumed to be 85% for class ISO ePM1 50% [9] and 50% for class ISO ePM10 50% (according to the definition of the class).

A typical solution is that in the outdoor air (before entering the RHE) and in the extract air (before entering the RHE) an ISO ePM1 50% filter is placed. Thus, the potentially contaminated air passes through only one filter.

4.3. Estimation of the ASTR including filter

The aerosol transfer ratio of an AHU $ASTR_{AHU}$ can be estimated as follow:

$$ASTR_{AHU} = ASTR_{RHE} \cdot (1 - f_{F,eta}) \cdot (1 - f_{F,sup}) \quad (3)$$

where

$ASTR_{RHE}$ is the ASTR of the RHE, acc. to Equation (2),

$f_{F,eta}$ is the separation efficiency of lung aerosols of an extract air filter (positioned before RHE),

$f_{F,sup}$ is the separation efficiency of lung aerosols of a supply air filter (positioned after RHE).

With the values shown in chapters 4.1 and 4.2, an ISO ePM1 50% filter in extract air and no additional filter

Table 1. EATR and ASTR, condensation wheel.

MP, -	v, m/s	n, rpm	Δp_{22-11} , Pa	EATR, %	ASTR, %
1.1	1	20	10	10.4 ± 0.3	7.5 ± 3.7
1.2	2	20	10	4.7 ± 0.2	3.8 ± 2.3
1.3	3	20	10	3.3 ± 0.2	2.4 ± 0.6
1.4	3	20	250	2.6 ± 0.2	1.6 ± 0.2

Table 2. EATR and ASTR, sorption wheel.

MP, -	v, m/s	n, rpm	Δp_{22-11} , Pa	EATR, %	ASTR, %
2.1	1	20	10	8.2 ± 0.3	6.3 ± 2.9
2.2	2	20	10	4.7 ± 0.2	2.7 ± 0.5
2.3	3	20	10	3.2 ± 0.2	1.7 ± 0.3
2.4	1	10	10	4.5 ± 0.1	2.8 ± 0.8
2.5	2	10	10	2.3 ± 0.2	0.9 ± 0.2
2.6	3	10	10	1.5 ± 0.2	0.6 ± 0.2

in supply air, the result is an $APTR_{AHU}$ of approx. 0.006 or 0.6% respectively. This applies to RHEs without purge sectors. With purge sector, values 10 times lower can be achieved.

4.4. Estimation of the infection risk

The amount of virus released into the air can be done by combining the concentration of viruses in the lung lining liquid with the size-distribution of microdroplets released during breathing and speaking and by taking into account the proportion that sediments rapidly [10]. To estimate the viral concentration at steady state in different situations, we used an indoor scenario simulator that is based on this emission concept [11]. In all the calculated scenarios, we assumed that a very contagious person (a so-called super-emitter) is in a room of 100 m³ volume and 3 air changes per hour. We then simulated a quiet office, a loud office (e.g. call centre) and a hospital situation with coughing COVID-19 patients. We further assumed that 1000 people are in this building with a ventilation flow rate of 30 000 m³/h. For the general population, a very high infection rate of 1% is assumed, for the hospital wing with COVID-19 patients a rate of 50% (50% patients, 50% staff). **Table 3** summaries the simulated virus concentrations in these scenarios in the individual rooms and in the extract air of the building.

The concentrations indicate viral copies as assessed by RNA assays. For the Delta variant about 1 in 300 and for the Omicron variant about 1 in 100 of these copies was found to be able to infect cells [12]. Thus, doses above 300 or even only 100 virus-copies seems to be critical for viral infections. This is supported by simulation of super-spreading events where the virus dose (the amount taken up) was estimated in the range of a few thousand viruses.

For the example of the call centre, it can be said that with an $ASTR_{AHU}$ of 0.6% and the virus concentrations in the extract air according to **Table 3**, the virus concentration in the supply air is 0.2 copies/m³. Even if the personnel directly inhale the supply air during an 8-hour shift

Table 3. Simulated virus concentrations (copies/m³) in individual rooms and in the extract air in different scenarios.

Scenario	Infection rate, %	Steady state in room, Copies /m ³	Extract air, Copies /m ³
Quiet office	1	1200	1.2
Call centre	1	40 000	40
Hospital*	50	500 000	250 000

*COVID section

(breathing air volume 0.6 m³/h), the amount of inhaled viruses is two orders of magnitude below the critical value for an infection risk. However, in a hospital situation with many highly emitting patients, the situation could rapidly become critical. Thus, the recommendation to use heat recovery systems without any risk of exhaust air transfer to supply air (e.g. tight plate heat exchanges or run around coil systems) in such settings is well warranted.

Eurovent 6/15 - 2021 [13] deals comprehensively and in detail with the prevention of air leakage in air handling units. According to this, an elementary measure is to ensure correct pressure conditions in air handling units. This depends primarily on the fan positions. For hygienically sensitive applications, a purge sector is also recommended.

It should be mentioned that the risk of exhaust air transfer also exists with other leakages in AHUs and ventilation systems that are not the subject of this paper.

5. Conclusion and outlook

The project investigated how aerosols, which behave similarly to human lung aerosols, are transferred in rotary heat exchangers without a purge sector under isothermal conditions. In the measurements on a condensation rotor, the exhaust air transfer ratio of the aerosols was around 1 percentage point lower than the exhaust air transfer ratio (EATR) of tracer gas. For a sorption rotor it was 2 percentage points lower. The results suggest that there is no risk of the used aerosols being transferred through the matrix with these rotary heat exchangers.

In the follow-up project further measurements with different products were carried out. The test report [14] is freely available, but the results have not yet been prepared for publication in a journal. However, it can be said that for rotors without a purge sector, the ASTR was always below the EATR, even with different air conditions. With a purge sector, EATR and ASTR were measured at a low level of 0.0 to 0.5%. Taking into account the measurement uncertainty, the EATR and the ASTR with purge sector can be described as approximately the same. ■

6. Acknowledgment

The authors would like to thank the company Hoval for initiating the project, the technical exchange, and the financial support.

7. References

Please find the full list of references in the original article at: <https://proceedings.open.tudelft.nl/clima2022/article/view/391>

▶ Uponor PEX pipes 50 years and still in love

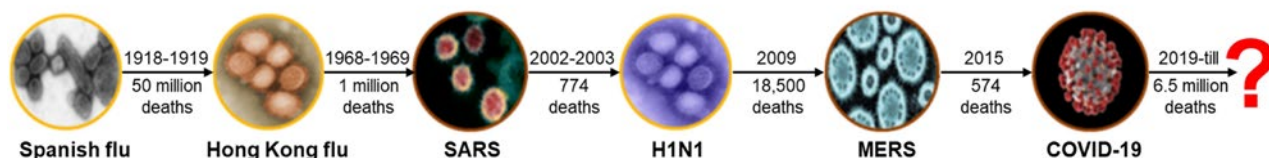
**RESISTANT, VERSATILE
AND EASY TO INSTALL**

In 1972, the first Uponor PEX pipes were launched worldwide and revolutionized the entire industry. 50 years later, they remain resistant and versatile. Uponor PEX Pipes, however, continue to evolve and create the basis for further sustainable innovations, such as the bio-based Uponor PEX Pipes Blue in 2022. Find out more about Uponor PEX pipes: www.uponor.com/50-years-of-uponor-pep-pipes



uponor

**Moving
> Forward**



Development of a non-contact modular screening clinic (NCMSC) for COVID-19



JINKYUN CHO

Dept. of Building and Plant Engineering,
Hanbat National University, Korea
jinkyun.cho@hanbat.ac.kr



JINHO KIM

Dept. of Fire Protection, Safety and Facilities,
Suwon Science College, Korea



JONGWOON SONG

Energy Solution Technology, E-SOLTEC Co., Ltd., Korea



SEUNGMIN JANG

Dept. of Building and Plant Engineering,
Hanbat National University, Korea

Under the global landscape of the prolonged COVID-19 pandemic, the number of individuals who need to be tested for COVID-19 through screening clinics is increasing. However, the risk of viral infection during the screening process remains significant. To limit cross-infection in screening clinics, a non-contact mobile screening clinic is developed. This study investigates aerosol transmission and ventilation control for eliminating cross-infection and for rapid virus removal from the indoor space using numerical analysis and experimental measurements.

Keywords: COVID-19, screening clinic, cross-infection, ventilation strategy, CFD, particle image velocimetry (PIV)

Introduction

In the past, most types of viruses that reached the pandemic level were respiratory infections such as influenza and coronavirus [1]. Particularly, the coronavirus causes a pandemic every 5 to 10 years because the cycle is getting shorter [2]. The WHO (World Health Organization) declared COVID-19 a global pandemic in 2020, which persists at the present. In the beginning, medical institutions isolated symptomatic patients from general patients through screening clinics. The screening clinic plays a primary role in screening suspected patients of infectious diseases. At the COVID-19 pandemic peak, more than 600 screening clinics (temporary, drive-through, walk-through and etc.) were installed and operated in Korea. However, there are no clear criteria and guidelines for the design,

installation, and operation of these screening clinics worldwide. A novel non-contact modular screening clinic (NCMSC) was developed that addresses the problems of existing screening clinics and the risk of cross-infection during the COVID-19 testing process.

Non-contact modular screening clinic

A NCMSC that uses biosafety cabinets and negative pressure booths enables safe, fast, and convenient COVID-19 testing. The NCMSC is a mobile modular unit that can be quickly moved, installed, and operated in the required area depending on the COVID-19 testing demand. This type of medical modular facility can reduce the risk of cross-infection between rooms by achieving the airtightness performance of the structure.

In particular, a non-contact automated system was applied to the entire testing process, from and body temperature measurements to specimen transport, to prevent infection from the source.

It increases the accessibility of patients to the screening clinic and provides adequate protection for healthcare workers (HCWs). The NCMSC is a safe medical facility equipped with negative pressure zones, an anteroom (AR) and a specimen collection booth (SCB), and positive pressure zones, such as an examination room (ER), as shown in **Figure 1**. Moreover, it implemented two-stage negative pressure control to prevent virus leakage. The air change rate was set to more than 12 ACH [3], [4], which is the standard for an airborne infectious isolation room, and the pressure differential was set to maintain maximum 25 Pa or above. Subsequently, ER maintained positive pressure and HEPA filter (PM_{2.5} 99.97%) were applied to prevent infection among HCWs. The total air change rate of the SCB was set to be maximum 30 ACH for an effective discharge of viruses. The ventilation system provides a safe air quality and space for HCWs and individuals to be tested against infection. Therefore, the appropriate arrangement of the supply air (SA) and exhaust air (EA) outlets of the ventilation system is an important consideration for adequate indoor airflow. The ventilation system and pressure differential performance should be reviewed and the airtightness and the area of opening of the structure should be optimized to maintain pressure differential through numerical analysis results and prevent aerosol viral diffusion and infection between SCB and ER.

Numerical analysis

A quantitative analysis of the effect of the cross-infection prevention and a ventilation strategy to prevent the transmission are needed and should be established in the developed NCMSC. The effects of the airflow velocity and room pressure control based on the operation of the ventilation system on the viral transmission were investigated. The dimension of the CFD domain was 4100 × 3000 × 2400 mm (L×W×H). **Figure 2** shows the division of SCB, AR, and ER. Both SA and EA systems were applied in the SCB for effective. On the other hand, only a SA system of ER was set to 6 ACH. Only an EA system was installed in AR and the airflow rate of EA was 12 ACH for Baseline and 30 ACH for Cases 2 and 3. Meanwhile, an EA outlet was installed in the SCB with an EA flowrate of

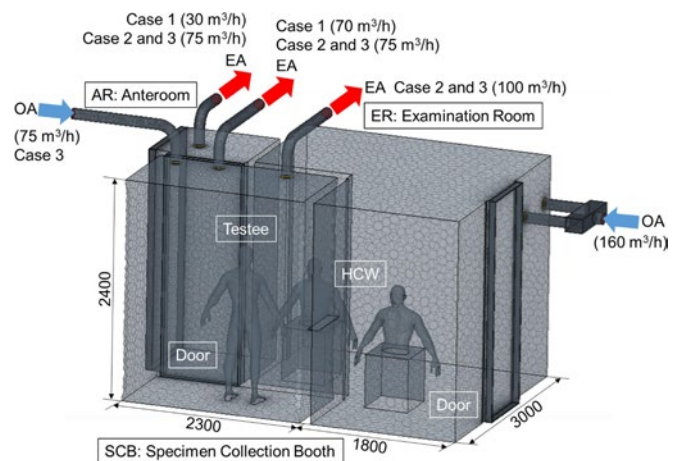


Figure 2. NCMSC mesh of the CFD model.

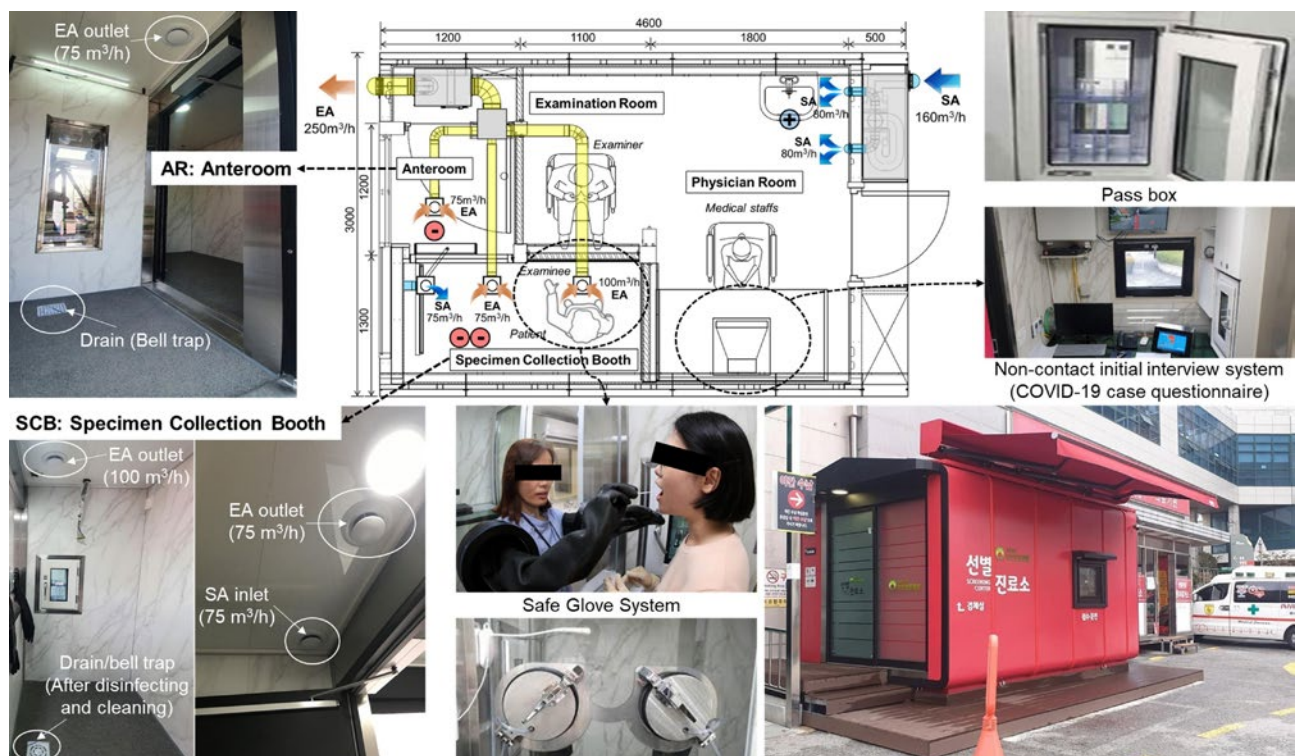


Figure 1. Layout of the COVID-19 NCMSC showing the optimized of SA/EA inlet/outlet locations.

12 ACH for Baseline. In addition, two EA outlets were installed for Cases 2 and 3 with total EA flowrate of 30 ACH. Furthermore, Case 3 applied the SA system was installed with a flowrate of 12 ACH. The negative pressure was controlled in SCB, and analysed with all doors closed. The shortage of SA for EA was supplemented through door gaps of adjacent rooms, and the direction of airflow was from the ER to the SCB.

The boundary conditions of the simulations are listed in **Table 1**. The velocity of air supplied through the SA inlet and gap of the door, the velocity of air exhausted through the EA outlet, and the pressure differential between rooms were evaluated. Then, the ventilation performance through which the virus is assumed to be an aerosol of SCB is predicted.

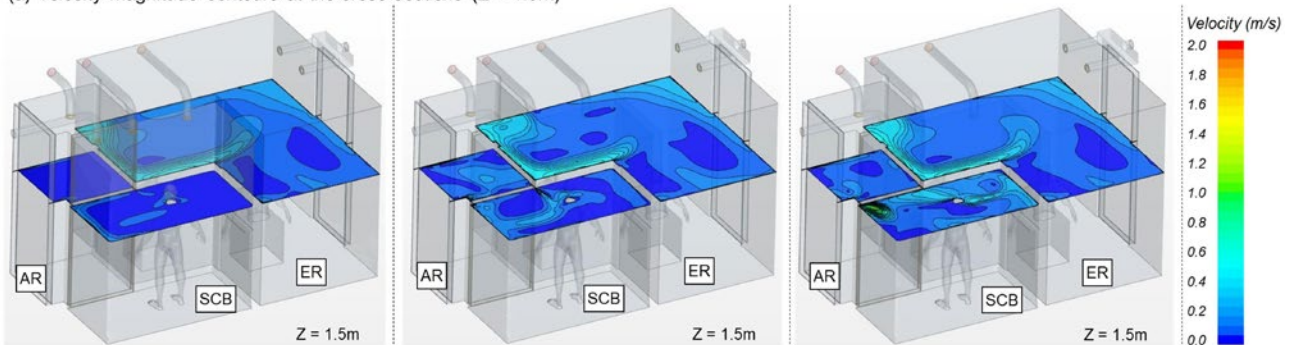
Airflow velocity

Figure 3(a) shows the horizontal airflow velocity profile at a height of 1.5 for each Case.

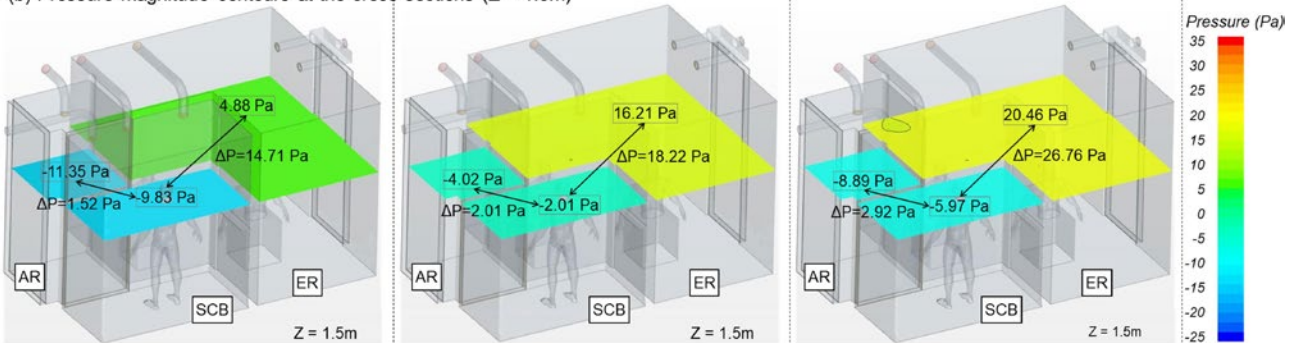
Table 1. CFD boundary conditions with airflow rates.

Ventilation system	Baseline	Case 2	Case 3
Supply (ER)	160 m ³ /h	160 m ³ /h	160 m ³ /h
Transfer (ER to SCB)	25 m ³ /h	40 m ³ /h	30 m ³ /h
Supply (SCB)	N/A	N/A	75 m ³ /h
Exhaust (SCB)	70 m ³ /h	175 m ³ /h	175 m ³ /h
Exhaust (AR)	30 m ³ /h	75 m ³ /h	75 m ³ /h
Transfer (AR to SCB)	45 m ³ /h	135 m ³ /h	70 m ³ /h
Lying manikins	Uniform heat flux: 62 W, no slip boundary		
Walls	2 and 1 W/m ² at ceiling/floor, no slip boundary		
Bedside	Adiabatic wall boundary condition		
Grid cells	8,176,419		
Turbulence model	Standard k-ε model		

(a) Velocity magnitude contours at the cross-sections (Z = 1.5m)



(b) Pressure magnitude contours at the cross-sections (Z = 1.5m)



(c) Streamline visualization of the velocity field

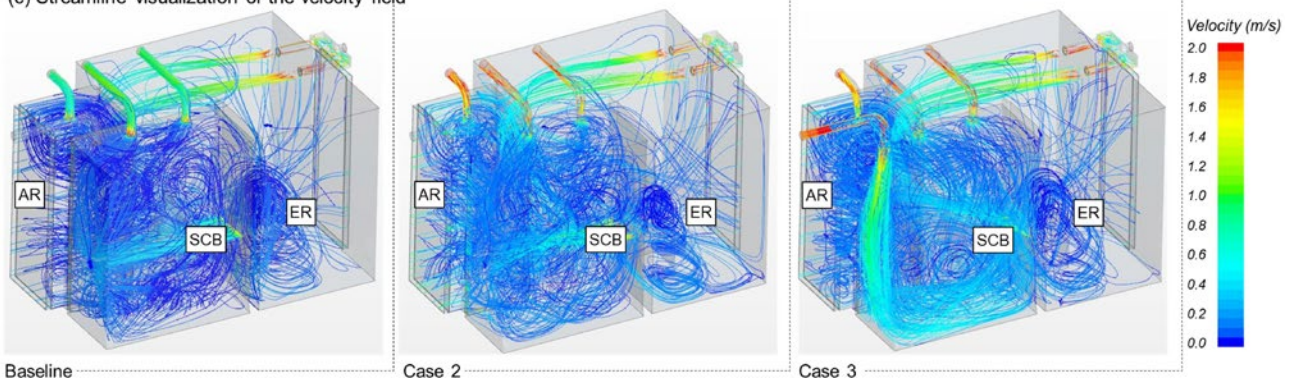


Figure 3. Results of CFD numerical analysis in the NCMSC for different ventilation conditions.

The air change rates for AR and SCB in Baseline, which only applied the EA system, was set to 12 ACH. The velocity values were in the range of 0.0374 to 0.0506 m/s by examining the average airflow velocity distribution for each height of the SCB, indicating that the airflow progressed slowly and the air was gradually exhausted. In the case of AR, the air was exhausted with a similar velocity of approximately 0.0365–0.0414 m/s with some of the air moved to the SCB. On the other hand, the air change rates for AR and SCB in Case 2, which only applied the EA system were set to 30 ACH. The average air velocity profile for each height of the SCB was in the range of 0.0852 to 0.0945 m/s, indicating that the airflow velocity was increased twice than in Baseline. The air in the AR is exhausted with a velocity range of 0.0931 to 0.1003 m/s with some of the air moves to the SCB.

Furthermore, the air change rates for AR and SCB in Case 3, which applied both EA and SA systems in the SCB were set to 30 ACH. The average airflow velocity range was from 0.1236 to 0.1781 m/s. The average airflow velocity profile was increased by approximately 1.7 times than in Case 2. The air in AR was exhausted with a velocity ranging from 0.1086 to 0.1166 m/s, and some of the air moves to the SCB.

Pressure differential

A negative pressure should be maintained in the contaminated zone (SCB) and a positive pressure should be maintained in the clean zone (ER) to ensure that the aerosol viruses in SCB do not flow to the ER. **Figure 3(b)** shows the pressure differential between SCB and ER for each case. It is less likely that viruses migrate from SCB to the ER if the pressure is great between these two rooms.

The average pressure differential for Baseline, Case 2 and 3 were -14.62 Pa, -18.17 Pa and -25.25 Pa, respectively. The analysis showed that the SCB was properly controlled for all cases to maintain the negative pressure. In addition, the effect of the cross-infection prevention of COVID-19 entering the ER is considerably enhanced because the pressure differential increases from Baseline to Case 3. The average pressure differential between SCB and AR for Baseline and Case 2, 3 were -1.39, -1.87 and

-3.02 Pa, respectively. However, the values for Baseline and Case 2 are not within the appropriate range of the recommended pressure differential of at least -2.5 Pa based on the airborne infectious isolation room [5].

Airflow considerations

Figure 3(c) shows the airflow streamlines across the entire MCMSC space. It is apparent that for SCB, which applied both SA and EA systems in Case 3, the ventilation is active across the entire room compared to Baseline and Case 2, which only applied the EA system. The airflow velocity results of 0.0587 m/s for Baseline and 0.112 m/s for Case 2 were obtained by examining the overall average airflow velocity of the room, indicating that the velocity of Case 2 increased by 1.9 times than Baseline. In addition, the airflow velocity was 0.1786 m/s for Case 3, indicating a velocity increase of 1.6 times than Case 2 and 3.0 times than Baseline. It is expected that Case 3 will enhance the ventilation performance and facilitate an effective discharge of the aerosol COVID-19 viruses.

Experimental analysis

Full-scale field measurements were performed under similar conditions used in the numerical analysis. PIV (particle image velocimetry) was used to conduct experiments for airflow behavior characterization and examination of the leakage area through visualization of particles simulating viruses in SCB and to verify the safety of the developed NCMSC against cross-infection.

Figure 4 shows the experimental setup and perspective view of the PIV set-up. Two-dimensional flow fields were measured at different positions of the camera and laser. At Position A, the camera was installed in the ER, and the laser and oil droplet generator were installed in the SCB. Moreover, at Position B, the laser was installed at the ER and the camera and the oil droplet generator was installed in the SCB to ensure that the droplet came out from the mouth of the manikin, an individual to be tested. Subsequently, the exhaust airflow was observed. Four different PIV measurements were performed for four different combinations, as shown in **Table 2**. First, the PIV measurement was performed at Position A for Case 2, where only the EA system was operated, and Case 3, where both EA and SA systems were simultaneously operated in the ventilation system of the SCB. Subsequently, the ventilation performance at Position B was examined with the door between the AR and SCB closed and open for Case 3.

The pressure differential can determine the effect of cross-infection prevention. The pressure differentials

Table 2. Measuring cases with the PIV equipment.

Measurement	Cases	Position	Door between SCB and AR
PIV A1	Case 2	A	Closed
PIV A2	Case 3	A	Closed
PIV B1	Case 3	B	Closed
PIV B2	Case 3	B	Open

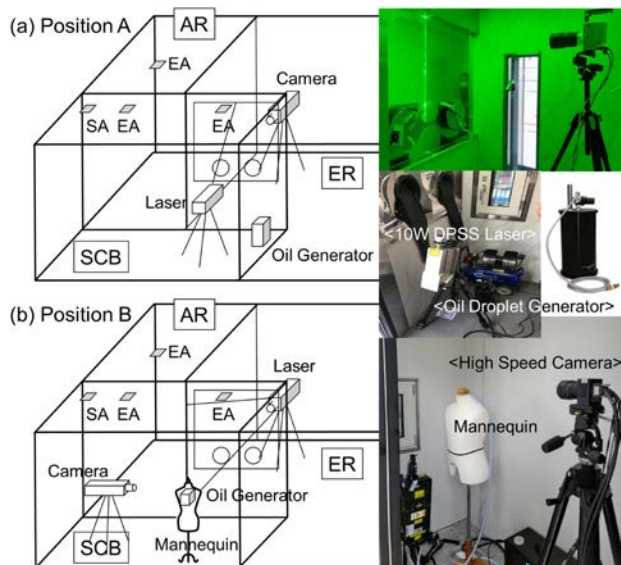


Figure 4. Experimental set-up for the PIV.

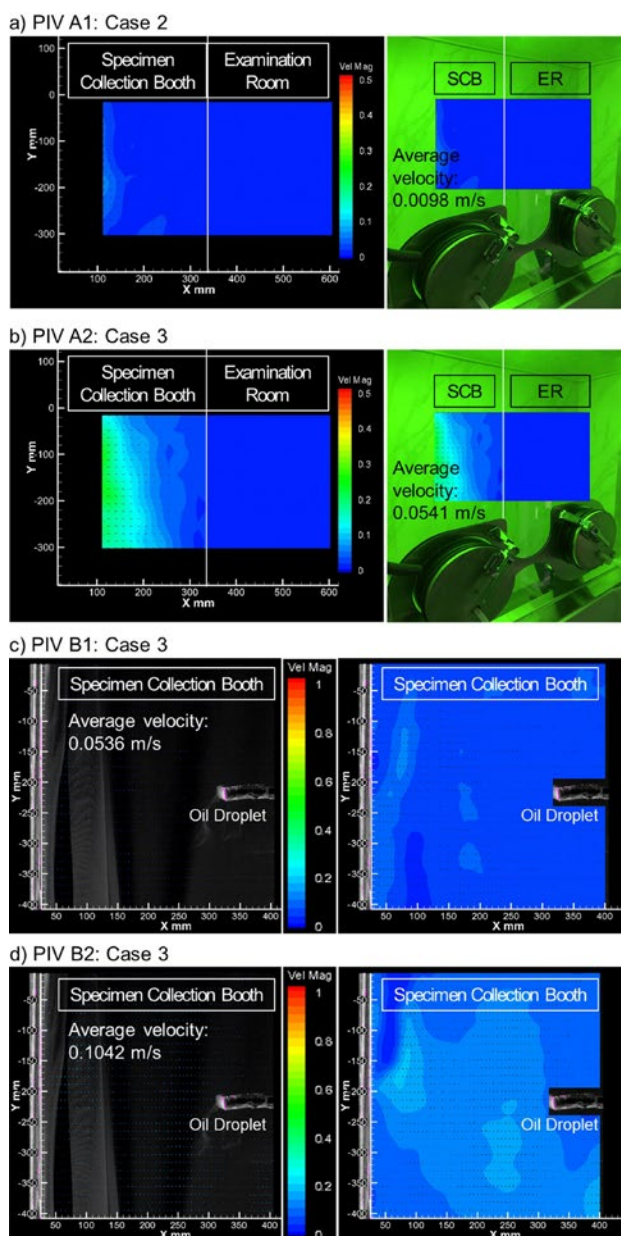


Figure 5. Time-averaged air distribution under PIV cases.

of SCB and ER with the ventilation system turned on are $\Delta P = -21.8$ and -29.3 Pa, respectively. The measured values and numerical analysis results were very similar. The negative pressure in the SCB was properly maintained for both cases (Cases 2 and 3). The experimental results were divided into two parts based on the location of the PIV measurements. Moreover, Figure 5 shows the experimental results for the vertical airflow velocity.

Figure 5(a) shows the average velocity of Case 2 for PIV A1. The particle movement velocity in the SCB was found to be very slow with almost no airflow for an average airflow velocity of 0.0098 m/s. On the other hand, the average airflow velocity of PIV A2 in Case 3 (Figure 5(b)), where SA and EA systems were operated, was 0.0541 m/s, indicating a four-time increase than PIV A1. The make-up air was smoothly supplied to improve the exhaust efficiency. In addition, the cross-infection by viruses is not expected to occur since there was no airflow from the contaminated zone (SCB) to the clean zone (ER) in PIV A1 and PIV A2. Figure 5(c) shows the average velocity of Case 3 for PIV B1. The average airflow velocity was 0.0536 m/s, and is the same as that in PIV A1 under the same ventilation conditions. Finally, Figure 5(d) shows the average velocity of Case 3 for PIV B2. The same condition was applied to PIV B2 as PIV B1, but the door to the AR was opened. In this case, the results showed that the average airflow velocity was 0.1042 m/s, and the velocity of the generated particles increased more than twice than that of PIV B1. However, it is a principle to close the door during specimen collection. Therefore, it is recommended to operate the ventilation system with the door open before the next individual to be tested enters to increase the cleaning and disinfection effect after collecting the specimen.

Conclusion

Based on the results of this study, the standards for the installation and operation of the screening clinics are proposed. It is necessary to implement space configuration and secure airtight performance to ensure that all tests can be performed using non-contact methods. ■

Acknowledgment

This work is supported by the Korea Agency for Infrastructure Technology Advancement (KAIA) grant funded by the Ministry of Land, Infrastructure and Transport (22TBIP-C161800-02).

References

Please find the full list of references in the original article at: <https://proceedings.open.tudelft.nl/clima2022/article/view/283>



For a healthy
and comfortable
room climate.

Webinar “The 7 Essentials for Healthy Indoor Air”

We assume that the air in buildings is “clean” and not harmful to our health. This makes it all the more surprising how little building users and operators actually know about the air quality in their spaces. Key variables such as humidity, CO₂ content or VOC concentration are almost never measured, much less displayed.

To find out where the about priorities lie in creating a healthy indoor air climate, Belimo conducted a global survey among experts of the ventilation industry and emerged seven fundamental factors for healthy indoor air in functional buildings.

Register for the Webinar “The 7 Essentials for Healthy Indoor Air” on 29.11.2022 and learn from our Expert Mikko Gisin how Belimo sensors and room operating units contribute to a healthy indoor air.



Thermal inactivation of the corona virus (SARS-CoV-2) in air volumes



ANDRÉ SCHLOTT

Fraunhofer Institute for Manufacturing Technology and Advanced Materials IFAM, Branch Lab Dresden, Dresden, Germany
andre.schlott@ifam-dd.fraunhofer.de



THOMAS HUTSCH

Fraunhofer Institute for Manufacturing Technology and Advanced Materials IFAM, Branch Lab Dresden, Dresden, Germany



EILEEN SAUER

Fraunhofer Institute for Interfacial Engineering and Biotechnology IGB, Stuttgart, Germany



JENS WETSCHKY

Fraunhofer Institute for Interfacial Engineering and Biotechnology IGB, Stuttgart, Germany



JANA HESSEL

Fraunhofer Institute for Interfacial Engineering and Biotechnology IGB, Stuttgart, Germany



SUSANNE BAILER

Fraunhofer Institute for Interfacial Engineering and Biotechnology IGB, Stuttgart, Germany



JOHN LAUBERT

Fraunhofer Institute for Manufacturing Technology and Advanced Materials IFAM, Bremen, Germany



STEFAN LÖSCH

Fraunhofer Institute for Manufacturing Technology and Advanced Materials IFAM, Bremen, Germany

Abstract: To control the spread of viruses (e.g., SARS-CoV-2) and other pathogens in a pandemic situation, slowing down the rate of spread is an essential goal that can be achieved by interrupting transmission chains. According to the current state of knowledge, SARS-CoV-2 is mainly transmitted by droplet infection through virus-containing aerosol clouds in the air. These aerosol clouds are mainly produced by exhalation and can be reduced by wearing medical masks. In closed rooms, there is an increased probability of infection by aerosols. Countermeasures include various recently developed air cleaning technologies. Most of these technologies available on the market are based on filters with a limited lifetime to remove the virus load from the air or different sterilisation methods like UV irradiation. The air cleaning technology presented focuses on the thermal inactivation of viruses beyond their temperature sensitivity by heating the air. In the developed apparatus, the potentially germ-carrying ambient air is sucked in and conditioned in such a way that it is exposed to a certain temperature for a defined period of time. Before the inactivated / hygienised air is returned to the environment, it is cooled down to almost room temperature. The recovered heat remains in the system and is used to heat the intake air. The use and combination of different technologies enable the most efficient air disinfection possible. Four different experiments were conducted. After determining a base line, the air was solely

passed through the pump, through the whole ‘Virus-Grill’ pressure free and with an elevated pressure of 1.5 bar. In all experiments (except the baseline) the number of active viruses were reduced below the limit of detection.

Keywords: Health, Thermal Sterilisation, Thermal Inactivation, Air Treatment, Air Cleaning Technology, Virus Inactivation, SARS-CoV-2, COVID-19, Heat Recovery, Energy Efficiency

1. Introduction

Aerosols containing viruses can accumulate indoors and lead to superspreading events [1]. Therefore, slowing down the rate of spread is an essential goal in order to control the pandemic spread of viruses (e.g. SARS-CoV-2) and other pathogens. That can be achieved by interrupting transmission chains.

Researchers all over the world work on air purification technologies. Possible air purifying technologies include filtration with HEPA filters, where the viruses are removed from the air volume. This is a common approach to reduce contamination in the surrounding air. With light in UV-C spectrum (200 to 280 nm), viruses are deactivated through critical damage to the genomic system of the microorganism by absorbing photons [2, 3]. With UV light, surfaces, e.g. door knobs, are sterilized [4]. To clean air volumes, an upper-room mounting of UV lights is possible [5]. Additionally, UV lights are installed in HVAC channels. A third method is the plasma air cleaning, which uses high-voltage electrodes to create ions in the air [6].

The developed apparatus ‘Virus-Grill’ reduces the probability of droplet infection by inactivating viruses. This inactivation is achieved by heating the viruses beyond their temperature sensitivity. (e.g. 70°C), the virus proteins, especially the surface proteins needed to dock to receptor molecules on the host cell membranes, are denaturated.

If this targeted process is carried out continuously, it can be used as a kind of “virus sink”. In order to return the inactivated air to the room, the air must be cooled down to nearly room temperature. The use of a heat pump enables efficient temperature control within the apparatus. The interaction of the components is ensured by a regulation and control software.

The aim was to construct and build up a test rig for the proof of the inactivation of viruses using a safety workbench. The developed principle itself can be integrated into climatization systems for closed volumes like rooms (bureau; waiting rooms; class rooms; passenger areas in aircrafts, hotels and ships).

2. Principle of Thermal Inactivation

The concept of the ‘Virus-Grill’ is that a partial quantity is extracted from a closed volume of air by the compressor and is specifically exposed to a higher temperature (e.g. more than 70°C) in the apparatus for at defined dwell time (e.g. 10 minutes in a dwell chamber). Before the air reaches this chamber, it is heated in three steps as shown in **Figure 1**. The heating steps one and two utilize the already treated and still hot air. While the first step is a passive heat recovery system, the second step uses an active heat pump to heat the air. The final heating step is the compressor itself, where the air reaches the temperature needed during compression. After that, the compressed air is stored in a heated chamber to inactivate the viruses.

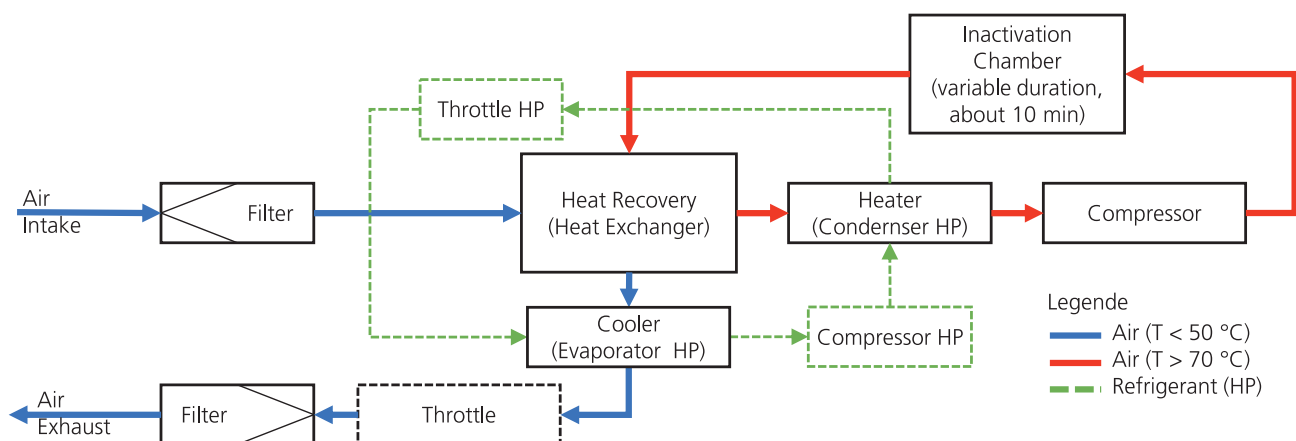


Figure 1. Flow chart of the sterilization process.

The viruses will stay in the treated air but because they are not infectious anymore, the air is considered inactivated / purified.

After releasing the sterilized air from the chamber, it goes through the heat recovery and the evaporator of the heat pump to reduce its temperature. Before leaving the apparatus, a throttle reduces the pressure of the air. Therefore, the air leaves the 'Virus-Grill' apparatus at ambient pressure and almost at ambient temperature.

3. Experimental Test Rig – The 'Virus-Grill' Apparatus

The set-up was done considering the planned tests with surrogate viruses in a safety workbench to characterise the effectiveness of the 'Virus-Grill'. Because of the limited space in the workbench, the test rig had to adhere to certain dimensions. Also, the required air volume of the aerosol generator and available electrical connection were considered at the design process of the test rig.

Figure 2 shows the set-up of the 'Virus-Grill' during the trials for the proof of efficacy.

The individual components play a special role in this process, the sum of which can achieve effective inactivation. The compressor works according to the

principle of a piston compressor. This causes pressure (change) and temperature to act for a short time. In addition, the pressure-resistant dwell chambers (here 3 bar) are tempered to a certain temperature by an external heater. In order to use energy more efficiently, the heat pump supports the heat recovery unit used. The developed system of solenoid valves enables almost continuous operation through appropriate control. The question of effectiveness was addressed as a complete unit as well as in partial component tests.

The 'Virus-Grill' control includes the collection and processing of numerous temperature and pressure sensor data and adjustable process parameters. Valves and compressor are controlled by control electronics containing market available and self-developed components. The 'Virus-Grill' is monitored by 16 temperature sensors (PT1000) and 16 pressure transmitters, whose data are processed by the controller. Switching operations on solenoid valves and air compressors as well as power control of the heat pump components are made possible by means of a Mosfet driver circuit and an external power supply. The control of the chamber heating is realised via standardised interfaces.

A microcontroller board is used as the central element of the control system, which has sufficient computing power and supports all necessary connections. The necessary firmware was programmed in C++ and

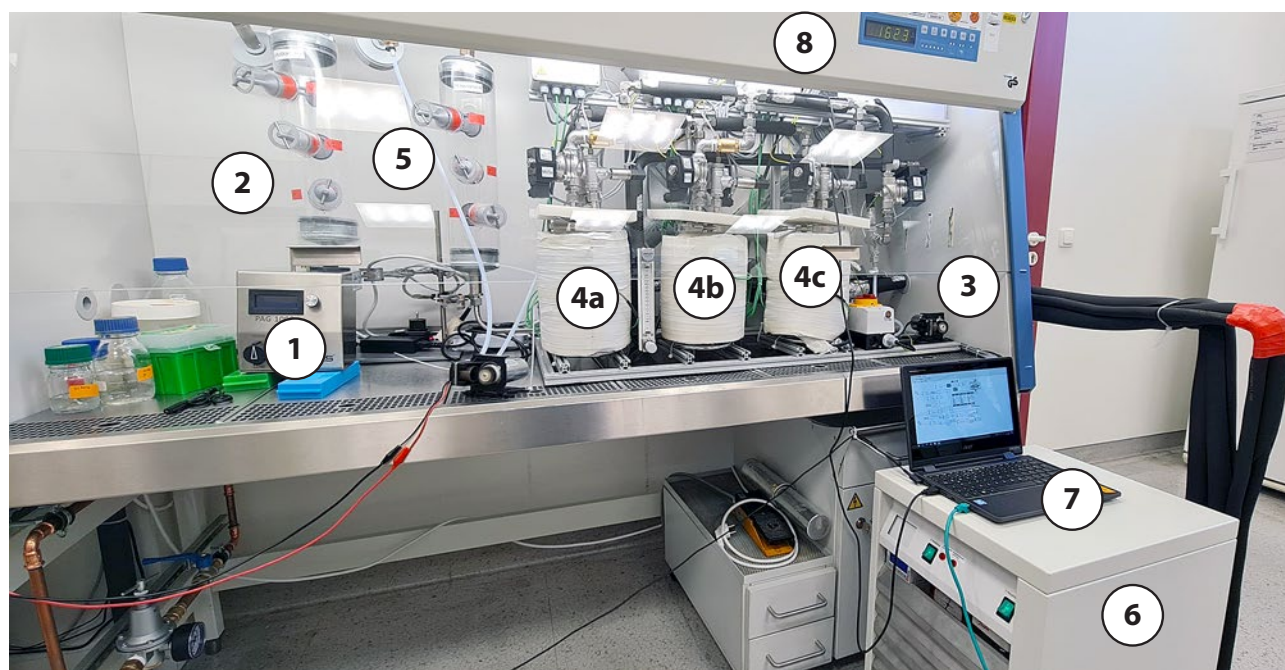


Figure 2. Prototype of the 'Virus-Grill' in the sterile bench environment to characterise the efficacy in terms of inactivation of aerosol-borne viruses. (1) aerosol generator, (2) virus chamber, (3) compressor, (4a-4c) holding chambers, (5) clean chamber, (6) heat pump, (7) measuring computer with control software, (8) safety workbench (sterile bench).

processes the measurement data, interprets process parameters and gives corresponding control signals. A wireless LAN access point including a webserver enables the user to interact with the 'Virus-Grill'.

A control software developed in C# establishes the necessary connection and displays the measurement data using a circuit diagram of the 'Virus-Grill' (Figure 3). The measurement data are stored in parallel for later evaluation. It is also possible to adjust the process parameters of the 'Virus-Grill'.

In order to take suitable samples, aerosol samples must be collected from a closed system, such as the virus and clean chamber, without manipulating the atmosphere in the system or allowing air contaminated with viruses to escape. Therefore, a small airlock for swabs was developed and four polycarbonate 3D printed components were created for each airlock, which were assembled with UV-resistant adhesive.

The construction is shown in Figure 4. The three-part airlock consists of a handpiece, a piston insert and the actual airlock chamber as well as the piston. The handpiece serves as a carrier/holder for the swab and at the same time as the "outer sluice gate". The piston insert combines inner and outer sluice gate including the necessary piston seals. The piston itself determines the volume of air exchanged when opening and closing the airlock.

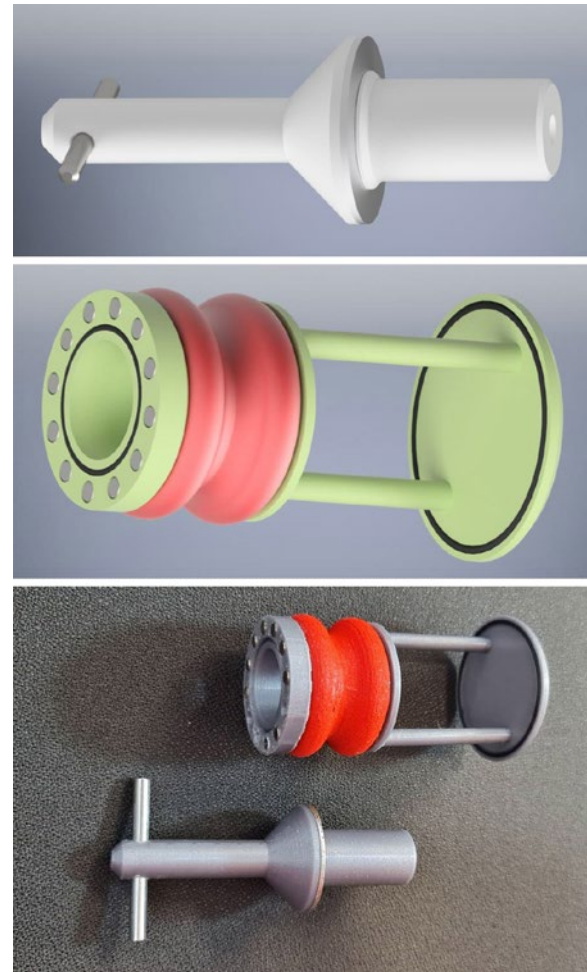


Figure 4. Three-part airlock for sampling (above: Handpiece/swab holder; middle: piston insert with sealing ring; bottom: printed components)

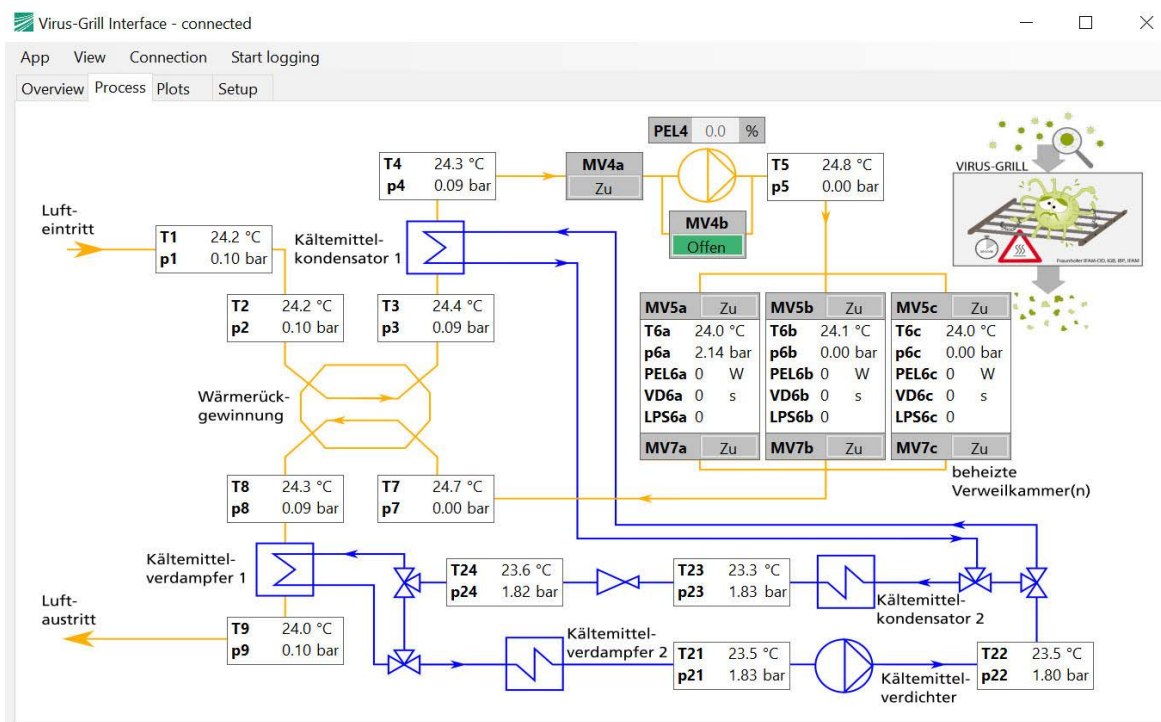


Figure 3. GUI of the control software.

The greatest difficulty in the CAD-supported development was the sealing ability of the piston rings. The tubes used, made of special solvent-resistant and UV-permeable acrylic glass, showed strong geometric tolerances, so that commercially available sealing solutions with rubber rings and lubricants and sealants did not achieve sufficient sealing. Therefore, piston sealing rings made of flexible filament were developed and manufactured by means of 3D printing, with which tolerances could be compensated and a sufficient seal achieved at both sluice gates. These are shown in red in **Figure 4**. Smooth sliding of the piston insert was also ensured.

To close the sluice gates securely, neodymium magnets are used to magnetically attract a metal ring on the handpiece itself or on the outer end of the piston, depending on the position of the handpiece. These metal rings required precise manufacturing in order to minimise the gap between the magnets and the metal ring so that the neodymium magnets can generate a sufficiently large magnetic attraction force.

4. Virological Test Setup

The current and still ongoing pandemic situation regarding SARS-CoV-2 requires standardised methods for the detection and analysis of airborne viruses in the form of aerosol. Since SARS-CoV-2 is classified as a biosafety level 3 virus, the number of laboratories that can culture and analyse infectious viruses is severely limited and the experiments require a high level of security measures for containment. For this reason, the bacteriophage Phi6 was established as a surrogate virus. Phi6 shows a high degree of similarity to SARS-CoV-2 in particle size, external structure, and the type of genome. In contrast to other surrogate viruses, Phi6 is a bacteriophage that only infects bacteria and poses no danger to humans, animals or plants. In order to assess the effectiveness of disinfection measures, two parameters were applied. i) The number of viral genomes that accounts for all viruses whether dead or alive, was determined by the molecular biological method of qPCR. ii) The viral activity or infectivity that accounts the number of infectious viruses was determined by the plaque assay.

4.1 Sample Preparation of surrogate viruses

The bacteriophage Phi6 was used as surrogate virus for the evaluation of the 'Virus-Grill'. Phi6 was propagated using its host bacterium *Pseudomonas syringae*. Stock solutions of Phi6 and *P. syringae* were kindly provided by Prof. Dr. Martin Hessling and Dr. Petra Vatter (Technische Hochschule Ulm). For propagation

of the surrogate virus, *P. syringae* was cultivated overnight in tryptic soy broth (TSB) at 25°C and 170 rpm. Bacterial culture was subcultivated in fresh TSB for starter culture. At an optical density of 0.3, Phi6 was added 1:10 followed by incubation to an optical density of 0.08. To obtain pure phage lysate, the culture was centrifuged to pellet the bacteria, and supernatant was filtered through a 0.45 µm filter (Fisher Scientific).

For all experiments performed, Phi6 lysate was rebuffed in water. The titer of the obtained Phi6 stock lysate was determined using a bacterial plaque Assay [7] and stored at 4°C until further usage. For the experimental procedures, the stock lysate was adjusted to 1×10^{10} PFU/mL and used for aerosolization.

4.2 Virological Data Acquisition

The individual steps of sampling with this airlock are shown in **Figure 5**. After inserting the swab into the handpiece, it was mounted in the piston insert. At the same time, the outer airlock is closed. For sampling, the entire piston insert is guided into the interior of the system, exposing the swab to the aerosols. When the piston insert is pulled out, the inner lock closes and the handpiece with the swab can be removed again. The escape of aerosols can thus be reduced to a minimum.

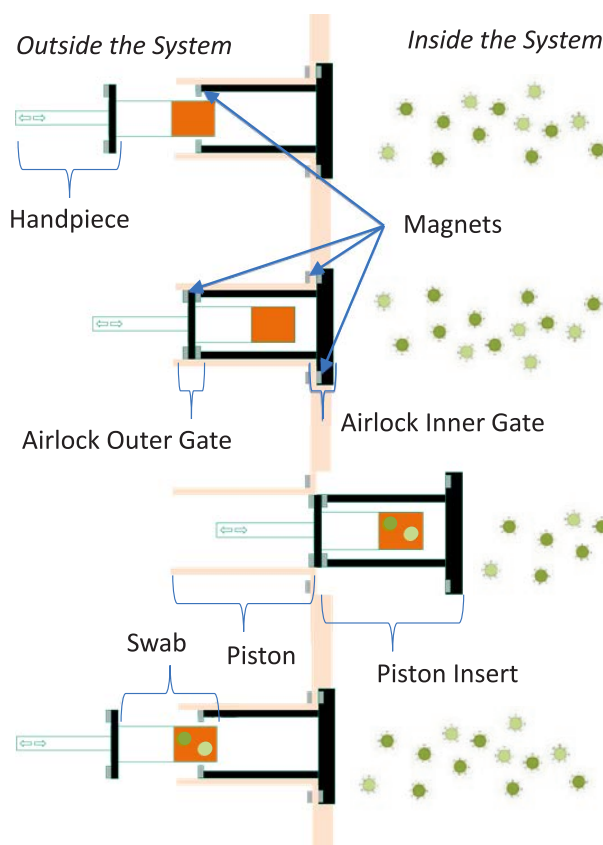


Figure 5. Sampling concept with airlock and swab

5. Measurements and Results

For the experimental set-up, a droplet aerosol with an average droplet size of 0.15 µm was generated from a phosphate-buffered saline (PBS) containing Phi6. The aerosol was collected and analysed at three positions before the experimental setup (virus chamber) and after the experimental setup (clean chamber) using swabs moistened in PBS. All samples were analysed for virus activity and total virus count.

Four different experiments were conducted to examine partial components of the ‘Virus-Grill’ and finally the entire test rig. In the first experiment (Exp. 1), the virus-containing aerosol was sucked from the virus chamber into the clean chamber. The pump was behind the clean chamber. This was done to find a baseline of surrogate viruses in the virus chamber and clean chamber with no treatment whatsoever. In the second experiment (Exp. 2), the virus-containing aerosol was pumped from the virus chamber through the pump into the clean chamber. In the third experiment (Exp. 3), the virus-containing aerosol was pumped pressure-free from the virus chamber through the ‘Virus-Grill’ into the clean chamber. Again, the pump was located at the end of / after the clean chamber. And in the fourth experiment (Exp. 4), the virus-containing aerosol was pumped from the virus chamber through the ‘Virus-Grill’, through the pump into the clean chamber at room temperature and 1.5 bar overpressure.

The results of the detection of the virus activity and the determined virus genome count are shown in **Figure 6** and **Figure 7**. It was shown that only in experiment 1, in which the viruses were sucked directly from one chamber to the other, were active viruses detectable in the clean chamber.

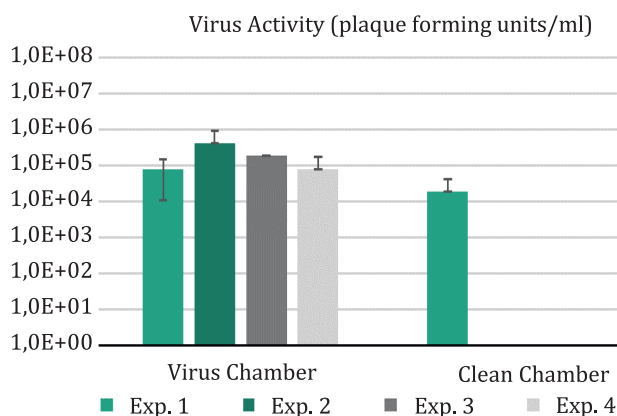


Figure 6. Comparison of virus activity in virus chamber and clean chamber.

The detected virus genomes in **Figure 7** show an increasing reduction of virus genomes when using the pump in experiment 2, the flow through the ‘Virus-Grill’ in experiment 3 up to the greatest reduction of virus genomes when operating the ‘Virus-Grill’ at room temperature and a system pressure of 1.5 bar in experiment 4.

Taken together, it was possible to aerosolise surrogate viruses in the experimental set-up, to transport them from the virus chamber into the clean chamber and to detect them. The use of the pump already leads to complete inactivation of the viruses used. This leads to the hypothesis that continuous inactivation is possible by using compressors based on the principle of the piston compressor for SARS-CoV-2. Furthermore, the use of the ‘Virus-Grill’ was able to reduce the total number of virus genomes.

6. Conclusions and outlook

The efficacy of the ‘Virus-Grill’ was validated with four experiments. Experiment 1 defined a baseline of viruses reaching the clean chamber with no treatment whatsoever. Experiments 2 to 4 tested different ‘Virus-Grill’ configurations. Experiment 2 pulls the virus-containing aerosol only through the piston pump into the clean chamber. In experiments 3 and 4 the contaminated air flows through the complete ‘Virus-Grill’ at ambient pressure and at an elevated pressure of 1.5 bar, respectively. The number of active viruses were reduced below the limit of detection in all three cases. The number of viral genomes in the clean chamber shows that there are inactivated viruses carried through the ‘Virus-Grill’.

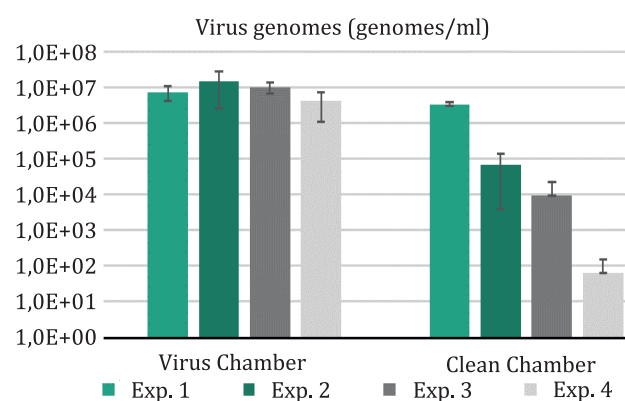


Figure 7. Detected viral genomes in virus chamber and clean chamber The viral genomes detect both inactivated and infectious viruses.

This process has very high potential in applications that dispense mechanical filtration. Here, maritime applications and integration into existing ventilation systems are mentioned in particular. The concept can also be adapted in the medical field for the ventilation of patients. Thus, a wide range of flow rates from a few l/min to several m³/min can be addressed through suitable design and scaling of the components. ■

7. Acknowledgment

The presented work was part of the project AVATOR and funded by the Fraunhofer-Society within the Fraunhofer vs. Corona campaign which is gratefully acknowledged.

Data Statement

The datasets generated and analysed during the current study are not available because of the ongoing validation and up-scaling process but the authors will make every reasonable effort to publish them in the near future.

8. References

Please find the full list of references in the original article at: <https://proceedings.open.tudelft.nl/clima2022/article/view/214>

REHVA is happy to welcome ZoonEx Systems as a new REHVA Supporter

Even with the highest level of manual cleaning, surfaces are at continual risk of contamination and the transferance of microbes to multiply and grow.

Mechanical Ventilation Systems can provide ideal conditions for microbial growth bringing unclean air into office spaces causing 'Sick Building Syndrome' (SBS), aiding the spread of viruses like the common cold, influenza and Coronavirus family among building users.

The ZoonEx™ System allows an antimicrobial treatment to bond to a clean surface, giving effective protection against bacteria and enveloped viruses (including Coronavirus family) for up to 30 days between treatments.

The coating bonds to the surface and forms a microscopic layer of pins that rupture bacteria and enveloped viruses, giving building occupants a protected/treated environment to work in.

More information: <https://zoonexsystems.com/>



SESSION 1
Achieving healthy Zero Emission Buildings with the EPBD

NOVEMBER 15, FROM 10 TILL 12

POLICY CONFERENCE
AT THE THON HOTEL BRISTOL STEPHANIE

join us in Brussels!

SESSION 2

REPower EU: phasing-out fossil fuels in buildings

NOVEMBER 15, FROM 13 TILL 15

MORE INFORMATION AND REGISTRATION



Health and energy assessment of a demand controlled mechanical extraction ventilation system



JANNEKE GHIJSELS
Ghent University



KLAAS DE JONGE
Ghent University &
FWO, Flanders Research
Foundation (ISA7619N)



JELLE LAVERGE
Ghent University

Abstract: Today, the assessment of residential demand-controlled ventilation systems only considers the perceived indoor air quality in terms of comfort, with CO₂ and humidity as the main parameters to investigate. However, the ventilation system and its controls also have an impact on the health aspect of Indoor Air Quality (IAQ) due to the higher exposure to unhealthy pollutants (Volatile Organic Compounds (VOCs), fine dust particles, e.g. PM_{2.5}). In this paper, two demand controlled mechanical extraction ventilation systems (DCV) and a continuous mechanical extraction ventilation system (MEV) of a typical Belgian apartment are modelled using Modelica. This allows to simulate the combined effect and interaction of temperature, airflow and IAQ. The model includes sources of CO₂, humidity, VOCs and PM_{2.5} to the indoor air. The combined approach using Modelica allows to do an in-depth analysis of the indoor air quality. A two-stage assessment method is performed, resulting in an overall performance (in terms of IAQ and energy use) of a DCV system in relation to the performance of the MEV reference system.

Keywords: Smart ventilation system, Indoor Air Quality, VOC, health and energy assessment.

1. Introduction

In the recent decades there has been an increasing awareness that the energy demand for buildings must be greatly reduced. Today, our buildings are better insulated and high-temperature heating is replaced by low-temperature surface-heating. The stricter insulation standards ensure an energy reduction and a better thermal comfort. The disadvantage is that, if we only focus on the thermal comfort, an adverse effect will be induced on the indoor air quality (IAQ) of our homes. In old houses there is natural ventilation through cracks and crevices [1] but in more modern houses, that are build more airtight, the pollutants will accumulate in the indoor air. This creates a greater risk of concentration problems, fatigue and other serious

health effects. Therefore, there is a need for a designed ventilation system that brings fresh air in and evacuates polluted air out of the home, preferably in a comfortable way.

A continuous, constant, airflow ventilation system will guarantee a good IAQ but will also provide more cold airflow that needs to be heated then strictly necessary to ensure comfort. This results in an increase of the energy use. The two main methods used in western-European residential ventilation systems to tackle this increase in energy use are the use of an air-to-air heat exchanger (heat recovery) and the use of pollution sensors to measure the indoor air quality and lower the ventilation flowrate when and where it is possible without

comprising the indoor air quality: demand-controlled ventilation systems (DCV). A DCV system can reduce the heating energy related to ventilation and electricity use of the ventilation system by 20 to 50% [2].

Nowadays, the assessment of a DCV system only considers the perceived IAQ in terms of comfort criteria (such as CO₂, humidity and odour) [3]. However, the big disadvantage of a DCV system is the accumulation of indoor pollutants in times of low occupancy. When the airflow rates are reduced, the VOC emissions of building materials and furniture will accumulate in the indoor air, resulting in harmful VOC concentrations and a poor IAQ. Therefore, the assessment of a DCV system must be extended from only comfort criteria to both comfort and health criteria.

2. Research methods

2.1 Simulation model

The simulation model is made in Dymola, an integrated environment for developing models in the Modelica language. This allows to simulate the combined effect of heat, moisture, airflow and indoor concentrations. In this study, the IDEAS library [4] is used in combination with proprietary models for modelling the airflows and pollutant sources. **Figure 1** shows the floor plan of the modelled three-bedroom apartment. This typical Belgian apartment has already been used several times and has been described in Heijmans, Van Den Bossche, Janssens (2007); Laverge, Janssens (2013) and De Jonge, Janssens, Laverge (2018). During modelling, a lot of attention is paid to the multi-zone representation of the apartment, the building envelope, the elements of the various ventilation systems, the occupant schedules, the ventilation controls, the emissions from the occupant activities and the emissions from the building materials and furniture.

2.2 Investigated DCV systems

The performance of two demand controlled mechanical extraction ventilation systems (DCV) are being compared to the performance of a continuous mechanical extraction ventilation system (MEV). The two DCV systems follow the same principles: fresh air is naturally brought into the dry spaces through trickle vents and will be mechanically extracted in the wet spaces. The first DCV system (DCV1) is a theoretical control system based on controls that can currently be found on the Belgian market. The ventilation flow rates (Q) are adapted on the one hand by a local detection and a local control in the wet areas. The bathroom is controlled on humidity, the kitchen on CO₂ and the toilet on VOC. Additionally, there

are also extra CO₂-sensors in the dry spaces that will increase the extraction flow rate in the wet spaces if the CO₂-concentration in the dry spaces becomes too high. For the increase of the extraction flow rate only the dry space with the maximum CO₂-concentration will be considered. The increase of extraction creates negative pressure in the building which force more fresh air through the trickle vents resulting in a larger supply of fresh air in the dry spaces.

The second DCV system (DCV2) is also a theoretical control system based on controls that can currently be found on the Belgian market. The ventilation flow rates (Q) are, just like DCV1, adapted by a local detection and local control in the wet spaces. Supplementary to these extraction in the wet spaces, there is an additional extraction in the dry spaces based on local CO₂-sensors. Due to the direct extraction in the dry spaces, the amount of supply through the trickle vents can be guaranteed. In addition, the extraction works in two zones, namely the bedrooms and the living space. The zone with the highest CO₂-concentration will be controlled based on this concentration and the flow rate of the other zone is lowered to the minimal flow rate. In that way, the zone with the highest occupation, receives the highest ventilation flow rate.

The working principles of both DCV systems is graphical represented in **Figure 2**. The nominal ventilation flow rates according to the NBN-D50-001 are represented for each zone in **Table 1**. Q_{nom} are the nominal flow rates for both systems and $Q_{nom, addition}$ are the nominal flow rates for the additional extraction in the dry spaces for DCV2. The zones are numbered like the floor plan in **Figure 1**. Lastly, the different sensors and their controls on the ventilation flow rates are represented in **Table 2**. The first four controls are for both DCV systems. The fifth and sixth control are respectively for DCV1 and DCV2.

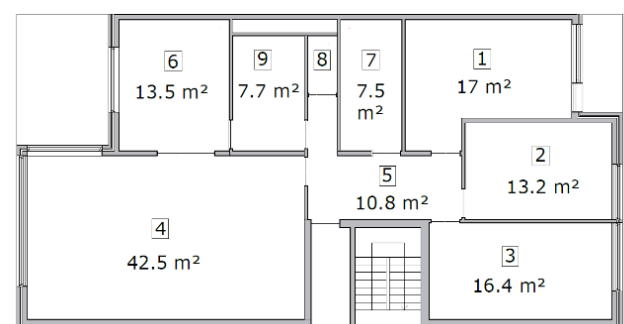


Figure 1. Floor plan of the reference apartment. Zone 1-4 are the dry spaces, zone 5-9 are the wet spaces.

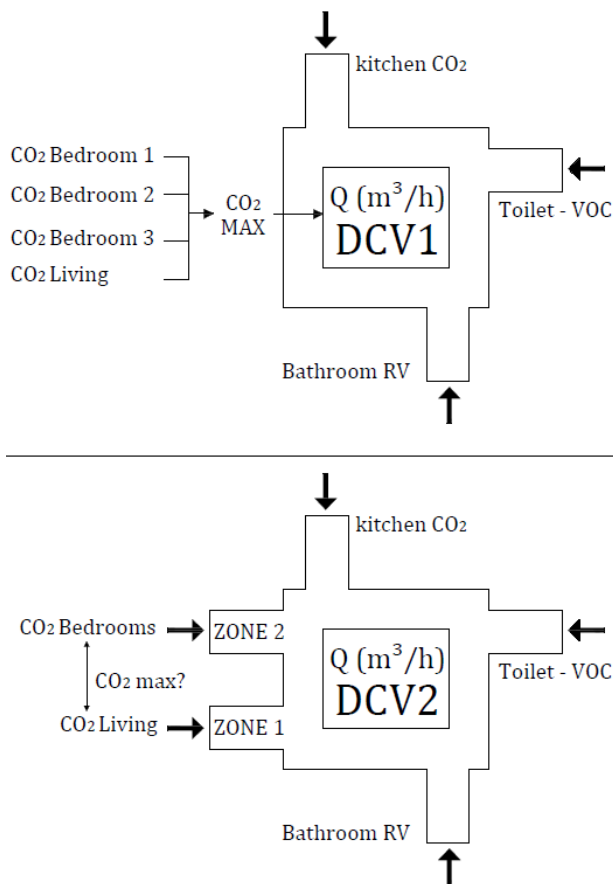


Figure 2. Graphical representation of the working principle of DCV1 and DCV2.

Table 1. Ventilation flow rates.

Zone	Q_{nom} (m ³ /h)	$Q_{nom_addition}$ DCV2 (m ³ /h)
1: Bedroom	43.92	25
2: Bedroom	35.26	25
3: Bedroom	38.88	25
4: Living room	108.32	60
5: Hall	16	-
6: Kitchen	60	-
7: Bathroom	60	-
8: Toilet	30	-
9: service room	60	-

2.3 Pollutants of concern and their emissions

More than 100 indoor pollutants are currently identified as (potentially) hazardous to our health. To obtain a priority list of target pollutants, 7 large studies are reviewed, each a conclusion of many other studies. The most important study is the AIVC-CR17 [5] study where, for Belgium, the concentrations of harmful pollutants were measured in more than 400 homes. As a result, 6 indoor pollutants and 3 outdoor pollutants are prioritized for the Belgian residential application, namely benzene, formaldehyde, naphthalene, limonene, toluene and particulate matter (PM_{2.5}) as indoor pollutants and (PM_{2.5}), nitrogen dioxide (NO₂) and ozone (O₃) as outdoor pollutants. The concentration of the outdoor pollutants will be modelled as constants. In the future, this can be further investigated.

To allow a clear representation of which emissions are implemented for each pollutant, the emissions will be divided into three categories, namely emissions from building materials and furniture, emissions from occupants and emissions from occupant activities.

Table 2. Controls.

Sensor	Control	Q (m ³ /h)
1. RV – Bathroom and service room	RV < 30%	10 %
	30% < RV < 65%	30 %
	65% < RV < 95%	60%
	RV > 95%	100%
2. RV – Bathroom	ΔRV > 2% in 5min	100%
3. CO ₂ (ppm) Kitchen	CO ₂ > 850	10%
	850 < CO ₂ < 950	Linear
	CO ₂ > 950	100%
4. VOC – Toilet	No presence	10%
	Presence	100%
5. CO ₂ (ppm) DCV1 Max. of dry spaces	CO ₂ < 1,000	10%
	1000 < CO ₂ < 1,200	Linear
	CO ₂ > 1,200	100%
6. CO ₂ (ppm) DCV2 Dry spaces extraction	Zone 1: zone with maximum CO ₂ -concentration. CO ₂ > 850 850 < CO ₂ < 950 CO ₂ > 950	10% Linear 100%
	Zone 2: zone with smaller CO ₂ -concentration	- 10%

A. Emissions from building materials and furniture

To determine the emissions of the building materials and furniture, it is assumed that the apartment is refurbished or newly built so that can be concluded that the floor and furniture are new. Therefore, all the emissions will be determined after a lifetime of 28 days. The furniture is calculated for an occupancy of two adults, two children and two babies. The furniture is considered wood, synthetic or gypsum. This means that only the pollutants benzene, formaldehyde, naphthalene and toluene are considered for these emissions. All the emissions of building materials and furniture are determined using the Pandora Database [6]. The summary of these emissions is given in **Table 3**. All these emissions are assumed to have a constant emission rate. One exception is made for the formaldehyde emission by the floor. The emission rate of the flooring is a dynamic source model based on the air temperature and relative humidity in the zone [7].

Table 3. Summary of the emissions from building materials and furniture for each pollutant.

Emission [ug/h/m ²]	formaldehyde	benzene	naphthalene	toluene
Floor (wood)	9.91	negligible	negligible	negligible
Furniture (wood)	3.06	1.40	5.68	-
Door (wood)	4.50	-	-	-
Other furniture (synthetic)	3.00	2.00	-	11.00
Carpet	4.27	0.21	0.47	0.20
Walls (gypsum)	negligible	negligible	negligible	0.50

Table 4. Summary of the emissions from building materials and furniture for each pollutant.

Emission [ug/h/m ²]	moisture	limonene	naphthalene	PM _{2.5}
Cleaning (3)	5.00 g/m ² (floor) [15]	1912 ug/h/m ² (floor) [6]	-	-
Cooking	0.60 L/s * 1.00 L/s * 1.50 L/s *	-	-	1260 ug/min [9] 1910 ug/min 2550 ug/min
Washing dishes	4.20 e-04 L/s	24.8 ug/h	-	-
Showering	0.50 L/s *	1200 ug/h [10]	3.76 ug/h [11]	-
Deodorant use	-	1438 ug/use [14]	-	12 ug/use [13]
Washing clothes	6.50 x e-2 L/s *	7833 ug/h [12]	-	-

* CEN 14788: Ventilation of buildings - Design and dimensioning of residential ventilation systems

B. Emissions from occupant activities

The impact of the occupant activities on the VOC concentrations is significant. To determine which activities must be implemented, the original occupant schedules, used in Belgian simulation studies for the determination of ventilation legislation [8], were reviewed. The original activities were cooking, showering and washing clothes and only the emission of moisture was recorded. Eventually, the activities were expanded with cleaning, washing dishes and using deodorant spray. The emissions of the activities, including the original activities, were expanded with limonene, naphthalene and particulate matter emissions. Existing research on emission values is very limited, which means that assumptions often must be made. When newer or more accurate research is published, the emission values can easily be adjusted in the model.

For cooking, PM_{2.5}-emissions were added based on the relationship to the moisture emission in the study of Poirier et al (2021) [9]. Extensive cooking results in a greater moisture and PM_{2.5}-production. Important is that the cooking emissions are considerably reduced by the implementation of a cooker hood with a flow rate of 200 m³/h and a capture efficiency of 0.7. This means that 70% of the emissions are captured by the cooker hood. For the activity of showering, the use of shampoo and shower gel was added, resulting in limonene [10] and naphthalene [11] emissions. For the activity of washing clothes, the use of washing liquid (wash pods of 27 gram) was added, resulting in limonene emissions [12]. For the use of deodorant, a PM_{2.5} [13] and limonene [14] emission was added to the occupant itself. The occupant uses the deodorant 3 times a day (0.5 gram) and carries these emissions around the house. Also, the emissions for the activity cleaning, were added to the occupant itself. When the occupant is cleaning, moisture [15] and limonene [6] emissions are released into the air where the occupant is situated.

All these emissions are summarized in **Table 4**. The references are given in the text and in the table. For a more in-depth explanation on how the emissions are obtained, reference is made to “Health-based assessment method for residential DCV systems” by Janneke Ghijsels (2022).

C. Emissions from occupants

Occupants produce both CO₂, H₂O and human odour. The CO₂- and H₂O-emissions are shown in **Table 5** for a metabolism (the degree of activity) equal to 1.6 met (very active). In the simulation these productions are scaled according to the metabolism of each occupant at each timestep.

2.4. Assessment method

To make a complete analysis of the impact of a DCV system on IAQ, the assessment method will be divided into two stages. The first stage is a **health performance checklist** that will rule out the possibility that the exposure concentrations cause harmful health effects for the occupants. If this criterion is not met, the controls can be adapted (e.g. increasing the nominal flow rates, increasing the minimal flow rates or adjusting the boundaries.)

When the quality of the indoor air is sufficient for the health of the occupants, the DCV system can be analysed by the second stage of this assessment method, namely the **overall performance rating** in terms of health and energy. A comparison will be made with the performance of the MEV reference system. In this way, a pareto optimum can be explored for each DCV system in which both the energy and health performance are better than the performance of the MEV reference system.

A. Health performance checklist

For the assessment of the health performance, a checklist will be followed in which first the exposure concentrations of each pollutant will be compared with the limit concentrations of the chosen exposure metrics. Both acute and chronic exposure concentrations will be checked to exclude both acute and chronic health effects.

The peak concentrations will be checked by the 10-minute AEGL-1 value (obtained by U.S. EPA) [18] and the average exposure concentrations over a time interval of 1 hour and 8 hours will be checked by the acute REL values (obtained by OEHHA) [19]. The chronic exposure concentrations will be checked by the chronic REL value. The summary of these limit concentrations is given in **Table 6**.

Table 5. Emissions by occupants themselves.

Production	1.6 met (light activity)
CO ₂ -production	
- Adult	19.0 l/h *
- Child	12.6 l/h [16]
- Baby	6.7 l/h *
H ₂ O-production	
- Adult	55.0 g/h *
- Child	41.3 g/h [17]
- Baby	18.3 g/h *

* Norm CEN 14788

After the control of the exposure concentrations, the lifetime average daily dose (LADD) is calculated for each pollutant [20]. The formula of the LADD is given in equation (1). Because the LADD considers both body weight and inhalation rate it is possible to obtain an estimation of the health effects for sensitive occupants, for example babies.

Babies will have a higher lifetime average daily dose than an adult, even though the exposure concentrations of the pollutants are the same.

$$LADD = \frac{E_i \times IR \times E_f \times E_d}{BW \times A_t} \times \epsilon \quad (1)$$

Where E_i is the timeweighted exposure (ug/m³), IR is the inhalation rate (m³/day) [21], E_f is the exposure frequency (day/year), E_d is the exposure duration (day), BW is the bodyweight (kg) where in this study 70 kg is used for adults, 23 kg for children and 11 kg for babies. A_t is the simulation time, in this study 365 days and ϵ is the absorption factor of each pollutant (for example 0.9 for formaldehyde).

The use of LADD makes it possible to exclude non-carcinogenic health effects by calculating the hazard quotient (HQ), given in equation (2). The LADD is compared by the reference doses (RfD) (obtained by U.S. EPA) [22]. When HQ is less than 1, the risk of non-carcinogenic health effects is considered negligible.

$$HQ = \frac{LADD}{RfD} < 1 \quad \text{Health effects are negligible} \quad (2)$$

Table 6. Emissions by occupants themselves.

Reference $C_{exposure}$ (ug/m ³)	10 min AEGL-1	Acute REL-1h	Acute REL-8h	Chronic REL
Benzene	415,000	27	3	3
Formaldehyde	1105	55	9	9
Naphthalene	-	-	9	9
Limonene	-	-	-	9000
Toluene	252,000	-	800	400
PM_{2.5}	-	-	25 (24h) *	10*

* WHO guidelines: air quality guidelines for particulate matter, ozone, nitrogen dioxide and sulphur dioxide: summary of risk assessment

B. Overall performance rating

If the DCV system passes the health performance checklist, it is evaluated by the second part of this assessment method. In this assessment method, the DALY-index (Disabled Adjusted Life Years) is used as health indicator. It quantifies the total years lost due to death or disability due to poor IAQ. It scales the harmfulness of the different VOC and PM_{2.5}-concentrations to allow a general health rating. The total DALYs are calculated based on the study of Logue et al. (2012) [23]. The DALYs of the outdoor pollutants (i.e. PM_{2.5}, NO₂ and O₃) are calculated using the IND-method. The DALYs of the indoor pollutants (i.e. benzene, formaldehyde, naphthalene, limonene and toluene) are calculated using the ID-method where the study of Huijbrechts et al. (2005) [24] provides the information on the (∂D/∂I)-factors.

When the total DALYs are calculated for each DCV system, this health indicator can be compared with the energy use of each DCV system. In that way it is possible to rate the overall performance of the DCV system. The performance of a DCV system is considered sufficient when there is a pareto optimum compared to the continuous MEV reference system. This means that both the energy use and the health impact of the DCV system must be lower than those of the reference system.

3. Results – Assessment method

Each DCV system and their controls are modelled in the Modelica model together with the different emissions and the activity schedules of the occupants. For each ventilation system 10 different families are simulated. The results are average exposure concentration of these 10 scenarios.

3.1 Health performance checklist

In this paper, the focus will be on one constant emission source (i.e. formaldehyde) and on one emission source that depends on the activities of the occupants (i.e. PM_{2.5}), because these two pollutants show to have the highest impact on our health. In **Figure 2** the exposure concentration of formaldehyde is compared for the two DCV systems and the MEV reference system. The acute concentration limit of 55 ug/m³ is not exceeded by any system. The chronic concentration limit of 9 ug/m³ is exceeded by the two DCV systems. DCV1 has a chronic exposure concentration of 11 ug/m³, while DCV2 has a much larger chronic exposure concentration of 18.8 ug/m³.

Figure 3 shows the exposure concentration of PM_{2.5} for the three systems. The acute exposure concentration is compared with the 24 hours limit concentration

of the WHO and is only exceeded by DCV2. The chronic exposure concentration is exceeded by all the ventilation systems. This is a result of a constant outside PM_{2.5}-concentration of 14 ug/m³ (according to MIRA 2019) [26]. In the future, it can be important to change the approach of the outside pollutants to more variable concentrations according to the environment (e.g. temperature) and the location (e.g. nearby industry, heavy traffic).

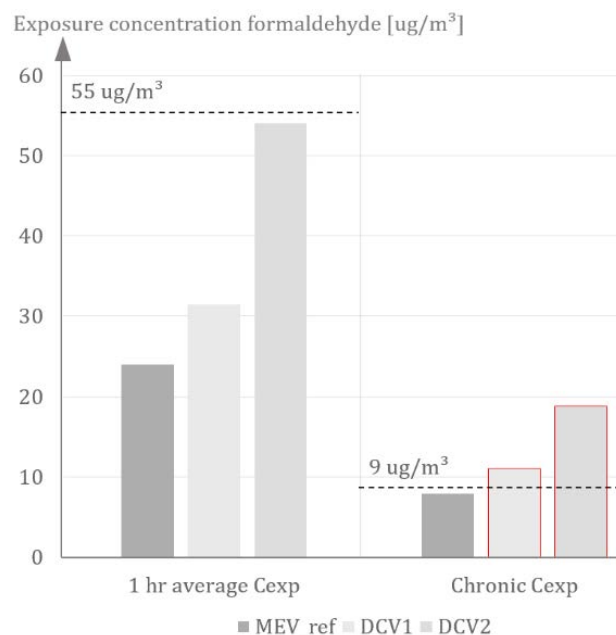


Figure 2. Comparison of the exposure concentration of formaldehyde between DCV1, DCV2 and MEV_ref.

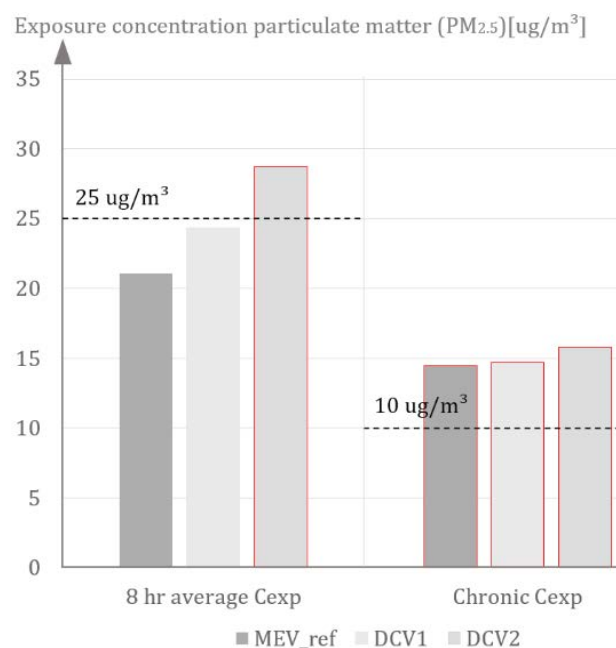


Figure 3. Comparison of the exposure concentration of PM_{2.5} between DCV1, DCV2 and MEV_ref.

In **Table 7** all the concentrations of the pollutants of concern are summarized. DCV2 scores too high for formaldehyde and PM_{2.5}. DCV2 has also higher exposure concentrations for all the other pollutants than DCV1.

To ensure that the IAQ, caused by system DCV2 does not cause any health effects on the sensitive occupants, the LADD is calculated. Subsequently the HQ of each pollutant is calculated by comparing the LADD to the reference dose (obtained by U.S. EPA). An example is worked out for benzene. In **Table 8** the average LADD of benzene of the 10 scenarios simulations is calculated for each occupant in the simulation. For DCV2, the LADD of benzene is higher than the reference dose (8.57×10^{-3} mg/ kg/day) for both the smaller children. Therefore, DCV2 will not ensure a good IAQ for the sensitive occupants.

It is necessary to adjust DCV2 to meet the minimum requirements of the health performance checklist. A new simulation is carried out where the minimum flow rates are increased from 10% to 30% of the nominal

flow rates. This adaptation changes the LADD of benzene for occupant 5 (Baby 1) from 0.01062 to 0.00784 mg/ kg/day and for occupant 6 (Baby 2) from 0.00915 to 0.00676 mg/ kg/day. All the average daily doses are now below the reference doses. Hence, it can be said that no important negative health effects will occur due to a poor IAQ. In the next paragraph, it is examined whether there is a pareto optimum between the two DCV systems, incl. the new DCV2 system and the MEV-reference system. The overall performance of the DCV systems, both in terms of energy and health, should perform better than the overall performance of the MEV reference system.

Table 8. Summary of all LADD of benzene for each occupant in the simulation for MEV_ref and the two DCV systems.

LADD Benzene	Adult 1	Adult 2	Child 1	Child 2	Baby 1	Baby 2
MEV_ref	0.00203	0.00254	0.00198	0.00195	0.00423	0.00400
DCV1	0.00278	0.00350	0.00264	0.00260	0.00564	0.00538
DCV2	0.00483	0.00599	0.00452	0.00408	0.01062	0.00915

Table 7. Summary of all the acute and chronic exposure concentrations of the pollutants of concern for DCV1, DCV2 and MEV_ref.

	Maximum C _{exp}	1 hour average C _{exp}	8 hour average C _{exp}	Chronic C _{exp}
MEV_ref				
Formaldehyde	21,94	24,03	19,15	7,92
Benzene	1,66	1,55	1,22	0,66
Limonene	565,41	581,52	-	12,56
Naphthalene	5,24	-	3,78	1,83
Toluene	11,15	11,12	8,64	5,55
PM _{2.5}	187,61	-	21,08	14,46
DCV1				
Formaldehyde	35,72	31,43	24,76	11,02
Benzene	2,77	2,27	1,65	0,87
Limonene	694,99	651,46	-	15,97
Naphthalene	8,69	-	5,13	2,42
Toluene	18,87	18,07	12,55	7,50
PM _{2.5}	215,70	-	24,35	14,70
DCV2				
Formaldehyde	73,01	54,07	42,75	18,84
Benzene	4,51	3,91	2,57	1,37
Limonene	856,91	736,12	-	22,12
Naphthalene	14,77	-	7,90	3,81
Toluene	35,87	34,80	25,80	12,16
PM _{2.5}	229,66	-	28,75	15,79

3.2 Overall performance rating

The total DALYs per 100,000 persons per year are calculated for each pollutant using the IND and ID method. The results are given in **Figure 4**. It becomes clear that the total DALYs are for more than 80% caused by PM_{2.5}. The second major pollutant is formaldehyde. All the other VOCs seem to have a very small impact and are therefore less harmful for our health. DCV1 has the smallest total number of DALYs. Even smaller than the reference system. This is caused by the smaller influence of the outdoor pollutants in periods of less ventilation. DCV2 has the largest total number of DALYs. This is caused by the higher formaldehyde concentrations and the higher PM_{2.5}-concentration in the kitchen during cooking periods.

The new DCV2 system, where the minimum flow are adapted to 30% of the nominal flow rates (instead of 10%) reduces the total number of DALYs from 41.1 to 32.8 DALYs per 100,000 persons per year. This is a reduction of more than 20% (8.3 DALY).

Now that the total DALYs are known, it is possible to generate an overall performance rating of the DCV systems. In **Figure 5** the total number of DALYs are compared with the energy use (electricity use of the fans and ventilation heat losses) of the ventilation system. To create a pareto optimum it is necessary that the DCV systems perform better in terms of health and energy. This means that the DCV systems must be located in the green frame shown in **Figure 5**. The system that is situated on the bottom, left, is the system that generate the best pareto optimum. At first, system DCV2 had a very low energy use. After the adaptation, the IAQ is improved with 20% (8.3 DALY) and the energy use increased with 35% (1,040 kWh/year). This increase in energy use seems very high, but the total energy use is still 40% (1,845kWh/year) lower than the energy use of the reference system with continuous flow rates. The overall performance of the new DCV2 is even better than the overall performance of DCV1. It is stated that with correct adaptations, it is possible to find a pareto optimum for each DCV system.

4. Discussion and conclusion

In this research, a very extensive emission model was combined with a dynamic temperature and occupancy model in the Dymola software. This allows an assessment of IAQ at every timestep for the different occupants with different ages, habits and metabolisms. Based on the determination of the exposure concentration at each time step and for each occupant, both

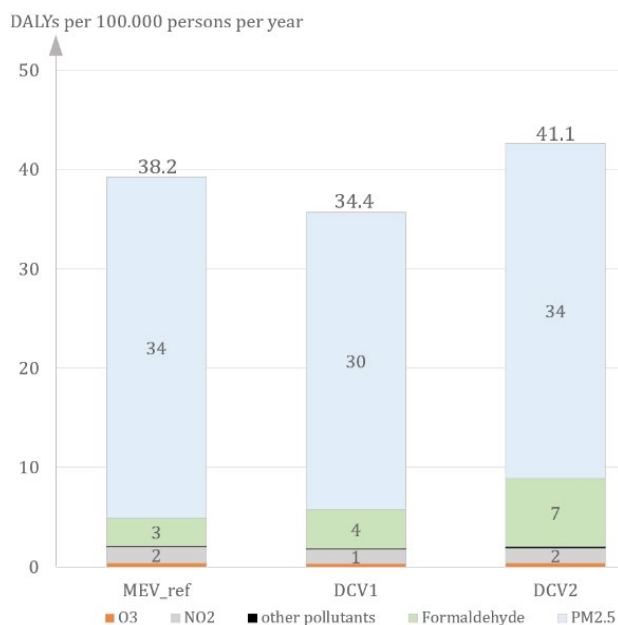


Figure 4. The share of each pollutant in the total number of DALYs (the health indicator in this research) per 100,000 persons per year compared for the two original DCV systems and the MEV reference system.

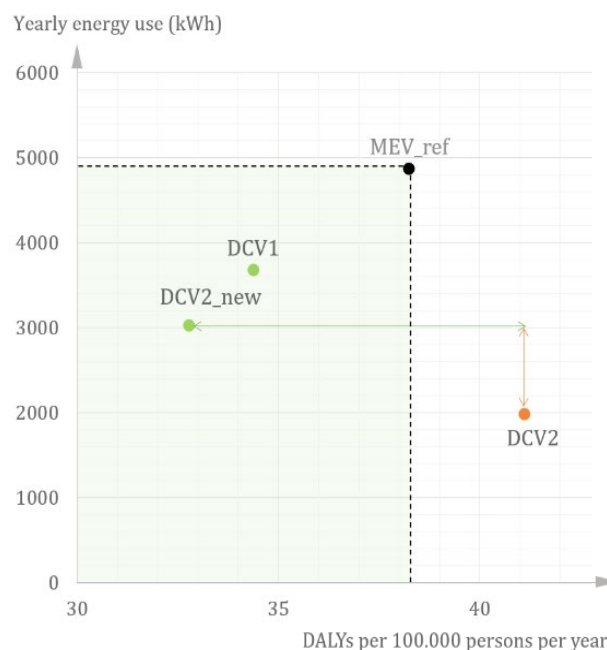


Figure 5. The overall performance of a DCV system in terms of energy and health compared to the MEV reference system. The overall performance of a DCV system is sufficient if there is a pareto optimum compared to the MEV reference system. DCV2_new scores best on the overall performance.

the average daily dose (LADD) and the intake can be calculated. These two parameters are both very important in the assessment method that was developed to determine whether a system ensures a good indoor air quality. The necessity for such an assessment method is high since the DCV systems are nowadays only assessed on comfort criteria such as CO₂, humidity and odour. Because the danger lies in the increased VOC concentrations in times of less ventilation, it is necessary that a DCV system, designed to ensure an energy saving, also ensures a sufficiently IAQ in terms of health.

The health and energy assessment method was designed as a two-stage assessment method in which first the exposure concentrations are checked on health risks for the occupants. The peak concentrations, acute concentrations and chronic concentrations are compared with the corresponding limit concentration from relevant exposure metrics. In this paper, the limit concentrations of the reference exposure levels [19] were used. It is possible to use other limit concentrations of exposure metrics that are for example drawn up in function of a legislation in the country where the research is being conducted.

The second stage of the assessment method is an overall performance rating where one health indicator, the total DALYs, is used as general health indicator of the system. The total DALYs scales the harmfulness of exposure to the different pollutants. In that way, the health performance of a system that ventilates more in the kitchen and induces lower PM_{2.5}-concentrations, can be compared to the health performance of a system that ventilates more in the living rooms and induces lower formaldehyde concentrations. The total DALYs

for each system are compared with the energy use of each system, resulting in an overall performance of the DCV system in comparison to the MEV reference system.

The conclusion of the two DCV systems is that, if there is minimum air flow rate of 10%, DCV1 ensures a better indoor air quality. This means that increasing the extraction flow rate by using CO₂-sensors in the dry spaces, works sufficient. The disadvantage is that DCV1 only ensures an energy reduction of around 25% (1,200 kWh/year) in comparison to the continuous MEV system, which is rather low. When the minimal flow rates of DCV2 are increased to 30%, it guarantees a better IAQ and a higher energy reduction than DCV1. That's why the adaption of a DCV system that initially guarantees a high energy reduction but a low IAQ, ensures mostly an improvement to the health/energy contradiction. In comparison to the continuous MEV system, the energy reduction of DCV2_new is around 40% (1,845 kWh/year) and the improvement of IAQ is around 15% (5.5 DALY).

The investigated cases show that DCV systems can be an effective measure to save energy and provide a healthier indoor air. Both systems, DCV1 and DCV2_new, guarantee a pareto optimum in comparison to the continuous reference system. It is stated that for every DCV system, an optimisation can be found where the health/energy contradiction disappears. ■

References

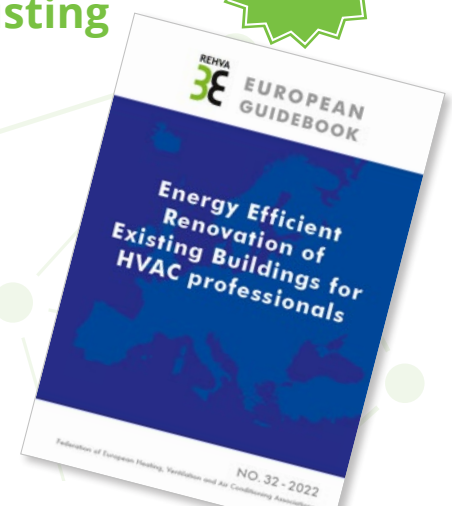
Please find the full list of references in the original article at: <https://proceedings.open.tudelft.nl/clima2022/article/view/155>

REHVA EUROPEAN GUIDEBOOKS Energy Efficient Renovation of Existing Buildings for HVAC professionals

No.32

Energy Efficient Renovation of Existing Buildings for HVAC professionals.

This REHVA Guidebook shows the baseline for specific energy efficiency and other renovation measures in existing buildings for which the HVAC systems play an important role. It presents the best available techniques and solutions that can be used as part of the energy modernization of the HVAC systems.



REHVA  40 RUE WASHINGTON 1050 BRUSSELS, BELGIUM
 +32-2-5141171  INFO@REHVA.EU  WWW.REHVA.EU

Low-temperature radiant cooling panel for hot and humid climate



GONGSHENG HUANG

Department of Architecture and Civil Engineering, City University of Hong Kong, Kowloon, Hong Kong
gongsheng.huang@cityu.edu.hk



NAN ZHANG

Department of Architecture and Civil Engineering, City University of Hong Kong, Kowloon, Hong Kong



YUYING LIANG

Department of Architecture and Civil Engineering, City University of Hong Kong, Kowloon, Hong Kong

Abstract: In this paper, the heat transfer and thermal environment of air-layer integrated radiant cooling panel (AiCRCP) was studied experimentally. AiCRCP was proposed in 1963, which was characterized by the use of an infrared-radiation transparent (IRT) membrane to separate the panel's radiant cooling surface from its external air-contact surface. Therefore, the panel's radiant cooling surface temperature can be reduced to increase the cooling capacity, while its external air-contact surface, due to the thermal resistance provided by the air layer and the IRT membrane, can be easily maintained at a high temperature to reduce condensation risks. The thermal performance of AiCRCP was investigated using a prototype. Several scenarios were tested to analyse the thermal performance of prototype, and the cooling capacity of the AiCRCP was also investigated according to the thermal performance of the prototype. The results demonstrated that this new type of radiant cooling systems could be more preferable to be implemented in hot and humid climates.

Keywords: Radiant cooling, air-layer integrated ceiling radiant cooling panel, IRT membrane, condensation, cooling capacity

1. Introduction

Radiant cooling has many benefits, such as its high thermal comfort, lower energy use, quiet operation, and smaller equipment footprint, compared with the methods of cooling air of indoor spaces through air circulation [1]. However, radiant cooling applications face great challenges in hot and humid climates from condensation and their limited cooling capacity [2]. In its cooling mechanisms, whether through panel cooling or slab cooling, the radiant surface is also the air-contact surface, as shown in **Figure 1(a)**, where a conventional ceiling radiant-cooling panel (CRCP) is used. In this CRCP, the cooling capacity increases with the decrease of the radiant-cooling surface temperature, but this will increase the risk of condensation. This dilemma has inhibited the commercialization of radiant cooling in hot and humid climates [3], and explains why CRCPs should be used together with

other air-cooling systems in practical applications to provide enough cooling for thermal comfort.

Many attempts have therefore been made to solve the condensation problem while increasing the cooling capacity [4]. A typical method is to maintain a low relative humidity so low radiant temperature can be used [5], but this dehumidification is costly and risks degrading the thermal comfort. By realizing that the radiant surface must be isolated from the air-contact surface to essentially solving this dilemma, Morse proposed a radiant-cooling panel covered with a sheet spaced several centimetres from it, filled with dry air, and sealed to prevent room air from contacting the cold radiant-cooling surface [6], referred to as an *air-layer-integrated radiant-cooling panel* (AiCRCP) and illustrated in **Figure 1(b)**. Thus, the air-contact surface and radiant cooling surface in the AiCRCP are physically separated.

It should be noted that the cover sheet must be transparent to the energy radiated from a body at a temperature range of 29.4°C to 35°C, and thus titled as infrared transparent (IRT) membrane. It enables the panel to act as a radiation heat sink, and heat from occupants in the vicinity can radiate through the transparent cover to the cold plate behind. Teitelbaum et al. [7] revisited this design, investigating several manufactured materials, such as low/high density polyethylene and polypropylene, using Fourier transform infrared (FTIR) spectroscopy to analyse its thermal performance. They also investigated the panel depth (spacing between the radiant-cooling panel and the membrane) to balance radiation, conduction, and convection when AiRCPs was applied to an outdoor environment.

In our research group, Zhang et al. established a two-flux heat transfer model for the AiCRCP, to analyse the optical, physical and thermal properties of the IR-transparent membrane [8]. Liang et al. investigated the thermal environment and thermal comfort created by an AiCRCP using CFD simulations, and they demonstrated that general thermal comfort indices could be satisfied even when the AiCRCP operated at a very low radiant temperature (e.g. -2.3°C) [9].

Previous literature has demonstrated that the enhanced cooling capacity and reduced condensation risk of AiCRCPs in addition to the thermal comfort they can

maintain give them potential applications in hot and humid climates. However, most of the work reviewed above was based on simulation or numerical studies. In this paper, the cooling performance of an AiCRCP prototype and the thermal environment created by the AiCRCP were investigated using experiments, which showed that the AiCRCP could provide higher cooling capacity and better condensation prevention.

2. Theoretical background

The heat transfer process of the AiCRCP is shown in **Figure 1(b)**, where the heat exchange between the AiCRCP and its thermal environment is mainly through two mechanisms. One is radiation that occurs directly between the AiCRCP and its thermal environment; and other is the combination of convection and conduction.

In the first mechanism, since the IRT membrane is assumed to have a poor ability to absorb infrared radiative heat flux and the air-layer is transparent to infrared radiation, the radiative cooling power of the radiant cooling surface will not be much affected by the IRT membrane. In the second mechanism, heat is firstly transferred to the IRT membrane from the air surrounding the AiCRCP through convection, and to the radiant cooling surface through the dry air convection (major) and conduction (minor). It should be noted that the IRT membrane is thin, its internal surface and external surface temperature could be consider as the same in the analysis of the thermal performance of AiCRCP.

Because the air layer has a large thermal resistance to both convection and conduction as shown in the previous work [8], the IRT membrane can be maintained at a high temperature even if the radiant cooling temperature is low, for example 5°C (much lower than 17°C used in conventional CRCPs). Therefore, a low radiant cooling temperature can be used to enhance the cooling capacity of the AiCRCP without increasing the condensation risk.

3. Experiment setup

3.1 Prototype of AiCRCP

Currently there is one prototype of AiCRCP in our laboratory with the dimension of 1 m × 1 m. This prototype uses a piece of aluminium plate: on one side high emissivity paint ($\epsilon \approx 0.95$) was coated and used as cooling radiant surface, and on another side heat transfer fluid (HTF) pipes were attached and fixed using screws.

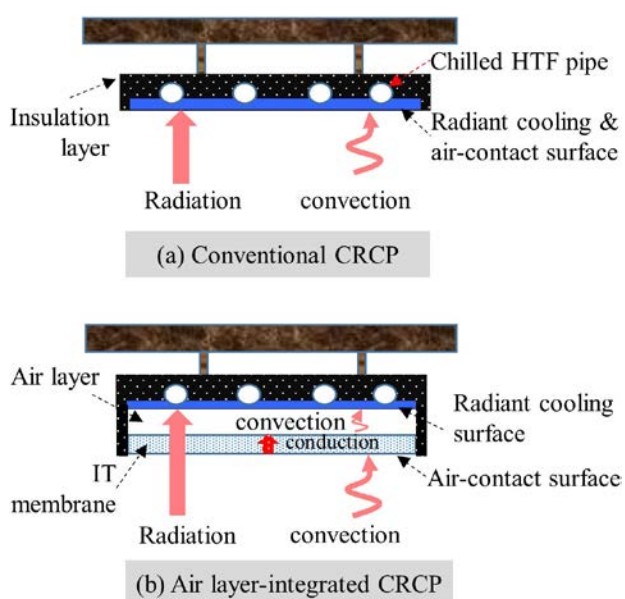
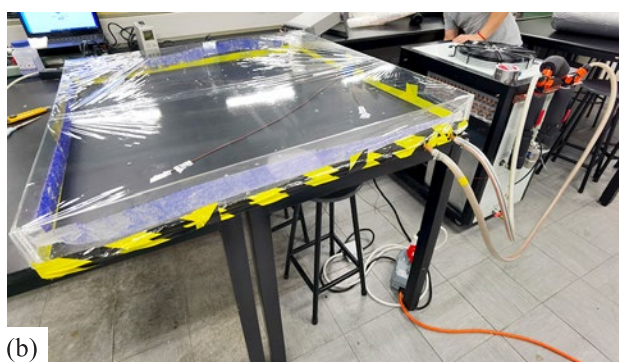


Figure 1. Diagrams of (a) the conventional radiant cooling unit, (b) the air-integrated CRCP.



(a)



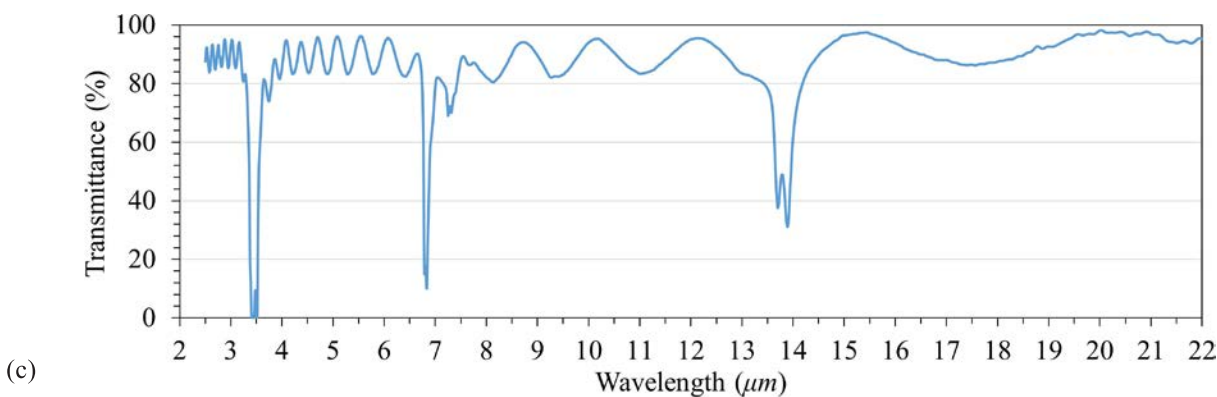
(b)

Thermal paste was used to increase the thermal conductivity between the HTF pipe and the aluminium plate, shown in the photo of **Figure 2(a)**. This side was covered with a insulation layer (Nitrile rubber) to prevent cooling loss. A photo of the prototype is given in **Figure 2(b)**. The prototype was connected with an air-cooled chiller that can provide heat transfer fluid with the temperature from -10°C to 20°C with the rated cooling capacity of 5.67 kW and coefficient of performance (COP) of 3.86. A 20 μm thick low-density *Polyethylene* (LDPE) was used as the IR-transparent membrane to seal a dry-air layer to separate the air-contact and radiant-cooling surfaces. The membrane has a good IR transparency property as shown in **Figure 2(c)**, where the spectral transmittance was measured using FTIR (Spectrum Two, PerkinElmer).

3.2 Thermal chamber and measurements

The thermal chamber is placed on a movable structure as shown in the photo of **Figure 3(a)**. **Figure 3(b)** shows the internal view of the chamber.

A number of sensors/flow meters were installed to measure the temperature, flow and humidity. The measured qualities, number of sensors and sensor uncertainty were summarized in **Table 1**.



(c)

Figure 2. (a) The radiant cooling panel covered by an insulation layer; (b) LDPE membrane covering the panel and sealing a dry air layer; (c) IR spectral transmittance through LDPE membrane using FTIR.

Table 1. Measured quantities, number and uncertainty of sensors.

Measured Quantity	Sensor	Number	Uncertainty
HTF Fluid temperature	T-type Thermocouple	2	$\pm 0.5^{\circ}\text{C}$
Surface temperature	T-type Thermocouple	18	$\pm 0.5^{\circ}\text{C}$
Dry bulb air temperature	Swema 03+	1	$\pm 0.1^{\circ}\text{C}$
Indoor air velocity	Swema 03+	1	$\pm 0.04\text{m/s}$
Relative humidity	Swema HC2A-S	1	$\pm 0.8\%\text{RH}$
Globe temperature	Swema 05	1	$\pm 0.1^{\circ}\text{C}$
HTF flow rate	Turbine pulse flowmeter	2	$\pm 0.5\%$
Infrared temperature	FLIR infrared camera	1	$\pm 4\%$

4. Experimental results and analysis

4.1 Testing scenarios

During the experiment, the thermal chamber was moved into a conditioned large hall, where the space temperature and humidity was maintained to be relatively stable. Inside

the thermal chamber, the cooling panel was installed horizontally on the ceiling, facing downward and working as ceiling cooling. In the test, the controlled variables were the indoor air temperature inside the thermal chamber and the radiant cooling temperature of the AiCRCP.



Figure 3. (a) an external view of the thermal chamber and (b) an internal view of the chamber.

There were three testing scenarios, defined according to the total power of the heaters. In scenario 1, the total power of the heater was the highest; while it was the lowest in scenario 2. In each scenario, the HTF supply temperature was varied in the range of $-5-15^{\circ}\text{C}$, and the cooling panel radiant surface temperature had a gradient change between 1°C and 19°C . The RH of the indoor air temperature was controlled at 3 levels, i.e. 70%, 60% and 50%. When any variable was changed, the temperatures were measured 20 min after stability. No mechanical ventilation was used during the experiment.

4.2 Temperature of the IRT membrane

The temperature of the IRT membrane surface (toward indoor air side) is an important variable that indicates the capability of the AiCRCP for condensation prevention. Please note that it is required at least 1°C higher than the dew point of indoor air to avoid condensation risk [1]. The average temperature of the IRT membrane under different radiant cooling panel temperature and different indoor air temperature and humidity were measured.

When RH was maintained at 70%, the cooling panel temperature should be higher than 13.5°C , 8.5°C and 3°C when the indoor air temperature was 28.9°C , 25°C and 19.4°C , respectively. However, when RH=60%, the cooling panel temperature should be higher than 6°C when the environmental temperature was 29°C . When the indoor air was lower than 25°C , the condensation would not occur on the membrane even if the cooling surface temperature was reduced to below 2°C . When RH=50%, the results showed that no condensation occurred on the membrane in these three different indoor air temperatures even the cooling panel temperature was reduced to 1°C .

To further analyse the capability of the condensation prevention of the AiCRCP, the minimum allowable cooling panel temperature allowed was defined, which was the minimal temperature of the panel that can guarantee the IRT membrane temperature being 1°C higher than the dew point of the indoor air. The differences between the minimum allowable cooling panel temperature of the AiCRCP and the conventional ceiling radiant cooling panel were shown in **Figure 4** when RH=70% and RH=60%. When RH=70% the minimum allowable temperature of the AiCRCP was around 10.8°C lower than the conventional CRCP; and when RH=60%, the value was about 15°C . Therefore, the AiCRCP has a good performance in preventing condensation in hot and humid climates with lower radiant temperature.

5. Cooling capacity of the AiCRCP

The cooling capacity of an AiCRCP depends on the thermal environment that is conditioned by the AiCRCP. Here we considered a room with the dimensions of $4\text{ m} \times 4\text{ m} \times 3\text{ m}$. We assumed that the whole ceiling was used as AiCRCP. The walls and floors had the emissivity of 0.9. Referring to the **Figure 2(d)**, the IRT transmittance of the membrane was assumed to be 80%. The temperature of the room air and the wall/floor surfaces were assumed to be 26°C .

The cooling capacity was the sum of radiative and convective heat fluxes. The cooling capacity of the AiCRCP was compared with that of the conventional CRCP in **Figure 5**. When the RH was 70%, 60%, and 50%, the dew point temperatures of the room air were 20.12°C , 17.66°C and 14.81°C , respectively. Therefore, the cooling panel temperature of the conventional CRCP were set as 21°C , 19°C and 16°C (approximated 1°C above the dew point). To maintain the IRT membrane temperature at 21°C , 19°C and 16°C , the minimum allowable cooling panel temperatures of the AiCRCP were 13°C , 8°C and 2°C respectively.

Figure 5(a) showed the comparison when RH was 70%. The cooling capacity of the conventional CRCP was 40 W/m^2 using a radiant temperature of 21°C . 7.5% cooling capacity enhancement was achieved by the AiCRCP when its radiant cooling temperature was 17°C . Since the minimum allowable cooling panel temperature of the AiCRCP could be down to 13°C , the maximum cooling capacity of AiCRCP reached 63.63 W/m^2 , improved by 59.1%.

Figure 5(b) showed the comparison when RH was 60%. At this condition, the cooling capacity of the

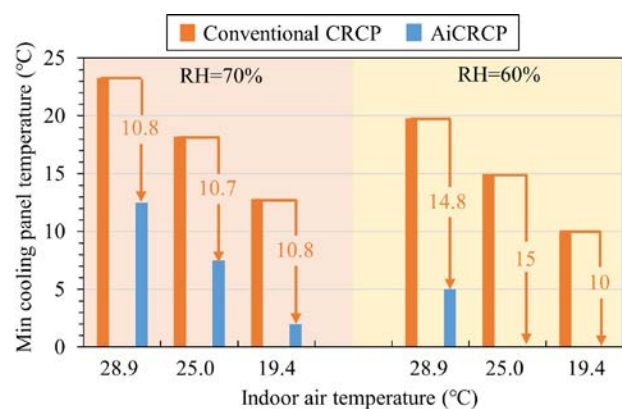


Figure 4. The minimum allowable cooling panel temperature of the AiCRCP and the conventional CRCP.

conventional CRCP was 59 W/m² using a radiant temperature of 19°C. Similar cooling capacity was achieved by the AiCRCP when its radiant cooling temperature was 14°C. Since the minimum allowable cooling panel temperature of the AiCRCP could be down to 8°C, the maximum cooling capacity of AiCRCP was improved by 52.2%, reaching 90 W/m².

The comparison when RH was 50% was shown in **Figure 5(c)**, where the cooling capacity of the conventional CRCP was 89 W/m² using a radiant temperature

of 16°C. When the radiant cooling temperature of the AiCRCP was 8°C, 2.2% cooling capacity improvement was achieved. Similarly, when we considered the minimum allowable cooling panel temperature of the AiCRCP that could be down to 2°C, the maximum cooling capacity of AiCRCP reached 121 W/m², improved by 35.9%.

Figure 5 also showed that due to a higher air contact surface temperature and a lower radiant surface temperature, the radiative heat flux of the AiCRCP was increased, while the convective flux was decreased when compared to the conventional CRCP. The enhanced radiative heat flux will benefit the heat exchange directly between heating sources (such as occupants) and the cooling panel.

6. Concluding remarks

This paper investigated the thermal performance of a prototype of AiCRCP experimentally and then analysed its cooling capacity of AiCRCP in a simple room environment based on the thermal performance of the AiCRCP prototype. The results have shown that

- The AiCRCP has much enhanced capacity to prevent condensation even in hot and humid climates. Due to a large thermal resistance from the sealed air layer, the IRT membrane can be maintained at a high temperature even when the radiant temperature is controlled to a very low temperature.
- Due the possibility of using a low temperature, the cooling capacity of the AiCRCP can be enhanced significantly. At a higher humid environment, for example RH = 70%, the cooling capacity can be improved around 60%.

Thus, the thermal performance of the AiCRCP could make it more preferable when the technique of ceiling radiant cooling is adopted in hot and humid climates. ■

7. Acknowledgement

The research work presented in this paper was supported by a grant from the Research Grants Council of the Hong Kong Special Administrative Region, China (Project No. 11212919).

8. References

Please find the full list of references in the original article at: <https://proceedings.open.tudelft.nl/clima2022/article/view/395>

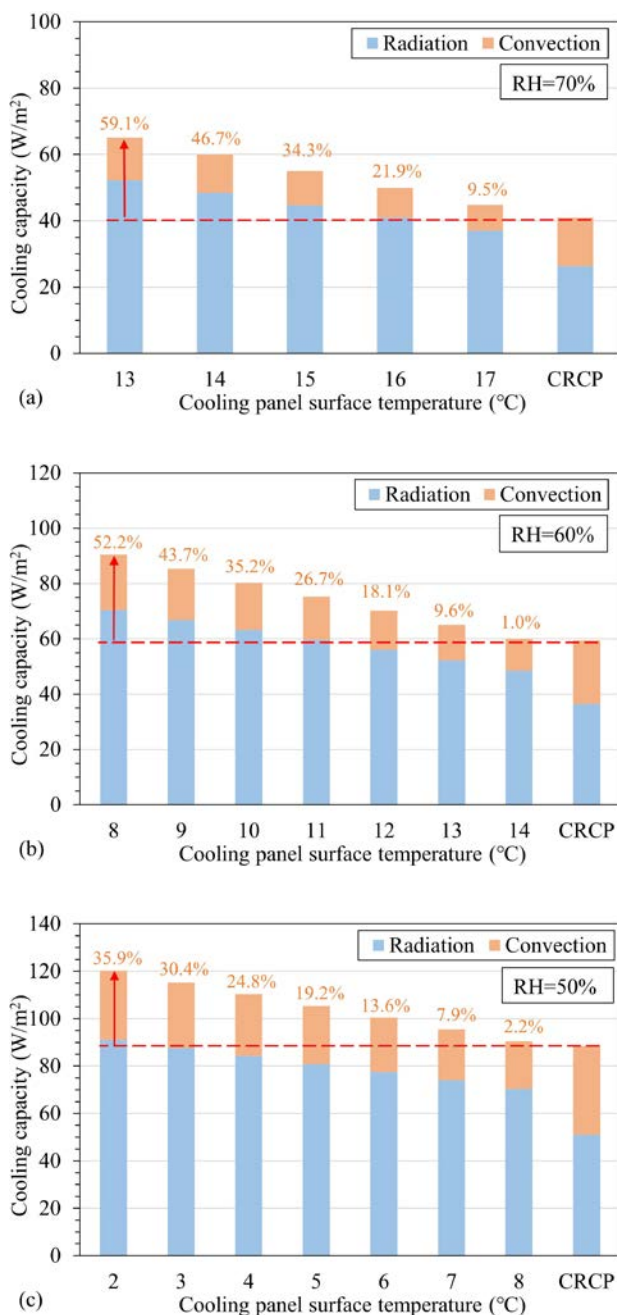


Figure 5. The cooling capacity of the AiCRCP and conventional CRCP.

Impact of future climate on the performances of ground-source cooling system



ABANTIKA SENGUPTA

PhD student, Faculty of Engineering Technology, KU Leuven, Belgium
abantika.sengupta@kuleuven.be



PIETER PROOT

Master Thesis student, Faculty of Engineering Technology, KU Leuven, Belgium



TOM TRIOEN

Master Thesis student, Faculty of Engineering Technology, KU Leuven, Belgium



HILDE BRESCH

Associate Professor, Faculty of Engineering Technology, KU Leuven, Belgium



MARIJKE STEEMAN

Associate Professor, Department of Architecture and Urban Planning, Ghent University, Belgium

Abstract: Newly constructed and renovated dwellings in Belgium are designed for the current climate context. However, due to the effects of global warming, extreme weather conditions like warmer summers and frequent heatwaves are expected in future climate scenarios. Future climate scenarios are nowadays mostly not taken into consideration during the building design process. This paper studies a case study dwelling equipped with a ground-water heat pump coupled with a heat exchanger to provide passive floor cooling, derived from two vertical boreholes with a depth of 100 meters. The aim of this study is the impact of future climate scenario on the thermal comfort and the performance of radiant floor cooling system in a Belgian dwelling. Monitoring of the case study building (April-October 2020) and Building Energy Simulations (BES) in Open studio and EnergyPlus were conducted. Future weather files (future mid-term-2050s and future long-term-2090s according to the RCP8.5-scenario) were developed in the framework of IEA EBC Annex 80 Resilient Cooling of Buildings. The performance of the floor cooling system was analysed for four different climate scenarios for Melle, Belgium: typical historical-2010s, 2020 including a heatwave (observational data obtained from RMI), typical future mid-term-2050s and long-term 2090s. The evaluation was based on two parameters, [1] thermal comfort and [2] cooling capacity of the ground heat exchanger. Results demonstrate that in the future (long-term) the current design of the building including the floor cooling system is inadequate to provide a good thermal comfort. Due to the rising indoor and ground temperatures, the maximum cooling capacity will decrease 22,5% in future long-term scenario compared to the typical historical weather scenario. Results also confirm that the occupancy has a big impact on the thermal comfort, especially in the sleeping rooms. This study also indicates the importance of implementing shading as a good solution to obtain a better thermal comfort in future climate scenarios.

Keywords: Climate Change, Future climate scenarios, Passive cooling strategies, Cooling capacity, Thermal Comfort.

1. Introduction

IPCC's Special Report on Global Warming of 1.5°C concludes there is a growing risk of overheating in buildings and an increase in severity and frequency of heatwaves in future climate scenarios [1]. As seen in **Figure 1**, if the current trend of global greenhouse gas emissions continues, that is Business as Usual (BAU), RCP8.5, by 2100 an increase of the outdoor temperature of approximately 5°C in Belgium is expected [2]. An increase of the outdoor temperature will have an enormous impact on the environment, soil and indoor climate. Given the uncertainty in future climate, mitigating the adverse effects of climate change is a high priority for the EU. To reduce the sensitivity of highly insulated dwellings to overheating, cooling systems (active or passive) are needed and will have an important role in the future [3].

In recent years, policies in Europe and worldwide focused on the energy efficiency of both new and renovated buildings. To avoid excessive increase of energy use for cooling, there is a need to examine alternative cooling concepts and passive cooling strategies in order to achieve the goals of the EU's Climate Change mitigation policies [4]. In new dwellings in Flanders, built between 2006 and 2018 [5], between 15-20% of new dwellings are equipped with a heat pump, out of which 30% are ground-water heat pump. Even though currently they are mainly used for heating, these numbers suggest a high potential for ground-source cooling. Ground-source cooling systems are gaining significant market share amongst low energy cooling technologies [6] [7].

The working principle of ground-source cooling is based on the fact that the ground temperature below approximately 10 m remains fairly constant all year round at about mean annual ambient air temperature [9]. It rejects heat to the ground by circulating a working fluid through ground heat exchangers. Ground-source cooling can be classified as direct ground cooling (passive) or ground source heat pump (active). As seen in **Figure 1** and **Figure 2**, in future climate scenarios, the outside air temperature and ground temperature will be higher, this will affect the cooling capacity of ground-source cooling [8]. Rising ground temperatures lead to the decrease in performance of a ground-water heat pump, as shown by a decrease in COP value during the summer. In the winter the COP will increase [10,11].

The objective of this study is to assess the performance of radiant floor cooling in future climate scenarios. This study aims to evaluate the increase in

cooling energy need in future climate scenario, even in moderate climates. The effect of climate change (increase in outdoor air temperature, solar radiation and ground temperature) is assessed to evaluate the performance of the floor cooling to ensure robust thermal summer comfort in a dwelling in Flanders (Belgium). In the following section, the case study building, model validation and methodology are described in detail, followed by a discussion of the main results and conclusions.

2. Materials and Methods

2.1. Case Study Building

The case study building examined is a terraced dwelling, located in Geel, Belgium and constructed in 2014. This building is also a part of the SCOOOLS-project

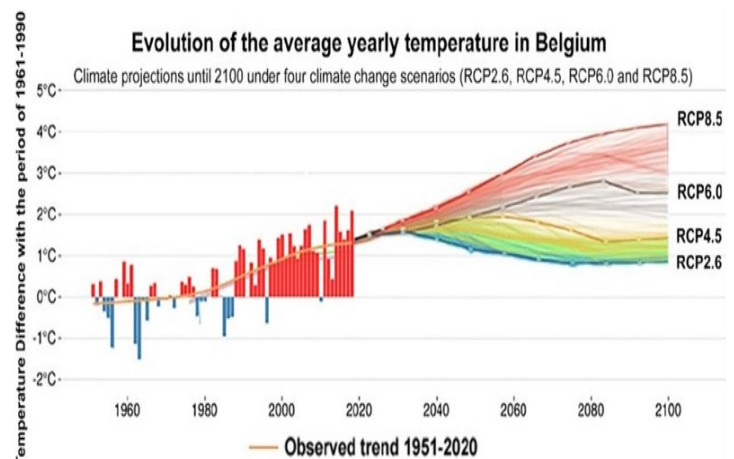


Figure 1. Evolution of the average annual temperature in Belgium. [2]

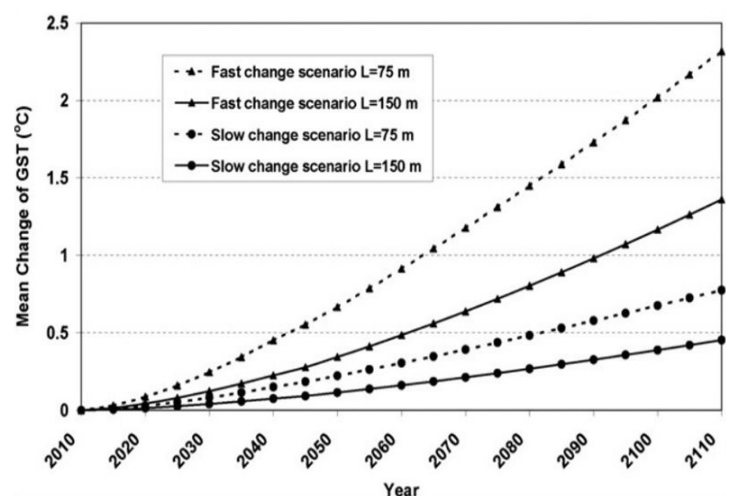


Figure 2. Evolution of ground temperature in future climate scenario. [8]

(2018-2021) which aims to evaluate the performance of low-energy cooling systems [12]. The building is South-West oriented and designed for a family consisting of 4 people. **Figure 3** shows the (southwest) facade of the building.

The building, apart from the parking in the ground floor, consists of two floors (3 m high each), with a total volume of 825 m³, an external surface of 440 m² and a compactness ratio (Surface area/gross heated volume) of 0.53. The dwelling is well-insulated and has a heavy thermal mass (calculated based on NBN EN ISO 52016-1) [13]. The average U-value of the construction is 0.42 W/m²K. The U-values of the construction elements are given in **Table 1**. The windows and the doors have a g-value of 0.55. The U-value of the fixed window and the skylights are 1.11 W/m²K and 1 W/m²K respectively. The glazing to floor ratio is 14%.

As seen in **Figure 4**, the case building is equipped with a geothermal heat pump of 8kW capacity coupled with a heat exchanger to provide floor heating in winter and during summer period, passive floor cooling from two vertical boreholes with a depth of 100 meters. One drilling of 100 m provides a cooling capacity of 2.5 kW and a heating capacity of 5 kW. Furthermore, a balanced mechanical ventilation system with total Airflow of 275 m³/h, with heat recovery is installed, which allows free cooling during the night.

2.2. Simulation Model

OpenStudio and EnergyPlus was used to perform the dynamic simulations [14] [15]. First, the building envelope is drawn in SketchUp using the OpenStudio SketchUp Plugin [16]. Then loads, schedules, HVAC-systems etc. are modelled in accordance with the real building, to set up a detailed simulation model.

The building was divided into 3 main floors, where: (a) ground floor was for entrance and storage, (b) first floor (day use)-living room, kitchen and (c) second floor (night use)- 3 bedrooms, bathroom, attic. However, for the simulation, the building has been divided into 13 thermal zones (see **Figure 4** and **Table 2**).

The internal loads are assigned for each zone and correspond to the heat gains due to occupancy, lighting and equipment (see **Table 3**). The occupancy is scheduled separately for weekday, weekend and summer vacations (See **Figure 6** for a typical weekday Schedule). Four people are assumed to be at work/school from 9h to 17h from Monday to Friday except Wednesday afternoon from 13 h. Hours of occupancy are 132 h/week. The



Figure 3. South-West facade of the case study building.

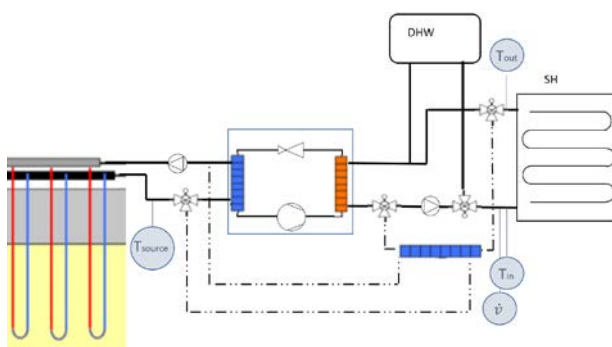


Figure 4. The scheme of the geothermal heat pump and the measurement locations.

Table 1. U-values of construction elements.

Construction	U-value (W/m ² K)
Ground Floor slab	0.21
External Wall	0.19
Common Wall	0.31
Internal Wall	2.39
Pitched Roof	0.13
Flat Roof	0.15

Table 2. Thermal Zones and Ventilation flow rates.

Thermal Zone	Ventilation Flow rates (m ³ /h)
Zone 1 (Entrance hall)	-
Zone 2 (Kitchen + dining) + Zone 3 (Living Room)	112.1
Zone 4 (Home Office/ Desk)	39.1
Zone 5 (Toilet-WC)	39.1
Zone 6 (Bedroom 1&2+ Dressing)	75
Zone 7 (Bedroom 3)	32.8
Zone 8 (Bathroom)	75
Zone 9 (Laundry)	62.6

‘radiant fraction’ is set to 0.5 for the persons, electrical equipment and lighting. This value is recommended by EN ISO 52016-1 when performing simulations [17].

Hours of occupancy in a space is a crucial factor impacting thermal comfort. In zone 2 and 3 (living room), it is assumed that the spaces are occupied during the daytime. Concerning zone 6 (bedrooms), two different scenarios are created for simulation. In the first scenario, the bedrooms are only occupied during the night (11 p.m. – 7 a.m.). For the second scenario, an occupancy from 4 p.m. till 7 a.m. is assumed. Since the case study building was not equipped with solar shading, a simulation scenario to evaluate the impact of solar shading on thermal comfort was implemented. An automatic solar shading with g-value of 0.55 has been implemented in the simulation model. The solar shading

Table 3. Internal loads for each space for heat gains. [17]

	Room	Persons (number)	Lighting (W/m ²)	Equipment (W)
level 1	Desk (Zone 4)	1	2	250
	Living area (Zone 3)	2	2	330
	Dining + kitchen (Zone 2)	2	1.7	108
level 2	Bedroom 1 + dressing (Zone 6)	2	2	0
	Bedroom 2 (Zone 6)	1	2	30
	Bedroom 3	1	2	30
	Bathroom	1	4.6	0
	Laundry room	0	0	3 200

Table 4. Adaptations in the simulation model for model validation.

	Adaptation	Description
1	Floor Cooling	<ul style="list-style-type: none"> – Setpoint cooling: 23°C ±1°C – Supply temperature: 18°C – Measure operative temperatures – Max Flow rate cooling: 1200l/h – Check parameters of circulation pump and heat exchangers
2	Air Flow	<ul style="list-style-type: none"> – Measure: Add zone mixing Object – Adjustments in the air flows between zones
3	Infiltration	– N50 = 2 h ⁻¹
4	Ground Heat Exchanger	<ul style="list-style-type: none"> – Ground Thermal conductivity: 2.1 W/Mk – Ground thermal heat capacity: 3400000 PA:K – Ground Temperature: 13°C – Pipe thermal conductivity: 0.42 W/mK – U_tube distance: 0.06 m – Pipe Thickness: 0.003 m – Flow rate loop: 0.00032 m³/s

is only applied to the windows located on the south-west side of the building, both for the bedrooms (thermal zone 6) and the living space (thermal zone 2 and 3). The solar shading is modelled to be ON, when the global solar radiation on the window reaches exceeds a value of 250 W/m². It remains ON for 15 min, after which the control checks the radiation on the window. If the solar radiation on the window exceeds 250 W/m², the shading remains ON and if the value is lower than the threshold value of 250W/m², the shading is turned OFF.

2.3. Model Validation

Before evaluating the impact of future climate scenarios on the performance of the floor cooling system, the simulation model must be validated. To do this, the indoor temperatures obtained from the model are compared with the indoor temperatures measured by sensors on site. For this reason, the operative indoor zone temperatures (from the model) are compared with the data from measuring devices placed on-site. A weather station TMK was placed with 2 minutes time step for monitoring the outdoor dry bulb temperature, relative humidity and solar radiation. Sensor HUBO MX1102 with time step 10 minutes was placed in the bedroom (See **Figure 5** for the position of the sensor in the bedroom) to monitor the temperature,

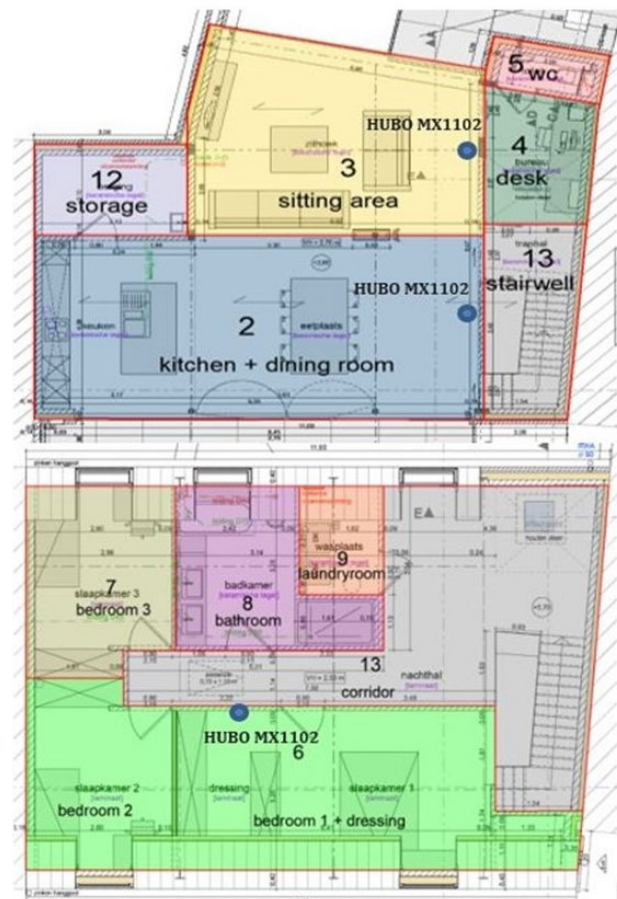


Figure 5. Thermal Zones.

relative humidity, CO₂ and dew point temperature. This sensor has a range between 0°C to 50°C with an accuracy of ±0.21°C in the given range. The comparison is performed for two periods of 10 days in July (6.07-16.07) and August (17.08-27.08-post heat wave period) of the year 2020 (see the weather data from July and August 2020 in **Figure 7**).

Figure 8 shows the measured data between 6th to 16th July 2020. The outdoor temperature reaches a maximum of 24.1°C on 13/07/2020 at 2 pm. The maximum indoor temperature for bedroom (23.5°C) and living room (25.2°C) was observed on 12/07/2020 at 8.11 pm.

Improvements on the simulation model were made on parameters of the floor cooling system, airflows, infiltration rates and ground heat exchanger to obtain the best result (see **Table 4**). The entire summer period of measured temperatures and simulated temperatures is compared (1st July – 14th September 2020). There are two conditions that the results of the simulation model must meet to be considered that the indoor temperatures as validated- (a) The MAE (Mean absolute value of error) should be less than 1°C and (b)RMSE (Root mean squared error) should be less than 1.5°C [18].

2.4. Climate Scenarios

The impact on the performances of a floor cooling system is assessed for four possible climate scenarios, representing historical, extreme weather data (heatwave period) and future weather data (midterm-2050s and longterm-2100s). The historical weather data of 2010 represent a moderate climate and are used as the reference scenario. The rising ground temperature is also taken into consideration for the dynamic-simulations. The weather data of Melle, for Scenario 1, 3 and 4 are based on RCP8.5 and developed adopting the methodology IEA EBC Annex 80-Resilient Cooling of Buildings [19]. Weather data of Melle for scenario 2 is based on the observations by RMI for year 2020 [20].

In **Figure 10**, we can observe, the maximum temperatures recorded in the summer months (April-August), shows rising temperature trend from the historical to the future long-term scenario. However, 2020, was an exceptionally warm year with heat waves in July and August and the observed weather data of 2020 had higher maximum temperature for the summer months than mid-term climate scenario. However, for radiation, the variation between the 2 scenarios (historical and midterm) in summer months are not significant.

Table 5. Model validation (Summer period: 1st July–14th September 2020).

Difference between simulated and measured temperature		Validation condition	Status	
MAE	living room	0.80°C	<1°C	Validated
	bedroom	0.83°C	<1°C	
RMSE	living room	1.03°C	<1.5°C	
	bedroom	1.03°C	<1.5°C	

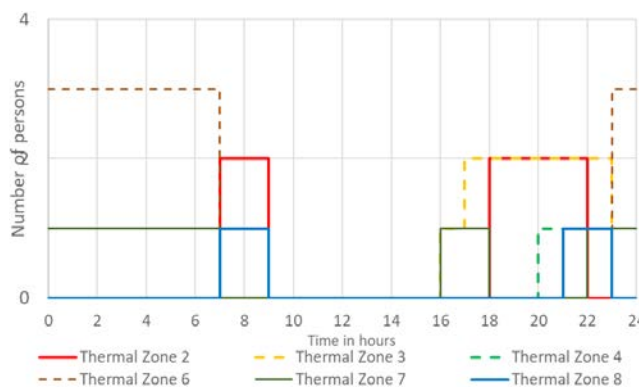


Figure 6. Weekday occupancy schedule.

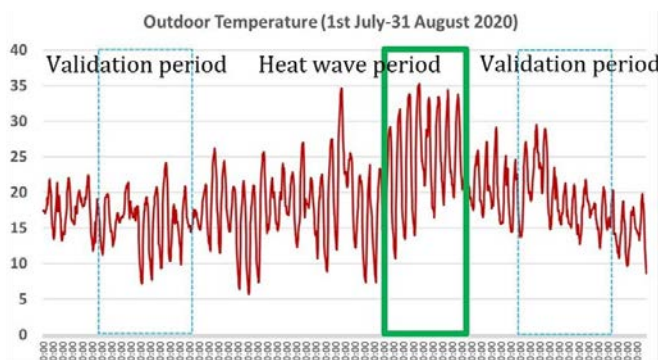


Figure 7. Weather data from 1st July to 31st August 2020 indicating the heat wave period in the beginning of August.

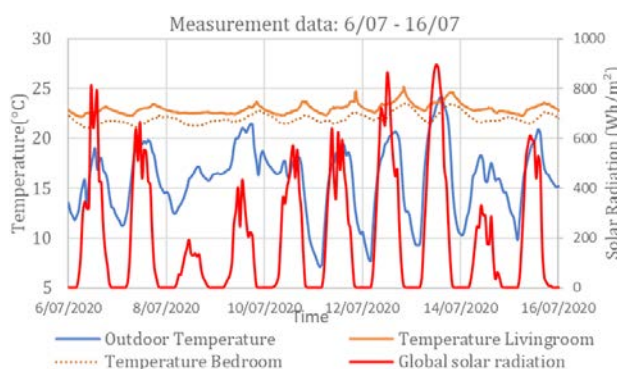


Figure 8. Measured outdoor and indoor temperature between 6th to 16th July 2020.

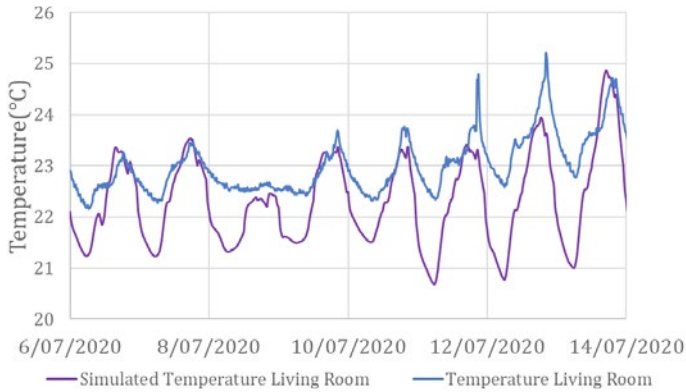


Figure 9. Comparison of the measured and Simulated temperature of the living room.

Table 6. Climate scenarios used for performance assessment.

Scenarios	Description
1	Historical weather data 2010s (2000-2020)
2	Weather data -Melle 2020 (heatwave)
3	Future mid-term 2050s (2040-2060)
4	Future long-term 2090s (2080-2100)

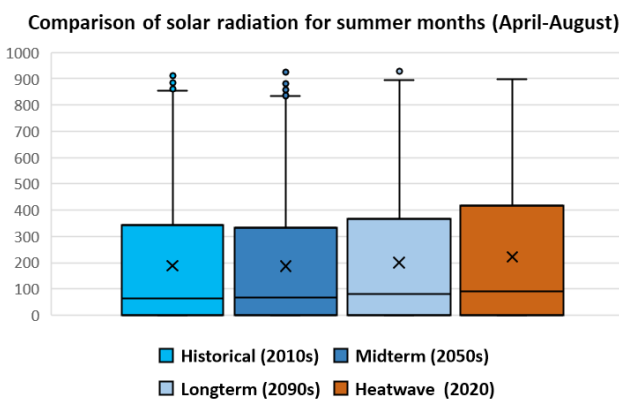
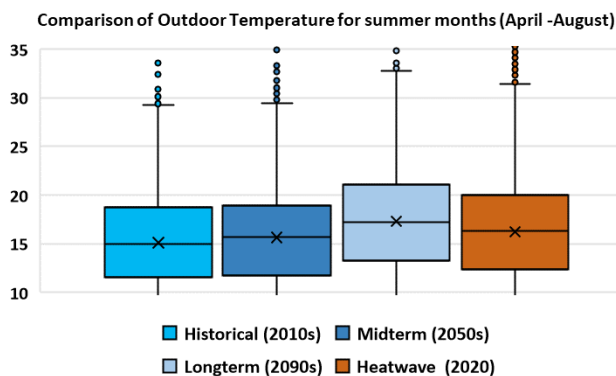


Figure 10. Temperature and solar radiation trends for the summer months for all 4 climate scenarios.

But for 2020, heat wave scenario, the solar radiation is significantly higher compared to the long-term scenario.

The OpenStudio/EnergyPlus manual shows that weather data (excluding specific ground temperatures) only has an impact on the ground temperature at the surface (up to 0.5 m). The ground heat exchanger is placed to a depth of 100 meters. It is therefore crucial that the ground temperature for the ground heat exchanger is manually adjusted for the future climate scenarios. For climate scenario 1 and 2, the ground temperature 13°C, 13.7°C for scenario 3 and 14.7°C for scenario 4 has been implemented. With boreholes up to 100 m deep, the choice was made to follow the fastest increasing scenario at a depth of 75 m [8].

2.5. Thermal Comfort and Cooling Capacity Assessment

Method A as described in Annex F of the EN 15251 (15) is selected for the evaluation of summer comfort. For this study, the percentage of occupied hours when the operative indoor temperature is above 25°C, 26°C and 28°C is evaluated for a period from the 1st of April until 31st October. The temperature thresholds also verify with the heat stress impact on human body, studied by [21]. The analysed period is an extension of the meteorological summer because, assuming future climate scenarios, summers can be longer. If the percentage above 25°C is lower than 5%, the thermal comfort is considered acceptable while lower than 3% is considered good.

The cooling capacity is calculated using the energy equation (1). The cooling capacity of the floor cooling system is increases/decreases depending on the inlet and outlet temperature of the ground heat exchanger (ΔT).

$$Q = \dot{m} \cdot c \cdot \Delta T \quad (1)$$

For the calculations on the supply side of the heat exchanger, the following parameters have been extracted from the simulation model (per time step of 1 hour):

- heat exchanger: inlet temperature (°C)
- heat exchanger: Outlet temperature (°C)
- Flow rate flowing through the heat exchanger (kg/s)

To evaluate the thermal comfort, only the most critical zones (living space (2&3) and bedrooms [6]) are considered. To improve the thermal comfort, the impact of solar shading is also investigated for all the zones.

3. Results and Discussion

3.1. Thermal comfort assessment

3.1.1. Bedroom (Zone 6)

Zone 6 (Bedroom) is only occupied during the night. Two types of occupancy profile (11pm to 7 am) and (4 pm to 7 am) has been simulated. Both the occupancy scenarios are simulated with and without solar shading interventions.

As seen in **Figure 11**, a good thermal comfort can be guaranteed in all 4 climate scenarios with a maximum of 1.4% of occupied hours above 25°C in the long-term scenario. Occupancy profile 1 (11 pm to 7 am) do not have any occupied hours above 26°C and 28°C threshold with or without shading. However, when the bedrooms are occupied for a longer period (4 am to 7 am), the percentage of occupied hours above 25°C in long-term scenario increases to 7.1% (see **Figure 12**). With higher occupancy, the percentage of exceeding hours in Future long-term scenario can be decreased from 7.1% to 3.5% with the intervention of solar shading (see **Figure 12**). For the climate scenarios-2020, historical and also midterm, solar shading decreases the exceeding hour percentage by 50%. There are no exceeding hours above 28°C with solar shading. However, without solar shading, there are 3.1% occupied hours exceeding 26°C, and 1.8% occupied hours exceeding 28°C.

3.1.2. Living Room (Zone 2&3)

Zone 2&3 (Kitchen+ dining and Living room) is occupied during the day. Zone 2 &3 is simulated with and without solar shading interventions. As seen in **Figure 13**, without solar shading, the percentage of occupied hours above 25°C is higher than the acceptable limit in all 4 climate scenarios. The percentage of occupied hours above 25°C threshold reaches up to 14.5 % in the long-term scenario.

With the intervention of solar shading, the percentage of occupied hours in historical and mid-term scenario can be improved and brought back below the acceptable 5% limit. However, even with solar shading, percentage of occupied hours above 25°C is above the acceptable level for the year 2020 (heat wave period) and for long-term climate scenarios (see **Figure 13**).

Figure 14 illustrates the percentage of occupied hours above 26°C threshold in Zone 2 &3, without and with shading. Without shading, only in long-term scenario, the percentage of occupied hours are above acceptable limit (9.8%). Historical and mid-term scenario are in good limits (below 3%), whereas year 2020 is 3.5%.

However, with the intervention of shading, all 4 scenarios are within the acceptable limit. Thus, Solar shading will reduce 50% of occupied hours above 26°C for the long-term scenario and will guarantee

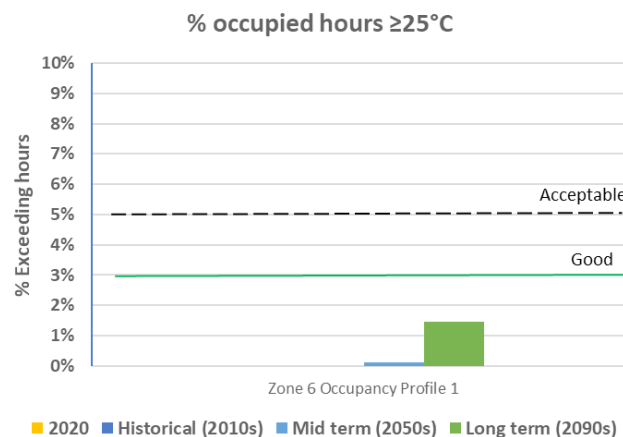


Figure 11. % occupied hours >25°C occupancy between 11 pm to 7 am, with and without shading

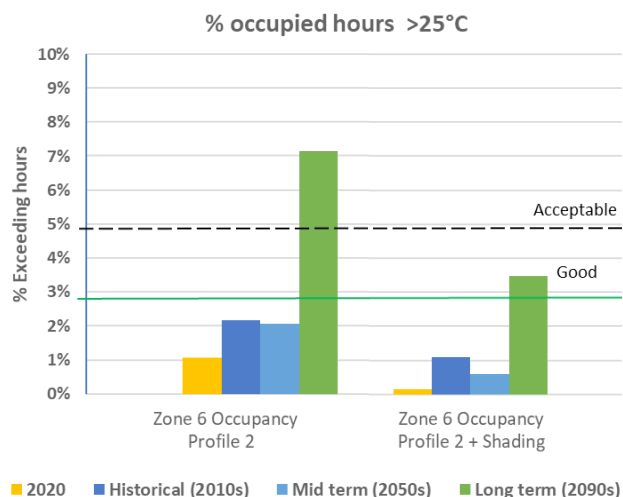


Figure 12. % occupied hours >25°C (Zone 6- Bedroom with Occupancy between 4 pm to 7 am, with and without shading).

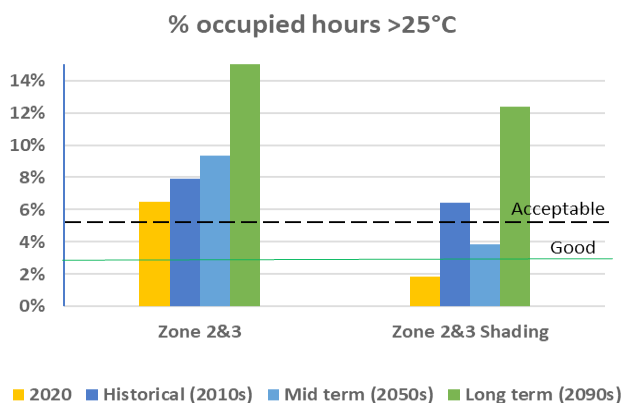


Figure 13. % occupied hours >25°C (zone 2&3) without and with shading.

a good thermal comfort in the other scenarios. In the long-term, the indoor temperature will rise above 28°C (0.5%) without solar shading. With shading, no indoor temperatures above 28°C are measured.

3.2. Cooling capacity assessment

The impact of future climate scenarios on the cooling capacity is illustrated in **Figure 15**. The results from the simulation confirm, climate change will have a

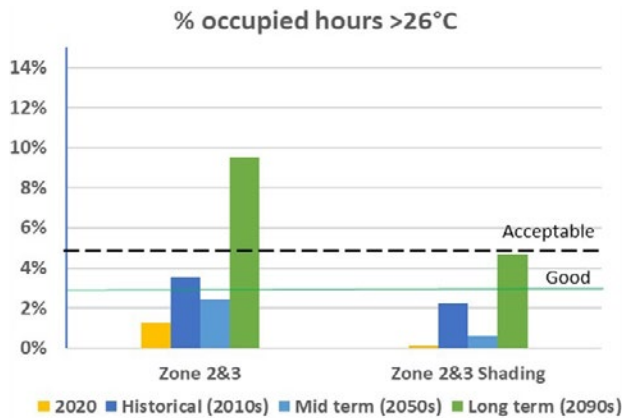


Figure 14. % of occupied hours in Zone 2 & 3 above 26 without and with solar shading.

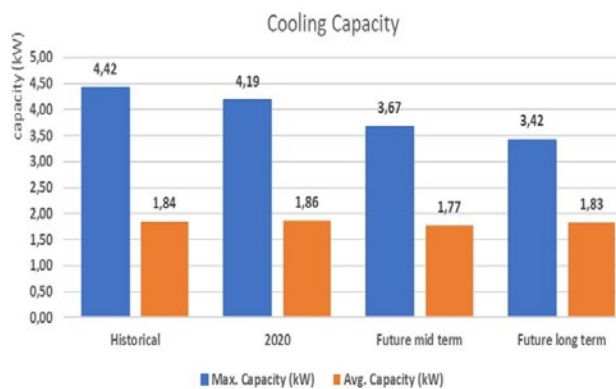


Figure 15. Cooling Capacity heat exchanger.

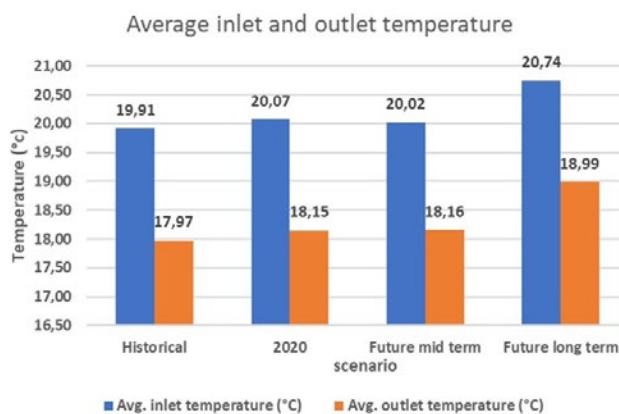


Figure 16. Average inlet and outlet temperature (Floor cooling).

negative impact on the cooling capacity, even for cooling devices used in this case study.

However, the technical data sheet of the system shows a peak cooling capacity of 5Kw. This value was never exceeded during all 4 climate scenarios, proving the current system should be able to deliver the peak cooling capacity in future climate scenarios. However, peak cooling power decreases 1 kW over 80 years. This is due to the rising ground temperature as a result of global warming. **Figure 16** illustrates the inlet and outlet temperatures on the supply side of floor cooling. The supply temperature of the floor cooling system was set at 18°C to avoid condensation and this setpoint was used in the actual system on site as well. For climate scenarios 2, 3 and 4, this supply temperature cannot longer be guaranteed. There is a rise in the inlet temperature (0.15°C for 2020, 0.16°C during mid-term and almost by 1°C for the long-term scenario).

Analysis of the cooling capacity shows that the maximum power output will decrease in the future climate scenarios. For example, the maximum power output will decrease by approximately 17% by 2050 and 22.5% by 2090. The average cooling capacity will remain approximately the same. The decrease in maximum cooling capacity is due to the faster increase of the outlet temperature compared to the inlet temperature of the heat exchanger. For example, in climate scenario 4 (2090) the supply temperature of 18 degrees cannot be guaranteed over the entire period. On average, the supply temperature rises to almost 19°C, which is the result of a rising source temperature in the boreholes.

4. Conclusions

The results of the thermal comfort show that occupancy has a major impact on whether or not the predetermined upper limits are exceeded. If the analysis is performed for the living space with an upper limit of 25°C, good thermal comfort cannot be guaranteed for any climate scenario. If the upper limit is raised to 26°C, the floor cooling system will only fail in 2090 and in rest 3 climate scenarios, it can guarantee acceptable hours of thermal comfort. In the long-term, only 0.5% of occupied hours was measured, with the indoor temperature exceeding the upper limit of 28°C. For the bedroom, assuming occupancy only at night in the bedrooms, good thermal comfort is achieved for all climate scenarios. With the occupancy profile from 4 pm to 7 am, good thermal comfort cannot be guaranteed 7.1% occupied hours above 25°C in 2090. In the bedroom, assuming an upper limit of 25°C

for both occupancy patterns, good thermal comfort can still be guaranteed. However, implementation of solar shading shows much improvement in the thermal comfort in the bedroom and especially in the living-dining room (Zone 2 &3). In the living space, good thermal comfort is only obtained if the comfort temperature limit is raised to 26°C, even in historical climate scenario. However, with intervention of solar shading this can be improved for the 4 climate scenarios. This verifies the necessity of solar shading especially in highly glazed and south or west facing zones in the buildings.

The decrease in cooling capacity of the floor cooling in mid-term climate scenario is 17%. In the long-term, the impact of climate change is greater. Even assuming an upper limit of 26°C, good thermal comfort is not obtained. With regard to the cooling capacity of the floor cooling, the decrease is also greater-22.5% compared to the existing condition. In the future, the system will therefore have to be dimensioned differently, for example by increasing the flow rates or additional (active or passive) cooling systems will have to be implemented. In the long-term, the current design of this dwelling including

the floor cooling system will not be able to reduce the temperature below 26°C in each thermal zone. The inlet temperature of 18°C can't be guaranteed in future climate scenarios, which results in a lower maximum cooling capacity.

Thus, it can be concluded that in future climate scenarios, shading is indispensable. Also, the cooling systems needs to be dimensioned keeping in mind the rise in air and ground temperature to guarantee good thermal comfort to the users. ■

5. Acknowledgement

This study was conducted as part of the curriculum for Master thesis of students Pieter Proot and Tom Trioen under the supervision of Prof. Hilde Breesch and PhD student Abantika Sengupta. The data of the case study building and the monitoring data was provided by Thomas More University of Applied Sciences as a part of their sCOOLS project.

6. References

Please find the full list of references in the original article at: <https://proceedings.open.tudelft.nl/clima2022/article/view/326>.





SOUTH ASIA'S LARGEST EXHIBITION ON AIR CONDITIONING, HEATING, VENTILATION AND INTELLIGENT BUILDINGS

ACREX India 2023

14-16 MARCH 2023 | BEC, MUMBAI



ENGINEERING TOWARDS NET ZERO

The 22nd edition of ACREX INDIA is scheduled from 14th to 16th March 2023 at Bombay Exhibition Centre, Mumbai. The focus will be on engineering advancements and driving technological solutions towards net zero goals in the HVAC-R sector, which is pivotal in creating a better future.

ACREX INDIA 2023 shall stand tall as the most coveted, comprehensive conglomeration for industry professionals from around the globe. Experts from all over the world would come together to meet people, cultivate and expand networks and conduct business.

ACREX INDIA 2023 FEATURES

 450+ Exhibitors	 35000+ Attendees	 32000 Sq m. Gross Exhibition Space	 Participation from 40 countries	 Technical Seminars and Workshops	 Interactive Panel discussions	 ACREX Awards of Excellence	 ACREX Hall of Fame
--	---	---	---	---	--	---	---

EXHIBITOR PROFILE	VISITOR PROFILE
<ul style="list-style-type: none"> * Packaged Chillers * Air Handling & Distribution Products * Unitary Products (Air conditioners) * Products (Refrigeration) * Refrigeration Accessories * Water distribution * Water treatment <p style="text-align: right;">and many more...</p>	<ul style="list-style-type: none"> * Contractors (HVAC, Refrigeration, Plumbing, Mechanical, Controls) * Consulting Engineers * Mechanical Engineers * Architects * Wholesalers/Distributors * Importers/Exporters * Public Utilities <p style="text-align: right;">and many more...</p>

SUPPORTED BY	PARTNERS						
  Federation of European Heating, Ventilation and Air-conditioning Associations	ACREX Award Night Partner 	ACREX Hall of Fame Partner  ENGINEERING TOMORROW	Titanium Partner 	IAQ Partner  We breathe air into your life	Silver Partners  	Bronze Partners  A Division of AIRUTE	

For Sales & Partnership | Rohan Chopra | M: +91 9873201377 | E: rohan.chopra@informa.com
 Saiprasad Terde | M: +91 9920050415 | E: acrex-india@informa.com
For Marketing & Alliances | Murtaza Dhankot | M: +91 9820597939 | E: murtaza.dhankot@informa.com

A Multi-Domain Approach to Explanatory and Predictive Thermal Comfort Modelling in Offices



EUGENE MAMULOVA
Eindhoven University of Technology, Eindhoven, the Netherlands
e.mamulova@tue.nl



HENK W. BRINK
Eindhoven University of Technology, Eindhoven, the Netherlands & Hanze University of Applied Sciences, Groningen, the Netherlands



MARCEL G.L.C. LOOMANS
Eindhoven University of Technology, Eindhoven, the Netherlands



ROEL C.G.M. LOONEN
Eindhoven University of Technology, Eindhoven, the Netherlands



HELIANTHE S.M. KORT
Eindhoven University of Technology, Eindhoven, the Netherlands

Abstract: It is well known that physical variables, such as temperature, exert a significant influence on occupants' thermal comfort in office buildings. Despite this knowledge, models that are currently used to predict thermal comfort fail to do so accurately, resulting in a mismatch between design conditions and actual thermal comfort conditions. The assumption is that exclusive attention to physical variables is insufficient for understanding or predicting thermal comfort. The question arises as to how a multi-domain approach can aid in explaining and predicting thermal comfort in offices. In this study, a unique dataset containing indoor environment, demographic, occupancy and personality related variables is used to construct two types of thermal comfort models. The dataset contains 524 observations, collected during summertime in two office buildings in the Netherlands. Firstly, structural equation modelling (SEM) is used to construct an explanatory model, with the aim to identify significant variables affecting thermal comfort, as well as the interactions between them. Secondly, machine learning is used to train four binary classification models to predict thermal discomfort. For the investigated cases, SEM suggests that thermal discomfort is significantly affected by (i) temperature, (ii) sound pressure level, (iii) the interaction between temperature, sound pressure level and illuminance, and (iv) the interaction between gregariousness and occupancy count. The four predictive models are subsequently trained using only the significant variables. Nevertheless, the weighted F_1 -score for all four models ranges between 0.55 and 0.59, indicating weak predictive performance. The results show that significant influencers are not necessarily good predictors of thermal discomfort. Future researchers are encouraged to combine explanatory and predictive modelling techniques, in order to test whether variables that are relevant to the domain are useful for prediction.

Keywords: Thermal comfort, multi-domain, personal domain, interaction effects, structural equation modelling, machine learning.

1. Introduction

Thermal comfort is that condition of mind that expresses satisfaction with the thermal environment [1]. Building engineers refer to building standards to predict the thermal comfort conditions for a given design. However, current standards do not always produce adequate thermal comfort predictions [2]. Researchers in the field of thermal comfort seek to understand and predict thermal comfort, using explanatory and predictive models. Explanatory models typically employ statistical techniques that provide insight into what influences thermal comfort in offices. Predictive models are built to forecast the thermal comfort conditions for a given office space.

Recent research efforts have focused on multi-domain approaches that treat thermal comfort as a combination of variables belonging to four domains, outlined in **Figure 1** [3]. Their relevance is apparent but their presence in existing thermal comfort models is limited [4]. The combined presence of all four domains is almost non-existent [4]. Moreover, the majority of existing studies focus on explanatory modelling [4]. The rift between design conditions and real-world conditions is in part attributable to the absence of a suitable thermal comfort model. In consequence, it is important to pursue better prediction of thermal comfort in office buildings and it is worthwhile doing so using the multi-domain approach. This study looks at existing thermal comfort models to identify potential variables that may aid in better explaining and predicting thermal comfort.

1.2 thermal comfort variables

Existing multi-domain studies identify several variables that are of interest to thermal comfort modelling. A list of main effects and interaction effects that are supported or rejected by existing research on multi-domain thermal comfort in offices is composed [4], leading to the following hypotheses:

- M1*: Air temperature exerts a positive, exponential, effect on thermal discomfort.
- M2*: Sound pressure exerts a positive effect on thermal discomfort.
- M3*: Occupant gregariousness exerts a negative effect on thermal discomfort.
- I1*: Air temperature exerts a negative effect on the interaction effect between sound pressure level and illuminance on thermal discomfort.
- I2*: Occupant assertiveness exerts a positive effect on the effect of air temperature on thermal discomfort.
- I3*: Occupancy count exerts a positive effect on the effect of occupant gregariousness on thermal discomfort.

The aforementioned hypotheses are tested via an explanatory model, using field measurement data. The results are used to train a model that aims to predict whether office employees are experiencing thermal comfort or discomfort. The articulation of the modelling outcome is unprecedented in current literature, covering three physical variables (air temperature,

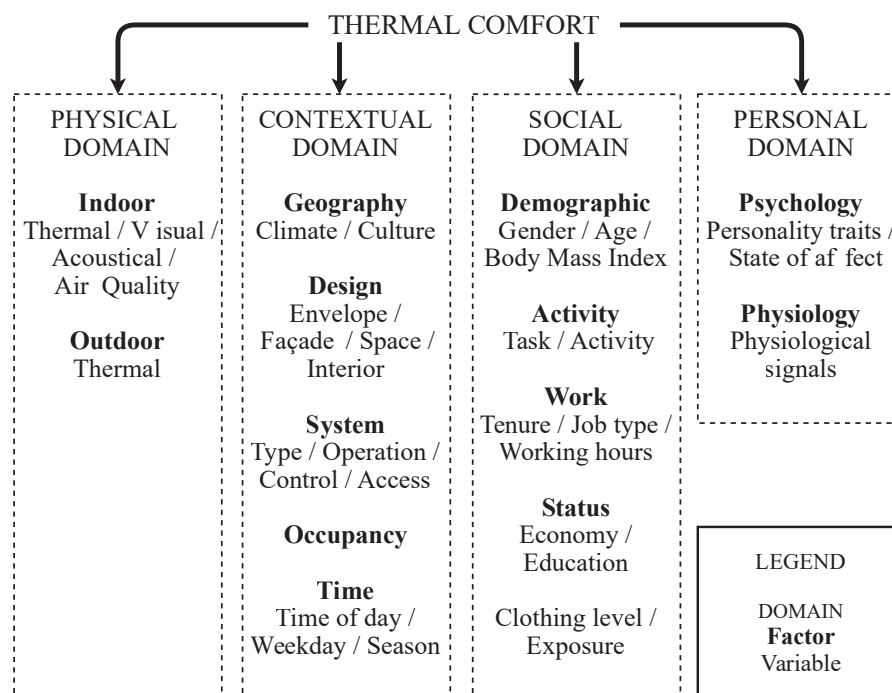


Figure 1. Physical, social, contextual and personal variables present in literature, adapted from [3].

illuminance and sound pressure level), one contextual variable (occupancy count), two personal variables (occupant assertiveness and gregariousness) and one social variable (gender), in the interest of testing whether such a multi-domain approach can aid in a better understanding or prediction of thermal (dis) comfort in offices.

2. Research methods

The data was collected prior to this study, in two office buildings in the Netherlands. The cross-sectional campaign was conducted during the years 2015-2018. The applied measurement protocol is described in a publication by Brink and Mobach [5]. The data points used in this study are limited to the warmer months of June and July 2016. 623 office employees participated in the measurements. The final sample size is equal to 522. The data consists of objective and subjective measurements.

2.1 explanatory modelling

Explanatory modelling is performed via structural equation modelling (SEM); a covariance-based technique that enables the inclusion of observable and unobservable variables. Visualization is done using standard LISREL matrix notation [6]. The computation is performed via the ‘lavaan’ package [7].

Table 1 provides an overview of the variables used, along with their notation. Variables T_{in} , SPL , E and

N_{occ} are continuous. Variables $a_1 - a_2$ and $g_1 - g_4$ are ordinal. All variables are normalized using min-max feature scaling. To account for multivariate non-normality, robust diagonally weighted least squares (DWLS) estimation, known as weighted least square mean and variance adjusted estimation (WLSMV) in ‘lavaan’ package, is used to compute the parameter estimates, robust standard errors and fit indices.

2.2 predictive modelling

The predictive model takes the form of a binary classifier that predicts whether a participant is experiencing thermal comfort or discomfort. The variables included in the model are listed in **Table 2**. Two linear and two non-linear classification algorithms are selected and trained using the scikitlearn Python library [8]. P_0 is used for linear algorithms, while P_1 is used for non-linear algorithms, as the latter are expected to capture non-linear relationships. The linear algorithms

Table 2. Variables used for prediction.

Variable	Symbol
Indoor temperature exponent	P_0
Indoor temperature	P_1
Sound pressure level	P_2
Sound × illuminance × temperature	P_3
Gregariousness × occupancy count	P_4
Gender	P_5

Table 1. Direct and indirect effects included in the SEM model.

Effect	Domain	Symbol	SEM	Variable	Range [unit]
Direct	Physical	$exp^{T_{in}}$	x_8	Air temperature	20 – 26 [°C]
		SPL	x_9	Sound pressure level	40 – 70 [dB(A)]
		E		Illuminance ^a	0 – 2,000 [lx]
	Personal	g_1	x_1	Gregariousness	
		g_2	x_2	Gregariousness	
		g_3	x_3	Gregariousness	
		h_1	y_1	General body discomfort	
		h_2	y_2	Lower body discomfort	
		h_3	y_3	Upper body discomfort	
Indirect	Physical	$SPL \cdot E \cdot T_{in}$	x_{10}	Sound, illuminance and temperature	
	Physical and personal	$T_{in} \cdot a_1$	x_4	Temperature and assertiveness	
		$T_{in} \cdot a_2$	x_5	Temperature and assertiveness	
	Contextual and personal	$N_{occ} \cdot g_1$	x_6	Occupancy count and gregariousness	$N_{occ} < 20$
$N_{occ} \cdot g_4$		x_7	Occupancy count and gregariousness	$N_{occ} < 20$	

^a The direct effect of illuminance is excluded but illuminance is used to compute $SPL \cdot E \cdot T_{in}$.

are logistic regression (LR) and linear support-vector machine (L-SVM), while the non-linear algorithms are random forest ensemble (RF) and non-linear support-vector machine that uses the radial basis function kernel (RBF-SVM). During the testing phase, the models are retrained on 308 observations, comprising the training and validation sets, and are tested on the remaining 77 observations. Common metrics such as the F_1 -score, accuracy (ACC) and the area under the ROC curve (AUC) are used.

4. Results

3.1 structural equation modelling

The outcome of the explanatory modelling phase is a SEM model. **Figure 2** shows the parameter estimates, variance/covariance estimates and factor loadings for the explanatory model. The parameter estimates are also shown in **Table 3**. The exponent of air temperature x_8 is expected to have a positive effect on thermal discomfort η_1 . According to the results, the effect of x_8 on η_1 is positive (see **Figure 2**) and significant at 99.9% confidence ($z > 3.09$, $p < 0.001$). Sound pressure level x_9 is expected to exert a positive effect

Table 3. Parameter estimates for the thermal comfort variables included in the SEM model.

	Estimate	SE	Z	P(< z)
x_8	0.643	0.203	3.177	0.001 ^a
x_9	0.357	0.151	2.368	0.018 ^b
x_{10}	-0.383	0.196	-1.951	0.051 ^c
ξ_1	-0.128	0.174	-0.736	0.462
ξ_2	0.104	0.382	0.272	0.785
ξ_3	0.394	0.198	1.988	0.047 ^c

^a CI – 99.9%, ^b CI – 98%, ^c CI – 95%.

on η_1 . The main effect of sound pressure level x_9 is found to be positive and significant at approximately 98% confidence ($z > 2.33$, $p < 0.02$).

The interaction between indoor temperature, sound pressure level and illuminance x_{10} is expected to exert a negative effect on η_1 , such that an increase in indoor temperature will result in a decreased audio-visual influence. The parameter estimate for the three-way interaction x_{10} is found to be negative and significant at

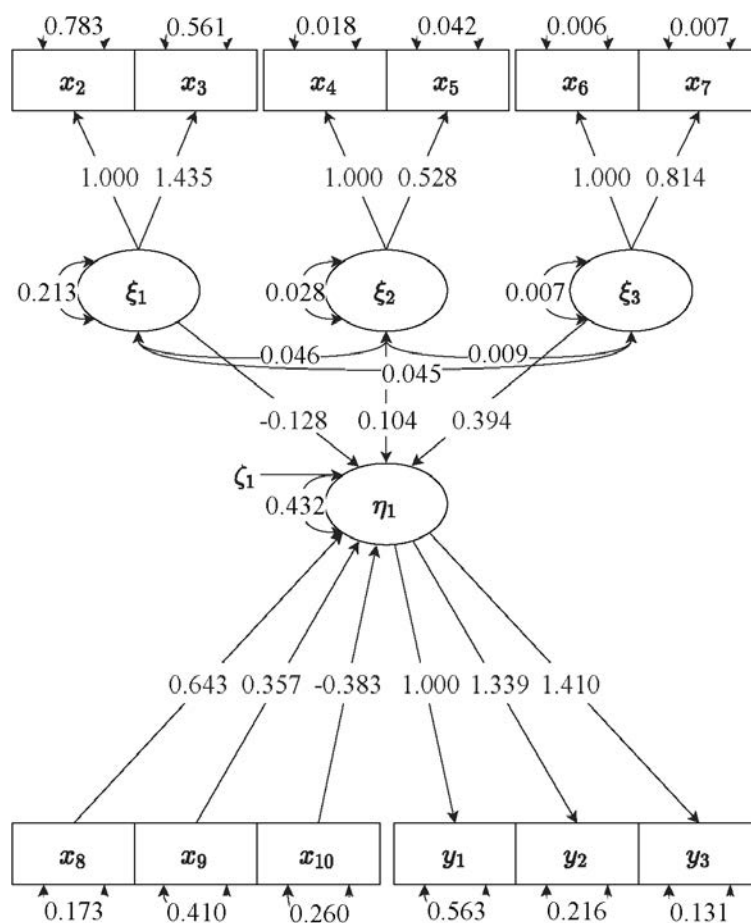


Figure 2. Graphical representation of model estimation.

95% confidence ($z > 1.96, p < 0.05$). Gregariousness x_1 is expected to exert a negative effect on η_1 . The effect of x_1 on η_1 is found to be negative but it is not found to be significant. The interaction between assertiveness and indoor temperature x_2 is expected to be positive, to the extent that an increase in temperature will result in an increased influence of assertiveness on η_1 . The two-way interaction x_2 is found to be positive but it is not found to be significant. The interaction between gregariousness and occupancy count x_3 is expected to be positive, such that an increase in occupancy count will result in an increased influence of gregariousness on η_1 . The two-way interaction x_3 is found to be significant at approximately 95% confidence ($z > 1.96, p < 0.05$). As a result, hypotheses $M1, M2, I1$ and $I3$ are not rejected.

3.2 binary classification

The outcome of the predictive modelling phase are four models; LR, L-SVM, RF and RBF-SVM. LR is fitted as shown in equation (1). The polarity of the parameter estimates is consistent with hypotheses $M1, M2, I1$ and $I3$, suggesting the model learned a similar pattern to the one captured using SEM.

$$P(Y = 1|X) = \frac{\exp(-0.27 + 0.29X_0 + 0.30X_2 - 0.13X_3 + 0.17X_4 + 0.23X_5)}{1 + \exp(-0.27 + 0.29X_0 + 0.30X_2 - 0.13X_3 + 0.17X_4 + 0.23X_5)} \quad (1)$$

The performance metrics for the validation and testing phases are reported in **Table 4**. The difference in performance across the models is very slight and all four models yield similar scores across all three metrics. While L-SVM and RF show better ACC and weighted F_1 on the validation set, they no longer outperform the other models on the test set. The increase in ACC during the testing phase for all four predictive models could be attributed to random variation between data splits. The predictive performance of the models is just

Table 4. Performance metrics (validation and testing).

Model	Set	AUC	ACC	F_1
LR	Valid	0.58	0.56	0.53
	Test	0.68	0.56	0.56
L-SVM	Valid	0.58	0.61	0.61
	Test	0.67	0.55	0.55
RF	Valid	0.62	0.60	0.60
	Test	0.64	0.58	0.59
RBF-SVM	Valid	0.57	0.52	0.48
	Test	0.66	0.57	0.58

above random guessing (= 0.50) and is not sufficient for predicting thermal (dis)comfort.

5. Explaining thermal comfort

The interpretation of the SEM model addresses the hypotheses $M1-M3$ and $I1-I3$. The model estimates do not reject $M1, M2, I2$ and $I3$, leading to several implications that may be of interest to the understanding of thermal comfort in offices:

- During the cooling season, an increase in indoor temperature results in an exponential increase in thermal discomfort.
- An increase in sound pressure level results in an increase in thermal discomfort.
- An increase in air temperature decreases the effect that the interaction between sound pressure level and illuminance has on thermal discomfort, resulting in a negative three-way interaction.
- An increase in occupancy count increases the effect of occupant gregariousness on thermal discomfort, resulting in a positive two-way interaction.

The results support the notion that the model may be used to explain thermal comfort. However, the existence of a near-equivalent model is likely. The reliability of the subjective data, particularly assertiveness and gregariousness, is questionable. A better fit may be achieved via the use of a more extensive and well-known scale, such as the IPIP-NEO-120 [9].

6. Predicting thermal comfort

The SEM model suggests that P_0-P_5 significantly affect thermal comfort in offices. Yet, the four predictive models are not capable of adequately predicting thermal (dis)comfort. Looking at all four outcomes, the quality of the data may have introduced noise, masking the patterns necessary for making reliable predictions. However, real-world data is noisy and constitutes a pitfall for even the most prevalent models. A predictive model can be expected to perform even worse in practice than it does on the mother data set. The results show that thermal comfort is a complex, multi-domain construct that is difficult to predict. However, the performance of the four predictive models does not cast a definitive shadow over the prospect of accurate prediction. Predictive models that include a larger number of thermal comfort variables and higher quality subjective measurements may yield better predictions. Moreover, other, more advanced modelling techniques, such as stochastic modelling, may be better suited for thermal comfort prediction.

7. Conclusion

This study applies the multi-domain approach to thermal-comfort modelling. An explanatory model is constructed using SEM. The specified model examines the influence of indoor temperature, illuminance, sound pressure level, occupancy count, gregariousness and assertiveness on thermal discomfort. The SEM model is unique, as it is the first explanatory model, derived from field measurements, to include multiple physical and personal variables, while also including contextual variables. The following conclusions are derived from the explanatory model:

- Thermal discomfort increases at higher indoor temperatures and higher sound pressure levels, suggesting that both should be optimized and maintained.
- Uncomfortably high indoor temperatures decrease the effect that sound pressure level and illuminance otherwise have in a comfortable thermal environment. This highlights the importance of designing for optimal temperature conditions and constitutes a basis for the use of personalized strategies.
- Gregarious individuals may be more thermally comfortable than non-gregarious individuals when there are many occupants in the room. Designers are encouraged to account for inter-individual differences by providing flexible working conditions.

Four predictive models LR, L-SVM, RF and RBF-SVM are trained using significant variables P_0 – P_5 . The models examine the predictive potential of the explanatory model. All models struggle to predict thermal (dis)comfort, despite the inclusion of significant thermal comfort variables. The results bring to light several conclusions:

- Significant thermal comfort influences are not always adequate predictors thereof.
- Researchers are advised to precede future thermal comfort studies with explanatory modelling, to facilitate the creation of predictive models that contain a large variety of variables.
- Combined use of explanatory and predictive modelling is necessary, to test whether variables considered in thermal comfort research hold theoretical relevance, predictive potential, both or, perhaps, neither.

This study is part of a broader research effort to achieve better prediction of thermal comfort in offices, which is an essential step in the building design process. The results formulate a basis for further research on the influence of indoor climate, occupancy and personality traits on thermal comfort in offices, as well as the interaction between the different influences. Moreover, the findings have direct implications for the engineering sector, as they suggest that influences such as sound pressure level, occupancy and personality traits, should be considered when designing for optimal thermal conditions.

6.1 limitations

This research is subject to several limitations, the mitigation of which is encouraged in the future. Firstly, prominent variables such as correlated colour temperature and air velocity are not included in the study. Similarly, variables such as age, relative humidity, clothing insulation and metabolic rate are excluded due to insufficient variability in the measured data. Secondly, extreme indoor conditions are not observed during field measurements. In addition, the measurements are limited to summer conditions in the context of the Netherlands and are not representative of cooler conditions or other climate regions. Due to this limitation, the relationship between temperature and thermal discomfort is assumed to be exponential. Future studies are encouraged to include cold sensation data and thereby model a parabolic relationship between temperature and thermal discomfort, where thermal discomfort increases at lower and higher temperatures both. Thirdly, the internal consistency of the personal variables is poor and they are not sufficiently representative of the Big Five personality traits. Lastly, the quality of the predictive models may be improved via the use of advanced hyper-parameter tuning, a larger variety of machine learning algorithms and more advanced modelling methods. ■

7. Acknowledgement

The data is provided by the research group of Mark Mobach at the Hanze University of Applied Sciences. The authors acknowledge the contribution of Yasin Toparlar, Deerns Groep B.V.


8. References

Please find the full list of references in the original article at: <https://proceedings.open.tudelft.nl/clima2022/article/view/181>

International Conference

World Sustainable Energy Days 2023

28 February - 3 March 2023
Wels/Austria



Energy
transition
=
Energy
security!

Conferences:

- European Energy Efficiency Conference
- European Pellet Conference
- Industrial Energy Efficiency Conference
- Smart E-Mobility Conference
- Young Energy Researchers Conference
- Innovation Workshops

www.wsed.at



Exploring futures of summer comfort in Dutch households



LENNEKE KUIJER

Future Everyday Group, Department of Industrial Design and Eindhoven Institute for Renewable Energy Systems, Eindhoven University of Technology, Eindhoven, the Netherlands
s.c.kuijer@tue.nl



LADA HENSEN CENTNEROVÁ

Building Performance Group, Department of the Built Environment, Eindhoven University of Technology, Eindhoven, the Netherlands

Abstract: This article describes the results of a qualitative study into cultural aspects of summer comfort in Dutch households. Results show that two main ways of preventing overheating – shading and summer night ventilation – compete with active cooling. Moreover, it identifies potential for technologies, policies and procedures to support adaptation to higher temperatures.

Keywords: Summer comfort, Netherlands, cultural change, qualitative study, dwellings, energy.

Introduction

The Dutch Meteorological Institute (KNMI) defines a heatwave as a period of at least five consecutive days with daily maximum temperatures exceeding 25°C, with at least three of the five days reaching maximum temperatures above 30°C. In the coming decades, heatwaves are expected to become longer, warmer, and more frequent [1]. On top of this, dwellings in the Netherlands have long been built with a focus on keeping warm during winter, resulting in high levels of insulation and airtightness that increase the risk of overheating. Other factors contributing to risks of overheating are large windows, urbanisation, and an ageing society.

Dutch households are beginning to adjust their lives and homes to these new circumstances. For those who can afford it, mitigating discomforts and health risks of hot weather are within reach, but tend to require high amounts of energy. Essent, one of the main energy providers in the Netherlands reported a 30% increase in energy demand during the August 2020 heatwave [2], and a 2021 study by research institute TNO [3] showed that 20% of Dutch households already have a form of active cooling, while 26% is considering to get it.

At this point in time, Dutch responses to global warming can still go in many directions, some of which are undesirable from health, inclusivity, and environmental points of view. Therefore, it is important to try and anticipate, and where possible redirect these pathways.

Actions in the present, such as building policies, proposing standards (e.g. EN ISO 52000-1, EN ISO 52016-1), designing infrastructure, building technologies, and passing on instructions have an effect on shaping futures of summer comfort in Dutch households. These actions, in turn, are informed by visions, assumptions and expectations of what futures are possible, desirable and likely to come about. However, insight into these futures from a Dutch household perspective is so far limited.

This raises questions like: To what extent are mainstream Dutch households equipped and able to equip themselves to deal with longer, warmer, and more frequent heatwaves? Which strategies do households apply and aspire to achieve comfort in times of hot weather, and which currently not? What are possible consequences of these strategies for levels and patterns of energy demand, and general well-being? What are developments outside of these households that may affect these strategies?

This article summarizes a selection of findings from a qualitative exploration of the future of domestic summer comfort in the Netherlands. A full version of the study results is available in an open access stakeholder report [4]. While the focus of the study is on the Netherlands, its outcomes may be relevant beyond this context, particularly in countries where active cooling is currently on the rise due to global warming.

Method

The study consisted of a set of interrelated research activities, primarily involving 21 household interviews and 10 domain expert interviews.

The household interviews were designed to capture the main daily domestic activities that are relevant to summer comfort. These were: (1) cooking and eating, (2) personal care and clothing, (3) laundering and cleaning, (4) home working, (5) free time, (6) sleeping, and (7) ventilating, shading and cooling.

The interviews were conducted around a heat wave in August 2020 (**Figure 1**). No actual measurements of indoor temperatures were made, so conclusions regarding temperatures are based on self-reported values, which tend to be less reliable. The use of workbooks with daily exercises, which primed participants to notice their indoor temperature values in the week before the interview, partly compensated for this.

The domain experts included HVAC, sleep, physiology, fashion, architecture, building standards, social housing and domestic shading. These interviews and additional sources, such as trade fairs and observations were used to identify and extrapolate current cultural, demographic and technological trends in domestic summer comfort.

Findings

Overall, the study confirms the expectation that the use of active cooling in Dutch dwellings is likely to increase in the future. This is reflected in growing sales figures of cooling systems, but also in actual and experienced overheating in dwellings, as well as frictions with emerging practices of shading and ventilation. The latter, along with embodied acclimatisation, have potential to

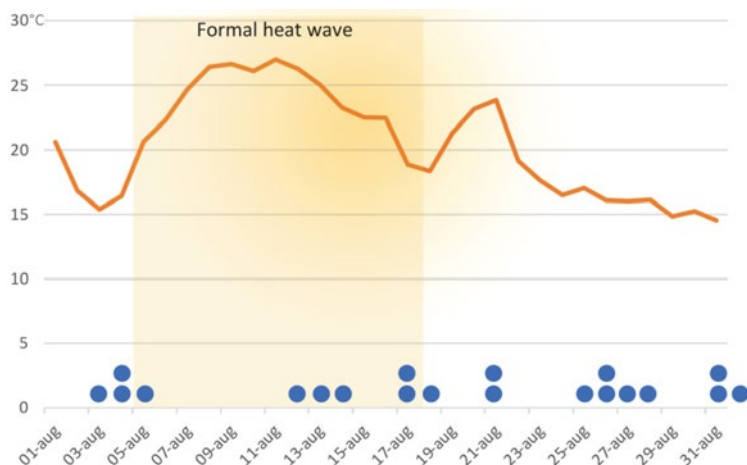


Figure 1. Timing of household interviews in relation to the August 2020 heatwave. Graph shows average temperatures measured at De Bilt weather station obtained from KNMI.nl. [4]

contribute to summer comfort in a low-energy manner. However, their establishment is hampered by existing infrastructures, historically shaped cultural values and habits, and competition between different activities. The sections below elaborate on these points.

Actual and experienced overheating

Overheating is already an issue in Dutch households. From the perspective of the NZEB (Net Zero Energy Buildings) standards, several dwellings in the study (all apartments) exceeded the threshold of 450 WHO_s (the Weighted Overheating Hours), which in the Dutch TO_{juli} -indicator start counting above 27°C. Overall, reported indoor daytime temperatures during the heat wave ranged from 24°C to 45°C for dwellings without cooling. The dwellings that reported temperatures over 30°C in their main living areas were all rented city apartments.

Stories of residents confirm that these dwellings become practically unliveable during a heat wave. Moreover, most households in the study considered their dwelling to be overheated well below the formal overheating threshold. Indoor temperatures above 25°C were considered too high by all but four participants, particularly for working and sleeping. These higher temperatures inhibited their freedom of movement and capability to go about their daily business, such as focusing on work, sleeping well, and performing housework.

These issues were absent for households with active cooling, but they were inhibited in other ways, particularly, in being outdoors. The data indicated that households with active cooling have a stronger tendency to take the car instead of walk or cycle, because stepping outside from a cooled space felt like 'hitting a wall'. In other words, spending time in cooled spaces reduced their willingness and ability to tolerate the higher outdoor temperatures.

With climate change, these overheating issues are expected to grow. The next sections go deeper into the strategies that households currently apply and aspire to deal with these issues.

Acclimatizing

Participants that were able to enjoy or accept the heat and modify their daily schedules around it were most capable of getting through the heatwave without too much discomfort. For example, families that had their summer holidays during the heat wave or a young person practicing mindfulness. However, the freedom to adjust one's daily schedule is not accessible for everyone, especially if heatwaves are to occur more often outside of summer holidays. Moreover, not all

bodies are equally capable of dealing with heat and these capabilities decrease with age [5,6].

However, the study shows that common knowledge among the general public on bodily responses to heat show a gap with state-of-the-art research, particularly regarding the role of sweat in dealing with heat (it is mostly seen as something negative) and the capability of bodies to adjust to higher temperatures over time. While research shows that people can adapt to heat by as much as 1°C per day as confirmed by the physiology expert, none of the participants referred to concepts of bodily adjustment to heat over time. This finding indicates that adjustments in knowledge, available products, skills, and attitudes to acclimatize could reduce people's experiences of being locked into their homes and bodies, and contribute to well-being in a low-energy manner. Put more strongly, the adverse mental and physical effects of reduced physical activity in hot weather might be partly mitigated if people (are facilitated to) acclimatize.

Cultural frictions with shading, ventilation and cooling

A seemingly embedded friction that arose from the interviews is the relationship that 'the Dutch' have with warm weather. Warm and sunny weather is associated with being outdoors and enjoying the light and warmth of the sun. In the spring, when days get longer and warmer, people open doors and windows to let fresh air in, extending their living spaces onto balconies and into gardens. Fluctuating temperatures mean that Dutch summers can have relatively cool spells that precede heatwaves. When temperatures go up, the sun is initially welcomed into the home. But when temperatures rise, this behaviour leads to overheating, which is then difficult to correct.

Proper, disciplined outdoor shading and summer night ventilation routines could reduce the extent to which indoor spaces heat up [7], but adopting these routines requires more than new equipment and behaviours. Viewing the sun as an 'enemy' instead of a 'friend' for part of the year requires a cultural shift. The Dutch friendship with the sun is deeply embedded in customs (opening doors, curtains and windows to enjoy light, views and fresh air), the built environment (ample, sun facing windows) and related professional practices such as architecture (disliking and sometimes prohibiting outdoor shading). For most of the year, the sun is and will remain a friend, helping to light and warm dwellings, and keep people healthy and cheerful. Learning to occasionally 'cool' this friendship requires a cultural shift that is necessary for the potential of shading and ventilation practices to develop (**Figure 2**).

Active cooling is more explicitly approached with reservation. Participants without active cooling are familiar with air conditioning, but find it too energy-consuming, noisy, expensive, and uncomfortable. However, even highly committed, knowledgeable residents in modern homes, equipped with the latest shading and ventilation technologies, had trouble maintaining a comfortable indoor climate without the use of active cooling. Many anticipated getting some form of active cooling in the future. Those who already had cooling were mostly content with their systems (except for mobile air conditioners). Although there are cultural and practical frictions to integrate active cooling into Dutch households, they seem easier to overcome than those related to shading and ventilating. Added to this lower barrier to uptake is the risk that active cooling creates a further threat for shading and ventilation practices to reach their potential because they compete.

Shading, ventilating and cooling compete

Shading and active cooling can complement each other in dwellings, but the study illustrates how they compete in the market. Both active cooling and outdoor shading require considerable investment.



Figure 2. Examples of inconsistent Dutch practices of shading and ventilating during hot weather (28°C). [Lenneke Kuijjer, August 2022]

If households have an opportunity to only invest in one, then cooling has the better position in terms of low-effort comfort. This competition is also visible in the current NZEB requirements, where adding a form of active cooling eliminates incentives for other, low-energy measures against overheating such as shading.

Cooling and summer night ventilation compete directly in the dwelling. While the cooling system is on, windows and doors need to be closed to retain the microclimate. This effect is even stronger for mobile air conditioners, used in three participating households, because securing the hose in the window can further hamper the opening of windows when the device is not in use. During the day, the hose in the window necessitates a (partly) open window enabling hot outside air to enter the dwelling (**Figure 3**).

In general, active cooling, when properly designed and installed, can secure comfortable temperatures in the dwelling regardless of other measures such as shading or ventilation. Shading and ventilation require the active involvement of residents. With active cooling in place, the incentive to invest money, time, and effort in them is reduced. Mobile air conditioners have a particularly problematic position in this respect because of their relatively low threshold, and energy-efficiency. While they can be life-savers on the scale of individual users, in the broader picture these appliances form undesirable symptoms of overheating in Dutch dwellings that contribute to the problem of climate change and heat islands [8].

Smart automation

These insights can be used to design measures that might slow down or prevent Dutch households from becoming dependent on energy intensive cooling

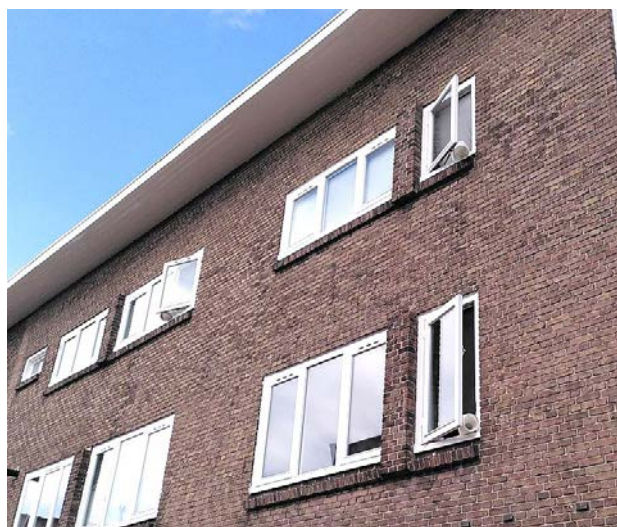


Figure 3. (Mobile) air-conditioners interfere with ventilating practices. [Lenneke Kuijer, August 2022]

equipment that could hamper the development of other strategies to deal with a warming climate.

Automation can play a role here. For example, when shading responds automatically to levels of solar gain, rain and wind, and ventilation to temperature and humidity differences inside and outside the dwelling. However, the role of residents cannot be ignored. Not only their autonomy in deciding whether to have these systems at all, but also in the ways they are used. The study revealed a wide array of circumstances in which people might disable automated shading, such as feeling locked-in, wanting more light, annoyance with repeated movement, wanting to open windows, etc. For ventilation systems, it became clear that their automated responses to CO₂ or humidity levels can conflict with summer comfort by drawing in hot outside air during the day, while summer night ventilation, in most homes, requires residents to open and close windows while they are sleeping. Further research is needed into this direction.

Pathways for active cooling

So far, active cooling is discussed as one practice, but in fact, different forms of active cooling are currently developing in parallel. Main pathways are radiant cooling and air-conditioning. Radiant cooling, mainly in underfloor settings powered by heat pumps or district cooling are relatively slow systems that cool the building mass. Such systems are likely to run continuously during hot weather. An advantage of these systems is that for ground source heat pumps, cooling can be provided on low-energy demand, or even energy-positive manners when heat is stored for use in winter (**Figure 4**).

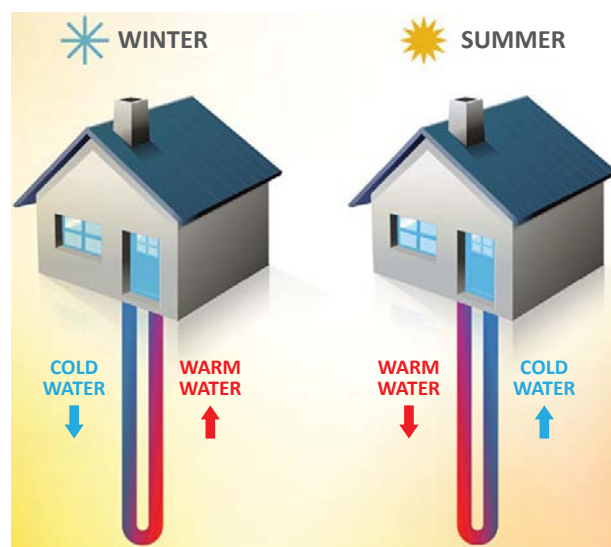


Figure 4. Storing summer heat in a ground source for use in winter. [4]

Air-conditioners work more quickly by directly cooling the indoor air and are more likely to be used based on occupancy and direct demand. Spaces also heat up again relatively quickly when they are off. Mobile air-conditioners allow for even more directed, person-oriented, albeit fleeting forms of cooling. Apart from their efficiency, these different patterns of use are likely to affect their overall energy demand.

Moreover, levels of energy demand for active cooling do not only depend on the type of systems and when it is used, but also on the set-temperature. At present, the temperatures to which households will set their cooling systems has not been settled or stabilised, but it is likely that norms around acceptable and normal temperature ranges will develop in the coming years and decades. With heating, for example, Dutch households presently tend to set their thermostat somewhere between 18 and 22°C. This normalised temperature range has formed and changed over a long time period [9], and varies per cultural context [10].

As illustrated in the introduction, building norms, standards and system design can play an important role in shaping these norms. Considering that technologies co-shape practices, it makes a huge difference for the way in which summer comfort practices will develop whether default settings, promotion

materials, media and installer instructions for cooling systems recommend setting the system to 18°C or 27°C, introduce some other metric like a combined humidity/temperature value, or are designed to offer a variable temperature that moves with the outdoor temperature and slowly increases over time to support acclimatisation.

Additional effects of warming on everyday life

The use of active cooling in the home seems to lead to a dependence on cooled spaces that extends beyond the dwelling. The examples in the study indicate a trend towards spending more time indoors, and the car becoming preferred over other means of transportation. Beside increases in CO₂ emissions and energy costs that accompany the increased use of most forms of active cooling, these trends indicate undesirable health effects resulting from lower activity levels and lower natural vitamin D intake.

Other areas in which increases in energy demand are likely to arise according to our finding are in increased capacity for cold food storage, showering and laundering. Several households reported that fruits and vegetables that are normally kept in dry storage are moved to refrigerators during hot weather, where they compete for space with more cooled drinks (**Figure 5**).



Figure 5. Demand for cold food storage increases in hot weather, but fridges and freezers heat up indoor spaces.

This leads to an increased demand for (larger) fridges and freezers—appliances which, in turn, directly contribute to overheating in dwellings due to the heat they produce.

The study also indicated that shower frequencies increase during hot spells. The main reason for more showers within the sample was not to cool down, but to rinse off sweat. This requires water, as well as energy to heat it. With a trend towards better insulated homes, these secondary effects could become significant.



Photo by Mandav / Shutterstock

Different consequences for different types of households and dwellings

While it is difficult to draw a strict line, some of the dwellings in the study were clearly overheated. These examples represent a larger group of households for which homes become unliveable for part of the year. Smaller, well-insulated dwellings, with higher window-to-content ratios, high sun exposure (e.g. in high-rise), little shading and ventilation opportunities, located in cities (heat islands) heat up quickly. Such dwellings are more likely to be occupied by lower-income households and are more often rented than owned. This might also mean that the potentially higher amount of time spent at home by the residents due to lower levels of employment could add to the overheating issues.

Also judging from recently introduced building standards in the Netherlands and elsewhere [11], overheating is slowly starting to be acknowledged as an issue, and social housing providers and landlords are beginning to contemplate on how to intervene. The study indicates that the costs of installing and maintaining outdoor shading on non-ground floor windows plays a role in hampering tenants and owners to act. Moreover,

explicit demand for shading and cooling seems low among social housing tenants. This could have all kinds of causes such as other more pressing issues on the tenants' minds, a fear of unmanageable rises in rent, unfamiliarity with the effects of shading and ventilation on overheating, or better skills of acclimatizing. Despite various efforts to involve low-income households, they were only present indirectly in the study through stories of higher income tenants, experts and observations during fieldwork. More research is needed into the specific issues, wishes and strategies of this group.

Conclusions

This study set out to gain more in-depth insight into the ways in which Dutch households are likely to deal with hot weather in their dwellings. Several opportunities were identified that might direct Dutch domestic practices of summer comfort onto more inclusive, healthy, and less energy-intensive pathways.

A range of opportunities present themselves around acclimatisation, i.e., modifying bodily relations with hot weather. There seems to be a gap between state-of-the-art physiological research on how bodies deal with heat and everyday knowledge among the households. The benefits of sweating (when combined with drinking enough water) as an effective way to deal with heat is not fully acknowledged. Moreover, none of the participants talked about bodily adjustment to heat over time, while experts confirm that this effect can be as strong as 1°C per day.

Outdoor shading during the day and ventilation during the night can reduce or prevent overheating in low-energy ways. The study shows that active cooling, while spreading quickly, reduces residents' acceptance of the experienced downsides of shading (including the costs) and lowers incentives and opportunities to utilise cooler night air. ■

Acknowledgement

We want to thank our experts and participants. This research was funded by the Dutch Research Council (NWO) under grant number VENI17343.

References

Please find the full list of references in the original article at: <https://proceedings.open.tudelft.nl/clima2022/article/view/388>

Correlation of subjective and objective air quality data in shopping centres as a function of air temperature and relative humidity



MAHMOUD EL-MOKADEM

RWTH Aachen University, E.ON Energy Research Center, Institute for Energy Efficient Buildings and Indoor Climate (EBC), Aachen, Germany



KAI REWITZ

RWTH Aachen University, E.ON Energy Research Center, Institute for Energy Efficient Buildings and Indoor Climate (EBC), Aachen, Germany



DIRK MÜLLER

RWTH Aachen University, E.ON Energy Research Center, Institute for Energy Efficient Buildings and Indoor Climate (EBC), Aachen, Germany

Abstract: Germany has 493 shopping centres mostly located in urban cities. According to STASTICA, the number of shopping centres was doubled in the last two decades [1]. For consumers, good indoor air quality (IAQ) is a basic requirement for their shopping experience. This leads to very high air exchange rates for current operation of HVAC systems in shopping centres. Accordingly, achieving good IAQ in combination with increasing energy efficiency is a main issue for operation of the shopping centres. Thus, in previous studies the intensity of shopping product emissions was evaluated by trained subject panels.

In this paper, we analyse the IAQ parameters not only by trained human panel, but also by analysing the volatile organic compounds (VOC) through objective tests. In a first step, we cluster five different product groups: books, clothing, shoes, coffee and perfume. Regarding these groups, we measure the emissions with objective and subjective tests for a variation of temperature and relative humidity. We use the results to investigate the influence of these environmental parameters on the subjective and objective intensity of the VOCs. Finally, we analyse the subjective data along with the objective data, to correlate the subjective evaluations with the measured sensor signal of the multi VOC sensor system. The evaluation is done with statistical data analysis methods such as Friedman test. The results show the potential for the metal oxide semiconductor sensors technology for detection of VOCs and for prediction of perceived intensity based on objective data. Furthermore, the results show an influence of air temperature and humidity on subjective perception.

Keywords: Indoor air quality, shopping centre, total volatile organic compounds, E-Nose, VOC

1. Introduction

Currently, air quality control in shopping centres is based on fixed high air exchange rates or on the measured CO₂ concentration, which is a good indicator for the emissions of persons and allows for demand-based supply

volume flow control. However, running the ventilation system with fixed volume flows does not lead to energy efficient operation and controlling the ventilation system based on only one parameter (CO₂) may not be sufficient from an air quality perspective. For example,

odours and contaminants emitted from shopping centre products are not detectable by CO₂ sensors.

Odours perceived by humans can often be traced back to so-called volatile organic compounds (VOCs). These substances occur in the air in the form of gases and vapours. Even low VOC emissions are often associated with significant odour perceptions and can lead to health problems. In contrast to CO₂ sensors, VOC sensors can detect mixtures of substances in the indoor air with a characteristic signal [2]. However, the control of ventilation using VOC sensors is rarely implemented, since no specific limit value is defined that could be used to as a setpoint.

Due to the large number of VOC emissions in shopping centres, the goal is to define acceptable objective limits for different product groups. Hence, extending current CO₂-based control by VOC-based control can improve air quality.

2. Methodology

2.1 E-Nose: Sensor Methodology

In this study, metal oxide semiconductor sensors are selected for the detection of volatile organic compounds. Their operating principle is based on the dependence of the electrical conductivity of metal oxides on the gas concentrations and gas types present. Metal oxide semiconductor sensors can be divided into thin-film and thick-film sensors and exhibit, among other things, high sensitivity to low gas concentrations, a long service life and a low price, which potentially qualifies them for use in the demand-based control of ventilation systems. On the other hand, their non-linear sensor characteristics depending on the gas concentration make calibration difficult. Moreover, drift and aging behaviour cannot be neglected. Furthermore, there is a cross-sensitivity of additional parameters such as relative humidity and air temperature [3].

2.2 E-Nose: Sensor system development

For the setup of the VOC sensor system, different metal oxide sensors of the MQ sensor series are used to enable the detection of several gases, such as CO, CO₂, H₂, NH₃, NO_x, ETOH, alcohol, and formaldehyde. The MQ sensors are connected to a single board Arduino Mega microcontroller for power supply and data transfer. In addition, a temperature sensor and a humidity sensor are integrated to compensate for cross-sensitivities. With the help of a TVOC sensor, the sum of volatile organic compounds can be recorded. Thus, total air pollution can additionally be estimated [4].

Figure 1 shows the final VOC sensor system.

2.3 Subjective and objective tests

The results of previous studies with subjective tests confirm the significant decrement of the acceptability of perceived air quality with increasing temperature and humidity [5–8].

The aim of the current study is to collect both subjective and objective data for the evaluation of odours or air quality for selected product groups and to derive possible limit values. In particular, the influences of air temperature and relative humidity are to be analysed. The objective evaluation is carried out with the developed VOC sensor system. The subjective evaluation is carried out with a group of test persons trained according to DIN ISO 16000-28 with regard to acceptance and perceived intensity by using acetone comparative scale [9].

2.3.1 Emission chambers

The study is conducted in the air quality laboratory of the Institute for Energy Efficient Buildings and Indoor Climate (EBC), RWTH Aachen University. The product groups are divided into 5 categories: clothing, books, shoes, perfume and coffee.

The products are filled into so-called emission chambers. The chambers are made of stainless steel to minimize the influence of oxidation reactions on the air. In addition, these chambers have a connection for introducing conditioned supply air via a central ventilation unit and an outlet fitted with a glass cylinder where test subjects can evaluate the air quality. Control of the supply air volume flow rate by measuring the actual condition via an orifice plate allows a precise adjustment of the air exchange in the emission chambers. To achieve good mixing even at low air changes, an additional mixing fan, which circulates the air in the chamber, is installed in each case.



Figure 1. Developed E-Nose.

Figure 2 shows an example of the positioning of the clothing and the sensor system in one of the emission chambers. The sensor system is positioned directly in front of the mixing fan.

2.3.2 Acetone comparative scale and subject panel

To evaluate the intensity of the shopping products emissions, an acetone comparative scale is used according to DIN ISO 16000-28. The test rig allows reproducible acetone concentrations. According to DIN ISO 16000-28, the acetone concentration in mg/m^3 can be converted into PI. Here, 0 PI corresponds to an acetone concentration of $20 \text{ mg}/\text{m}^3$. The increase by 1 PI corresponds to a linear increase of the acetone concentration of $20 \text{ mg}/\text{m}^3$.

In previous investigations Hegemann et. al used a maximum intensity of 14 PI for a shopping centre product (shoes) [10]. Since the current study also tests other products such as perfume, for which significantly higher ratings are expected, the upper end of the comparative acetone scale is extended to 28 PI ($580 \text{ mg}/\text{m}^3$). In choosing this value, the stated limits of $590 \text{ mg}/\text{m}^3$ by the National Institute for Occupational Safety and Health (NIOSH) for exposure over 24 hours are met [11].

According to DIN ISO 16000-28, the minimum size of a subjective group, for the evaluation of acceptance, is 15 persons (untrained) and for the evaluation of perceived intensity is eight persons (trained). For this study, 17 successfully trained test persons participated in the tests.



Figure 2. Positioning of the E-Nose and the product inside the emission chamber.

2.3.3 VOC classes for shopping centre products and method of detection

A classification of product groups from shopping centres or their emissions with respect to different VOC classes are investigated. Shoes, clothing, books, perfume and coffee, representing the food courts, are identified as relevant and suitable product groups for the main study. Sensors with correspondingly high sensitivity are also assigned to the VOC classes. For example, formaldehyde which can be emitted from new clothing, new shoes, or new books can be detected with HCHO sensor [12]. Sanaeifar et al. use the MQ-135 sensor for the detection of aromatic compounds emitted from food [13]. Perfumes and detergents contain alcohols, which can be detected with the MQ-3 sensor. Cosmetics containing alkanes can be detected with the MQ-2 sensor [14].

Since only three emission chambers are available, the study is divided into two sub-studies. In the first sub-study, clothing, shoes and perfume (variant 1) and in the second sub-study, books, coffee and perfume (variant 2) are evaluated. Perfume is tested for two source strengths, as the highest ratings were recorded here. The second variant corresponds to a 60% reduction in source strength compared to the first variant. In each sub-study, the group of test subjects is also divided into two sub-groups due to hygiene protection with regard to the COVID-19 pandemic, so that the first sub-group participated in the study in the morning and the second sub-group in the afternoon.

2.3.4 Test procedure

We selected one setting per day for the air temperature and the relative humidity of the supply air, which is kept constant during the day. Two hours before the arrival of the test subjects, the test stand is switched on to create stationary boundary conditions. After a welcome and brief acclimatization of the subjects, the evaluation begins. Once an evaluation is completed for all three emission chambers, the volume flow rate or air exchange rate is varied. During the test run, the subject group is almost exclusively in the air quality laboratory. After all assessments are completed, the subjects are dismissed. The parameter variations carried out were chosen to be inside the acceptable thermal comfort range boundaries [15]. Temperatures are chosen to 20°C , 23°C and 27°C , relative humidity is selected to 30% and 50% and air change rate is varied in 6 steps between 5.1 to 1 h^{-1} . This leads to 36 evaluations per subject and product.

In addition to the evaluation of the perceived intensity, the percentage of dissatisfied subjects is analysed using the question: "Imagine you were exposed to the air from the emission test chamber for several hours a day.

Would you rate the odour as acceptable?" "Yes" and "No" are available as response options. The proportion of no ratings is defined as the proportion of dissatisfied.

3. Results

3.1 Influence of temperature and humidity on the perceived intensity

In **Figure 3**, the ratings per air exchange setting averaged over all test subjects are plotted against temperature for a relative humidity of 50%. These mean values are shown as coloured circles per product group. Based on the results, a direct proportional relationship between air temperature and perceived intensity can be seen for each product groups. Furthermore, the difference in perceived intensity due to the product groups is significantly higher than the influence of temperature.

Figure 4 shows the effect of relative humidity on the perceived intensity for perfume (variant 1). The results for the relative humidity of 30% are shown as red circles, respectively as black crosses for 50%. In addition, the regression lines are drawn. Both regression lines run almost parallel with the same slope. However, the perceived intensity at 50% humidity is rated higher by about 2 PI compared to 30% humidity. The results for the other product groups show similar behaviour. Overall, it can be concluded that an increase in temperature and humidity leads to an increase in perceived intensity.

To evaluate the statistical significance of the temperature and humidity variation with respect to the subjects' evaluation, the Friedman test is used. The Friedman test is a statistical test suitable for evaluating non-parametric data as it does not assume a normal distribution of the data [15]. As a result of the test statistic, the "P-value" is compared. In our case, if $P > 0.05$, the null hypothesis cannot be rejected, and a difference between the samples distributions cannot be detected. If $P < 0.05$, the null hypothesis is rejected, and the alternative hypothesis is accepted.

The Friedman test leads to P-values smaller than the defined significance level ($P < 0.05$) with range from $3.30e^{-13}$ to $6.95e^{-55}$, so that statistically significant differences due to the variation in temperature and humidity can be assumed.

3.2 Influence of temperature and humidity on acceptance

Figure 5 shows the percentage of dissatisfied people for the perfume product (variant 1) across the different scenarios. The values in each scenario represent an

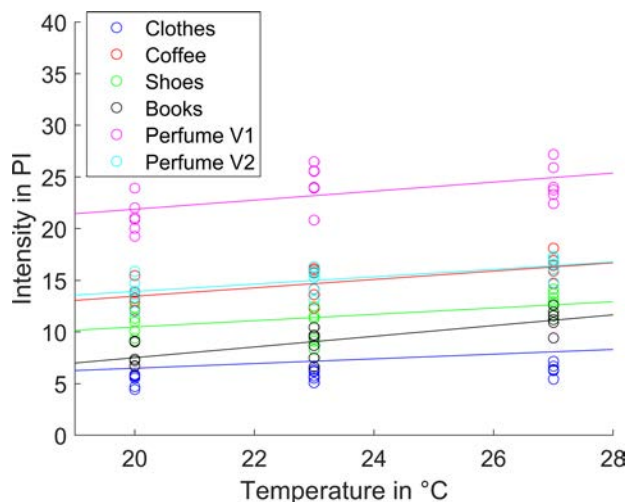


Figure 3. Influence of temperature on the perceived intensity at 50% relative humidity.

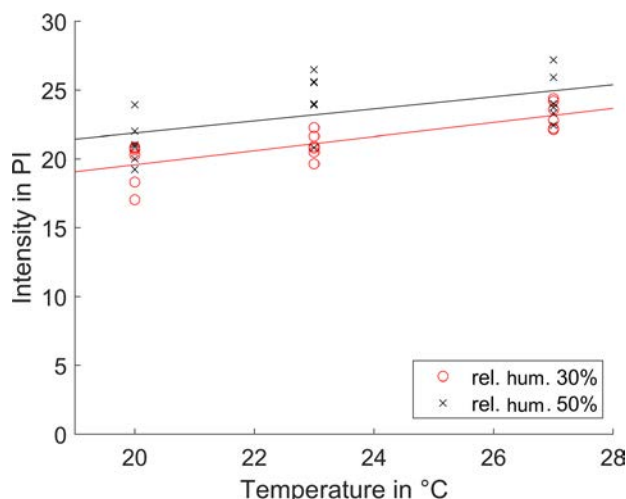


Figure 4. Influence of relative humidity (rel. hum.) on the perceived intensity for perfume (variant 1).

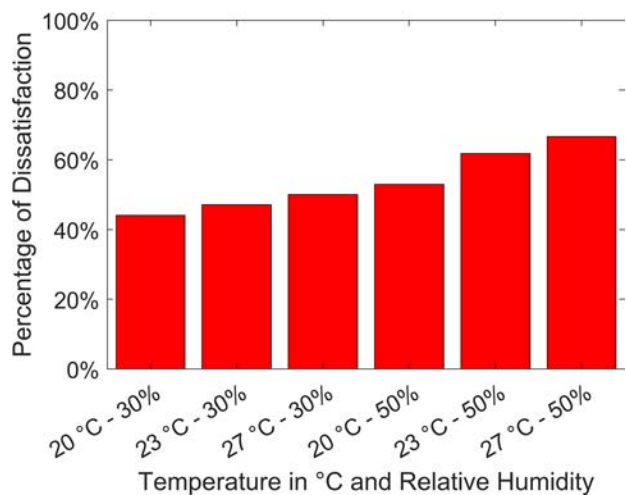


Figure 5. Influence of temperature and humidity on percentage of dissatisfied for perfume (variant 1).

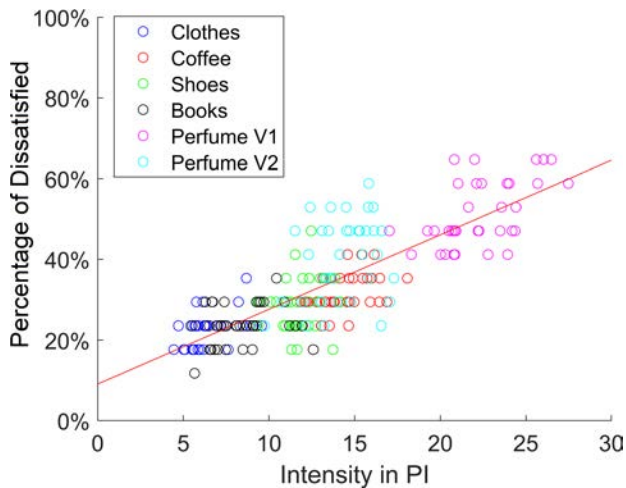


Figure 6. Correlation between perceived intensity and percentage of dissatisfied.

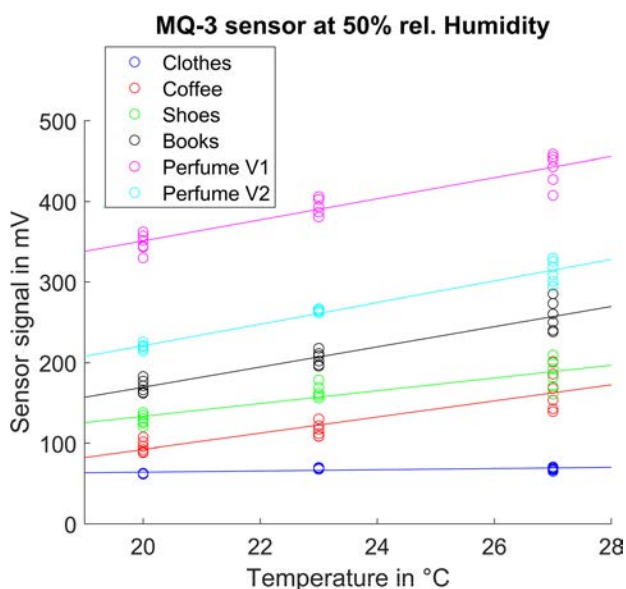


Figure 7. Influence of temperature on the sensor signal at 50% relative humidity for MQ-3 sensor.

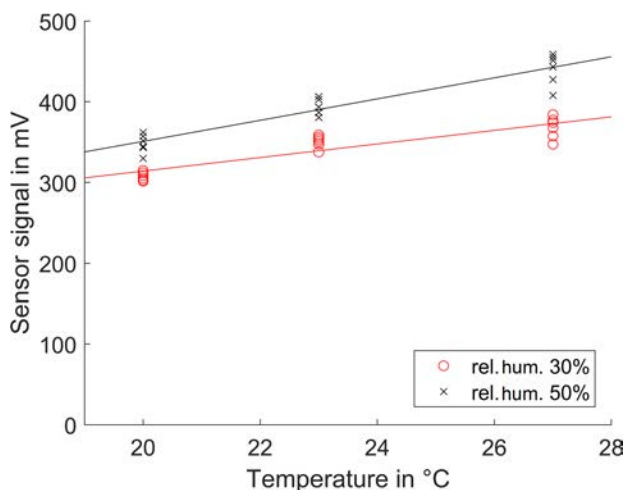


Figure 8. Influence of relative humidity on the sensor signal for perfume (variant 1) for MQ-3 sensor.

average value over all test subjects and analysed air change rates. The percentage of dissatisfied people increases with rising air temperature and rising relative humidity. The influence of the temperature is higher at a relative humidity of 50% than at 30%.

In **Figure 6**, the percentage of dissatisfied people is plotted against the perceived intensity. The coloured symbols are mean values of the 17 evaluations by the test persons for each combination of product, temperature, relative humidity and air change rate. The range of ratings for the products studied varies. The highest ratings for perceived intensity and the proportion of dissatisfied persons exist for the product perfume (variant 1). The lowest ratings occur for clothing and books, with an intensity of approximately 5 PI resulting in a proportion of dissatisfied of approximately 20%. The data shows that the proportion of dissatisfied people increases with the perceived intensity.

3.3 Influence of temperature and humidity on the sensor signal

In the following, the results for the MQ-3 sensor are presented since it has the highest sensitivity to the products investigated. **Figure 7** shows the sensor signal as a function of temperature for various products at a relative humidity of 50%. For all products except clothing, the sensor signal increases with increasing air temperature.

Comparing this with the subjective data from **Figure 3**, a similar behaviour can be seen for the sensor signal as a function of temperature. When looking at the order of the perceived intensities with the measured sensor signals, it can also be seen changing in the ranking of the products between the subjective and objective output. For example, the subjects rate coffee as more intense than shoes, books and clothing, whereas the sensor signal is only weaker for clothing than for coffee.

Figure 8 shows the sensor signal as a function of temperature for perfume (variant 1) at a relative humidity of 30% and 50% for the MQ-3 sensor. The sensor signal increases with increasing relative humidity. This behaviour is similar to the observation for the evaluation of perceived intensity in **Figure 4**.

3.4 Correlations between objective and subjective evaluation

To use VOC sensors for demand-controlled ventilation in shopping centres, limit values are needed that can be used as set points for the controlled variables. In **Figure 9**, the perceived intensity (subjective values) is plotted against the sensor signal for the MQ-3 sensor.

For the different product groups the point clouds in the diagram have different positions. In consequence, the correlation of the perceived intensity and the sensor signal should be done depending on the product groups. In addition, linear regression lines are shown

Table 1. Derived correlations between sensor signal in mV (x) and perceived intensity in PI (y).

Data	Correlation	R ²	RMSE
All data	$y = 0.05 \cdot x + 4.75$	0.65	3.2 PI
Books	$y = 0.026 \cdot x + 3.72$	0.40	1.4 PI
Coffee	$y = 0.026 \cdot x + 11.48$	0.30	1.5 PI
Clothes	$y = 0.053 \cdot x + 3.39$	0.40	0.9 PI
Perfume	$y = 0.05 \cdot x + 5.20$	0.65	2.5 PI
Shoes	$y = 0.026 \cdot x + 7.09$	0.20	1.5 PI

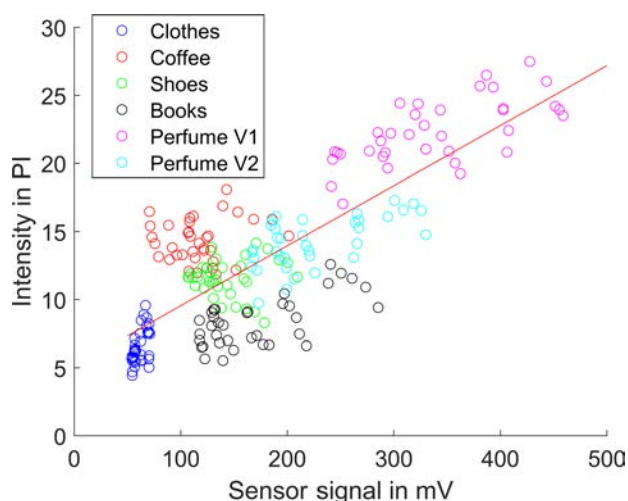


Figure 9. Correlation between the sensor signal of MQ-3 and the perceived intensity.

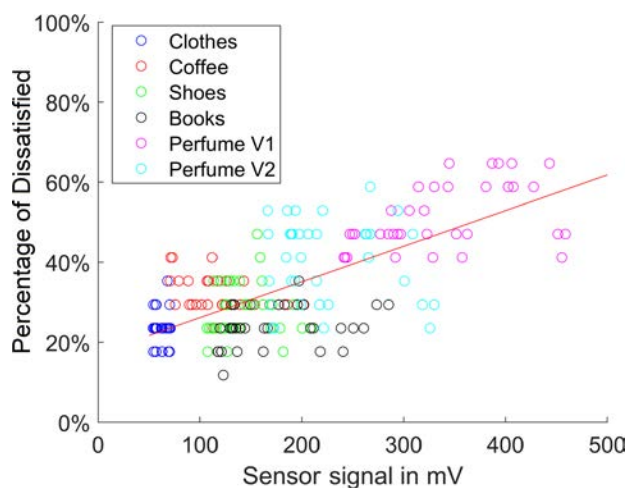


Figure 10. Correlation between the sensor signal of MQ-3 and the percentage of dissatisfied.

on the basis of the five product groups investigated, whose functions, the coefficients of determination R² and the root mean square error (RMSE) are contained in **Table 1**.

In each case, a linear regression approach is used to derive a correlation between the sensor signal in mV and the perceived intensity in PI. The coefficient of determination for the separate analysis of the product groups is smaller than the overall regression data. It is noticeable that for books, coffee, and shoes, the slope of the regression function is the same, and only the Y-axis intercept differs. In **Figure 10**, the percentage of dissatisfied persons is plotted against the sensor signal of the MQ-3 sensor for the product groups investigated. It can be observed, that with increasing sensor signal the percentage of dissatisfied is rising. However, a strong scattering of the data along the regression line drawn can be seen. This makes it difficult to derive an exact objective limit value to reach a specific percentage of satisfied people or not to be too restrictive to guarantee a minimum percentage of dissatisfied.

4. Conclusion

In order to detect emissions from building materials and products in shopping centres, VOC sensors are suitable in principle. Based on the results of the study carried out, it is possible to correlate the objective sensor signals with subjective evaluations for individual product groups. However, the determination of exact limit values in order to achieve a certain acceptance of the air quality must be set with caution due to the scattering of the data. With a larger amount of data, which would require further studies, it would also be possible to use machine-learning methods to analyse the data. With these, it might be possible to derive correlations between multiple sensor signals and subjective evaluations much more easily and robustly. Important findings were also obtained in connection with the influence of air temperature and humidity on subjective perception. Thus, for all products investigated, the perceived intensity and the proportion of dissatisfied persons increase with rising temperature and relative humidity. These findings can help implement an energy-efficient heating, cooling, and ventilation system operation in shopping centres. ■

5. References

Please find the full list of references in the original article at: <https://proceedings.open.tudelft.nl/clima2022/article/view/418>

Cross-infection risk between two people standing close to each other at different room temperatures



PETER V. NIELSEN

Aalborg University
pvn@civil.aau.dk

If we look at the exhalation flow from a person standing in a room with Mixing Ventilation and an air temperature T_a of 21°C, we will see that the exhalation will take an upward direction. The reason is that the pulsating exhalation flow has an initial temperature T_{exh} of 34°C. The exhalation will be entrained with room air in a forward movement and will decrease at temperature level, but it will keep a temperature higher than the surroundings and therefore have an upward movement, in principle to the ceiling level, **Figure 1**.

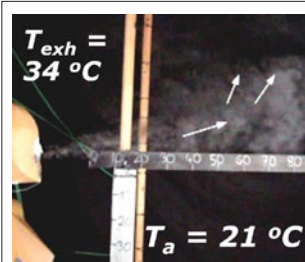


Figure 1. Pulsating exhalation flow in surroundings with fully mixed flow. Liu et al. (2009)

The horizontal length of the exhalation flow is a function of the temperature difference $T_{exh} - T_a$. If the temperature difference is large, as in cold surroundings, we will obtain a short length, but we will on the other hand have a substantial length in hot surroundings. The horizontal lengths will also depend on the person's activity level and on activities such as speaking, singing, coughing etc.

Things are different in a room with stratified flow as in the case of Displacement Ventilation. **Figure 2** shows that the exhalation will be stratified at a certain height, which could be just above the height of a person's mouth. The increased temperature versus height will lock the exhalation at a certain height.

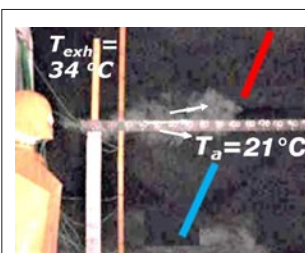


Figure 2. Pulsating exhalation flow in surroundings with stratified flow. The room temperature at the height of the mouth is 21°C. Liu et al. (2009)

When we conduct research, we often investigate the usual situations. For example, we consider the room temperature to be at comfort level, around 21°C. This is not the case in many practice situations where it could be more than 34°C in the summer in some countries and it could be 10°C in shops, for example, handling foods.

A COBEE 2022 conference paper shows new experiments with different room temperatures, Nielsen et al. (2022). The paper shows that the different lengths and directions of exhalation, obtained at different room temperatures, will influence the cross-infection risk between two people standing close to each other.

The paper shows that hot surroundings do increase the cross-infection risk to a high level at high room temperatures. It also shows that the cross-infection risk between two people standing close to each other will decrease in cold surroundings.

Figure 3 shows video stills of the exhalation flow from the index manikin. The exhalation flow is primarily governed by momentum in the first part, independent of the surrounding room temperature. It is obvious that the buoyancy effect changes the movement in an upward direction for the room temperatures 17°C and 25°C in the later flow.

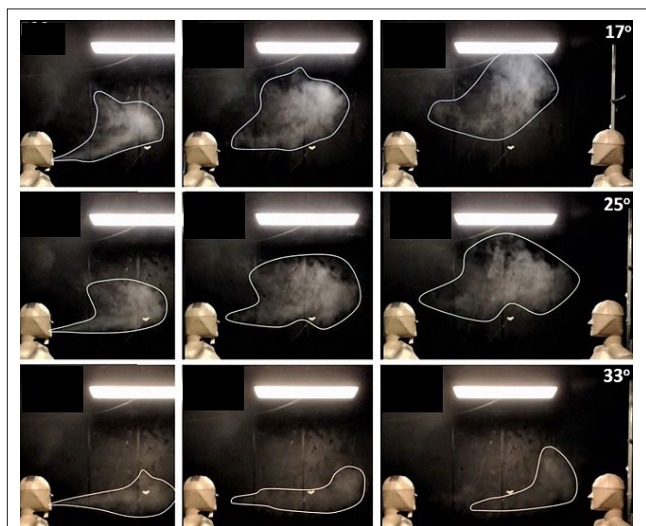


Figure 3. Exhalation flow from an index manikin standing 1.0 m in front of a susceptible (target) manikin. Each row shows the flow at one of the three room temperatures: 17°C, 25°C and 33°C.

When the room temperature is 33°C, there will be almost isothermal surroundings due to an exhalation temperature of the same level and the buoyancy effect will not be present. The horizontal direction seems to be blocked by the thermal plume from the target manikin. **Figure 3** shows that the growth rate of the vertical height of the exhalation flow is reduced in the $T_a = 33^\circ\text{C}$ case, indicating that it is a stratified flow with a reduced turbulence level.

The cross-infection risk is increased from 2 to 6, expressed as normalized exposure in case of mixing ventilation, when the room temperature increases from 23 to 33°C. (Distance between persons are 0.35 m). ■

Literature: please see the online version at rehva.eu

Smart air quality control in residences for optimised energy use and improved health of occupants



ELIZABETH COOPER

Dr, Lecturer
UCL Institute for Environmental
Design & Engineering



YAN WANG

Dr, Research Associate
UCL Institute for Environmental
Design & Engineering

Introduction

The premise of the work described here was to determine if a tailored application of building information and communication technologies might improve occupant comfort and health. This work explored the novel concept of connecting the predicted effects of a building control system with a health impact assessment, an important and innovative step in the creation of holistic and responsive building controls.

People in the UK, as with most of the Global North, spend nearly 65% of their time at home, where concentrations of particulate matter less than 2.5 μm in diameter, (PM_{2.5}) can be much higher than in outdoor air due to occupant behaviours such as cooking and smoking. PM_{2.5} has been linked to many serious health effects, including lung cancer, stroke, heart disease, and asthma. The good news is that previous research has reported that portable home air purifiers (HAPs) equipped with High Efficiency Particulate Air (HEPA) filters can effectively reduce PM_{2.5} levels in the rooms in which they are used. An important factor which has the potential to conflict with air filtration strategies in buildings, is occupants' operation of windows. The operation of windows also exerts a substantial impact on thermal comfort and building energy consumption. In this context, the research presented here aimed to develop a novel building control framework in which the operation of windows and the use of portable home air purifiers were optimised for energy efficiency and occupant health.

Building control systems play a central role in building operations and performance. Satisfying occupants' comfort and minimising building energy consumption

and carbon emissions are generally the intentions behind the design of a building control system. These systems, in general, share a common structure; first, the **sensor** measures an environmental parameter (e.g., temperature, CO₂ concentration); second, the sensor sends collected data to the **controller** which then uses pre-programmed control logic to determine the direction of change (if any). Window control systems have become a research topic gaining increasing interest in recent years, and research into HAPs has, independently, become a growing area of study. Although both automatic window controls and HAPs have, in recent years, but of increasing interest, an integrated system, which controls both window operations and HAPs, has not yet been investigated.

Methods

The proposed control framework included two modes; for the non-heating period, the control framework has both HAP and window controls running in parallel; during the heating period, windows are set to be closed, and the mechanical ventilation with heat recovery (MVHR) system operates continuously to provide background ventilation, and the HAP is enabled. The two control modes are shown schematically in **Figures 1 and 2**. In both modes, when the indoor PM_{2.5} concentration reaches the defined 'HAP-on' threshold (15 $\mu\text{g}/\text{m}^3$) the HAP switches on and continues to operate until the concentration falls below the defined 'HAP-off' threshold (5 $\mu\text{g}/\text{m}^3$).

When the residence is occupied, the default state of the window is fully open to optimise natural ventilation. However, the window is set to fully close

when certain conditions are met; either the indoor temperature falls outside the limits of EN 16798-1 Category II adaptive comfort temperature, or when both the outdoor PM_{2.5} concentration is higher than that indoors, and the indoor temperature is within the comfort zone, to reduce the working load of the HAP.

Quantitative health impact assessments are used to estimate future rates of mortality and morbidity from different interventions compared to what is predicted without such changes. In the work presented here, life-table models were used to quantify the impacts on mortality from reductions in indoor PM_{2.5}-concentrations due to the implementation of the control framework.

The life-table method is based on age- and sex-specific mortality rates, which are used to calculate probabilities of survival by year-of-age and calendar year. An impact assessment is performed using the underlying mortality rates which are adjusted to reflect changes in mortality risk from changes in exposure by applying relative risks calculated using available epidemiological evidence. Individual single-year survival probabilities are multiplied together to calculate cumulative probabilities of survival over multiple years. These cumulative survival probabilities are applied to a population allowing the calculation of life years lived by the population (where one life year is a full year of life lived by one person), which in turn can be used to estimate the average remaining life expectancy per person by age.

Results

The proposed hybrid control framework, along with either HAP or auto-window control alone for comparison, was tested in building simulations for a one-bedroom apartment. The simulation results for a summer week are presented below.

In the baseline scenario, without any control measures, there were morning and evening peaks of indoor PM_{2.5}

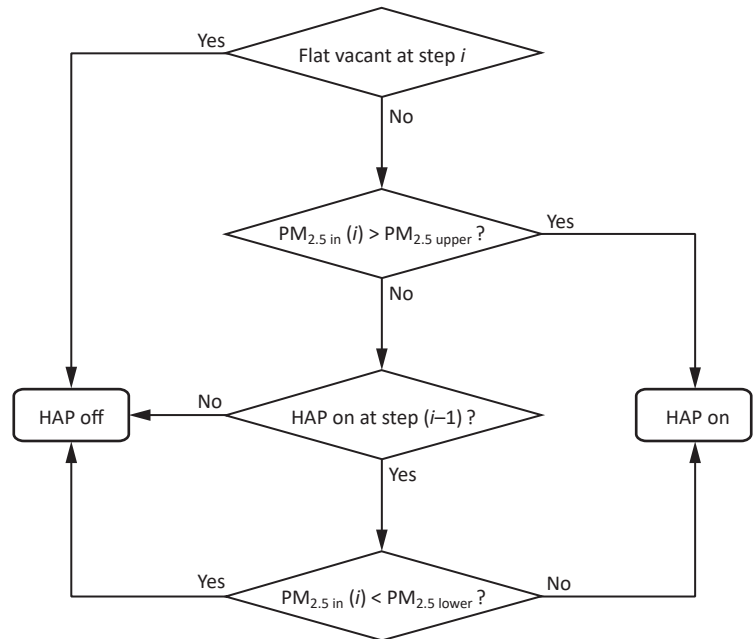


Figure 1. Algorithm for HAP control. (PM_{2.5} in: indoor PM_{2.5} concentration, PM_{2.5} upper: HAP-on threshold, PM_{2.5} lower: HAP-off threshold, *i*: time step).

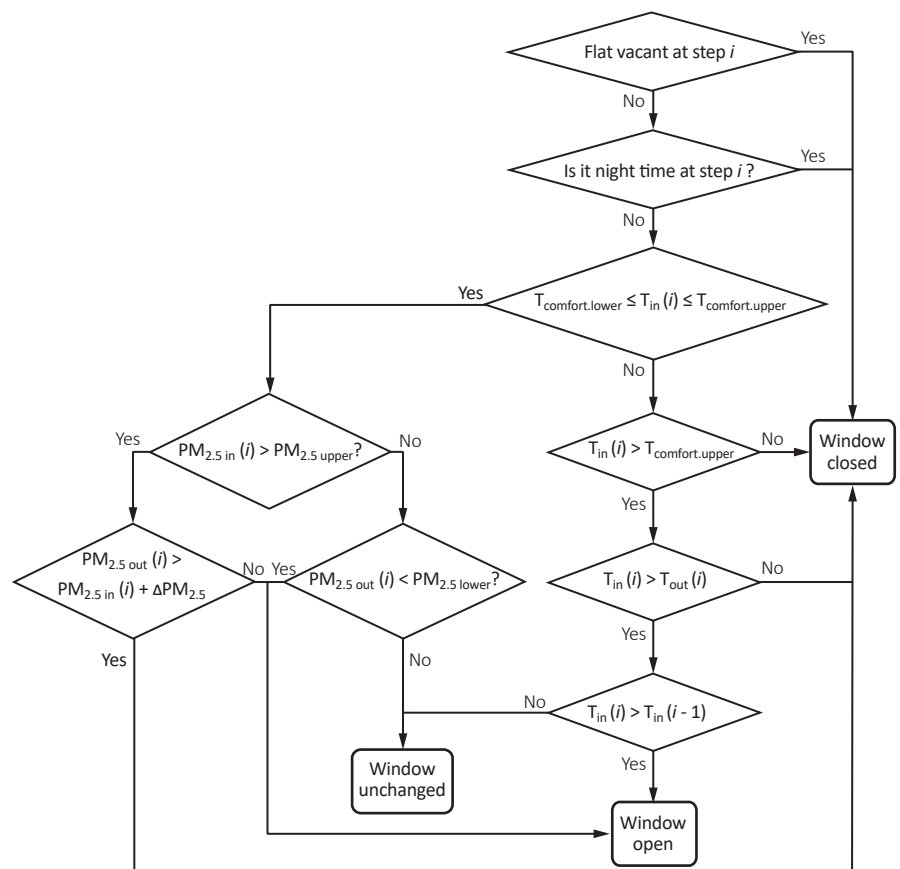


Figure 2. Algorithm for window control. (T_{in}/T_{out} : indoor / outdoor temperature, $T_{comfort.upper} / T_{comfort.lower}$: upper / lower limit of comfort temperature, PM_{2.5} in / PM_{2.5} out: indoor / outdoor PM_{2.5}-concentration, $\Delta PM_{2.5}$: the maximum accepted difference between indoor and outdoor PM_{2.5}-concentration, *i*: time step).

concentration, and the daily mean of indoor $PM_{2.5}$ concentration exceeded the WHO 24-hour limit ($15 \mu\text{g}/\text{m}^3$) for most of the week. However, the indoor temperature remained within the comfort range the entire week (Figure 3).

In the auto-window control mode (Figure 4), there was a significant reduction in the peaks of indoor $PM_{2.5}$ concentration. The number of days exceeding the WHO limit of $PM_{2.5}$ concentration fell by two from the baseline and occupant thermal comfort was still satisfied.

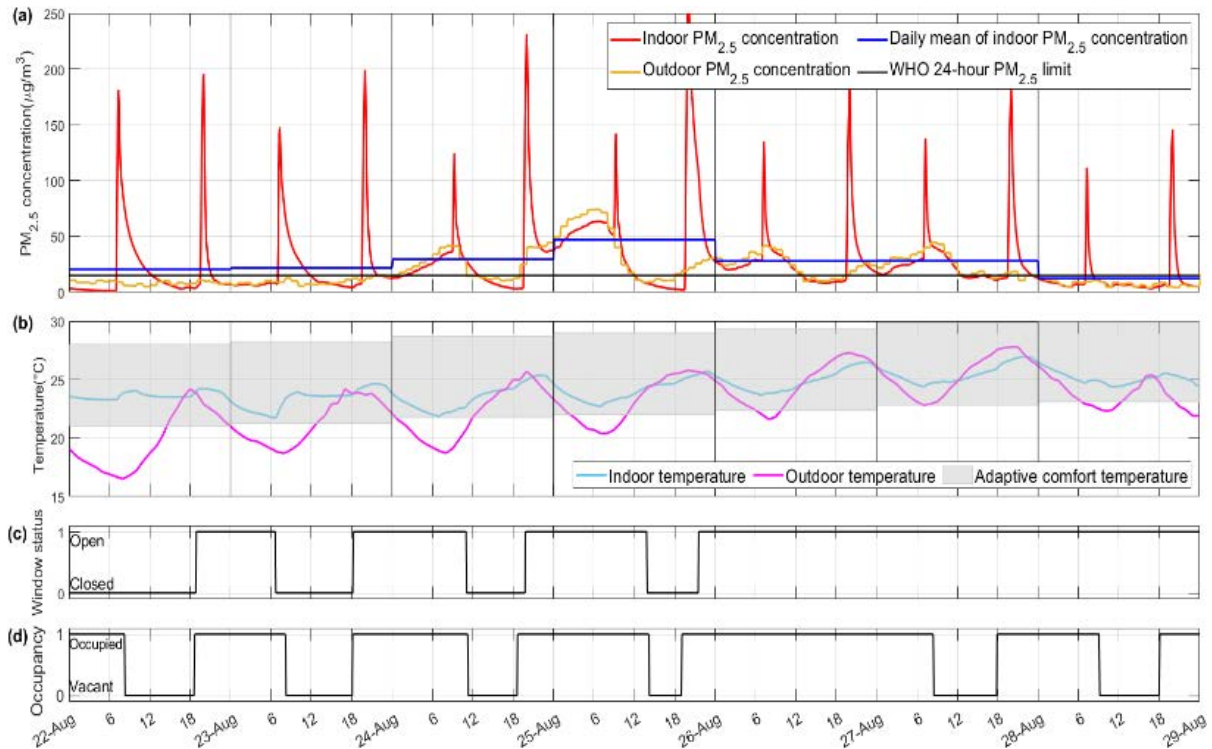


Figure 3. Summer week: Baseline. (a) Indoor and outdoor $PM_{2.5}$ -concentrations with the daily mean of indoor $PM_{2.5}$ concentration compared with the WHO guideline; (b) indoor, outdoor and adaptive comfort temperatures; (c) window state schedule; (d) occupancy schedule

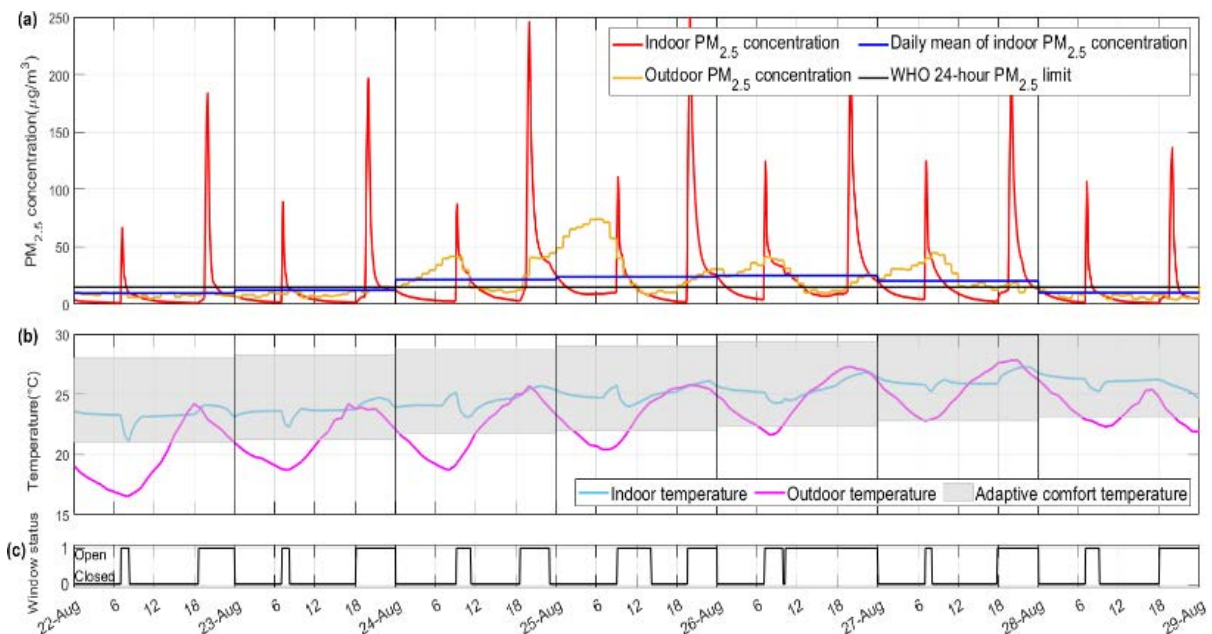


Figure 4. Summer week: Auto-window mode. (a) Indoor and outdoor $PM_{2.5}$ -concentrations with the daily mean of indoor $PM_{2.5}$ concentration compared with the WHO guideline; (b) indoor, outdoor and adaptive comfort temperatures; (c) window state schedule.

Figure 5 shows the HAP control mode where the peaks of indoor $PM_{2.5}$ -concentrations were further reduced from both baseline and auto-window control. However, because of high outdoor $PM_{2.5}$ levels, even with the use of HAPs there were still two days when the daily mean concentration of indoor $PM_{2.5}$ was above the WHO limit.

The hybrid control mode, shown in **Figure 6**, represents the proposed control method. With both HAPs and windows controlled, the indoor $PM_{2.5}$ concentration never exceeded the WHO daily limit, whilst indoor temperature was maintained within the comfort range.

The major advantage of the joint control of HAPs and windows was that the window could be shut when outdoor pollution was high before an accumulation of $PM_{2.5}$ could occur indoors. In this way, the indoor $PM_{2.5}$ concentration was lowered while optimising the HAP operation and efficiency. Meanwhile, the control algorithm was directed, when the outdoor air quality was good, to open the window to allow for natural ventilation.

The simulated reductions in indoor $PM_{2.5}$ -concentrations, from baseline, for each of the control modes were used to estimate the mean years of life gained (YLGs) for females and males in the UK over

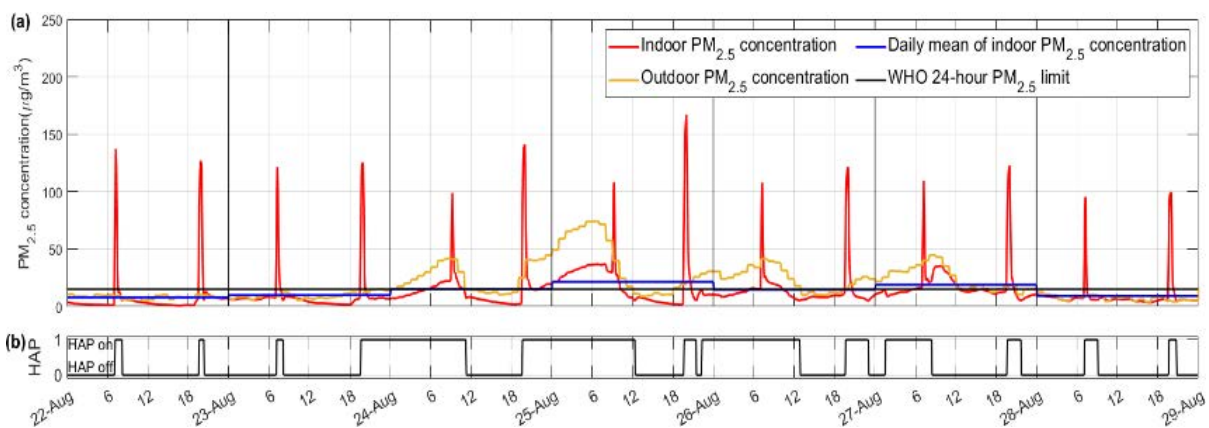


Figure 5. Summer week: HAP mode. (a) Indoor and outdoor $PM_{2.5}$ -concentrations with the daily mean of indoor $PM_{2.5}$ concentration compared with the WHO guideline; (b) HAP operation schedule.

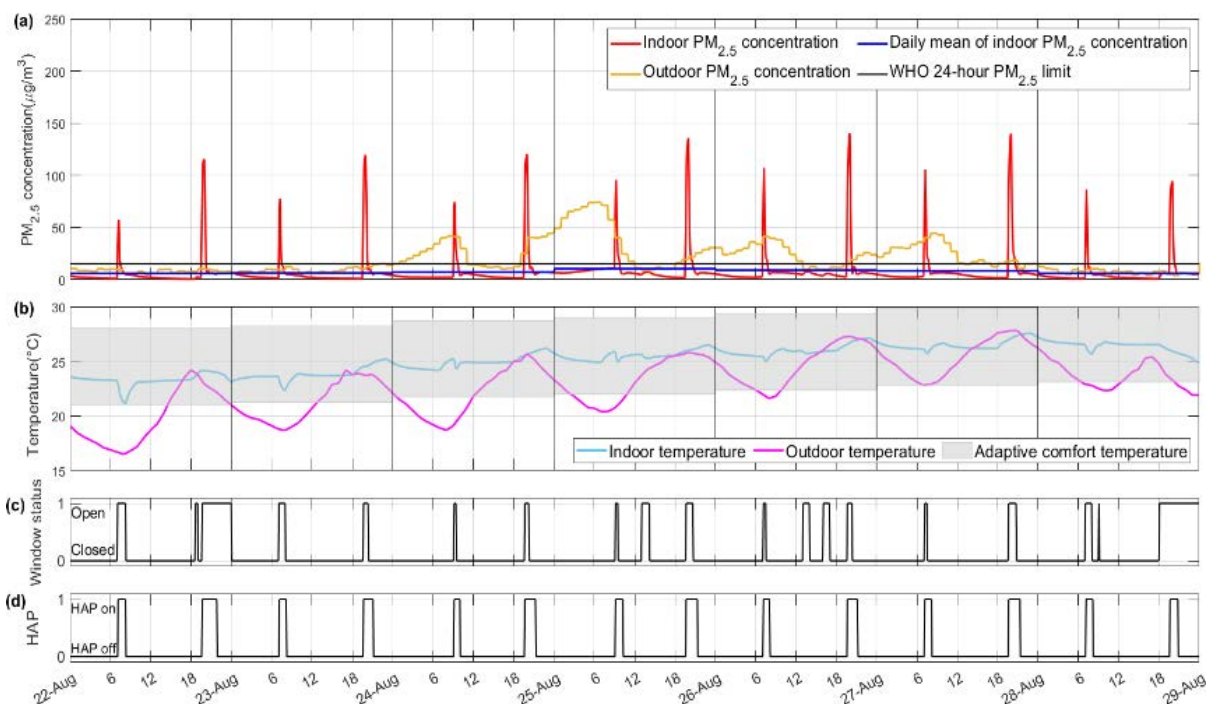


Figure 6. Summer week: Hybrid mode. (a) Indoor and outdoor $PM_{2.5}$ -concentrations with the daily mean of indoor $PM_{2.5}$ concentration compared with the WHO guideline; (b) indoor, outdoor and adaptive comfort temperatures; (c) window state schedule; (d) HAP operation schedule.

a lifetime (97 years). The mean YLGs for males were approximately 6.5 million, 15 million, and 18 million for the automatic window/MVHR, HAP, and hybrid modes respectively. For females YLGs were approximately 6 million, 14 million, and 16 million for the three intervention scenarios, respectively (Table 1). The reduction in exposure to PM_{2.5} from the implementation of the hybrid mode added a mean of nearly 6 months of life for both males and females.

Key Messages

For building designers and engineers, this work highlights the importance of recognising health impacts, as well as energy efficiency and environmental impacts, related to occupant-centric building design and operation.

For policymakers, this research adds technical evidence of the impact of including health metrics in the building sector.

Table 1. Summary of life-table model estimates of changes in mortality from different environmental control strategies based on modelled PM_{2.5}-concentrations in case study flat.

Control mode	Males		Females	
	YLG Mean	Mean days gained	YLG Mean	Mean days gained
Auto-window / MVHR	6,557,926	73	5,948,462	64
HAP	15,209,453	168	13,739,074	148
Hybrid	17,940,660	199	16,188,821	175

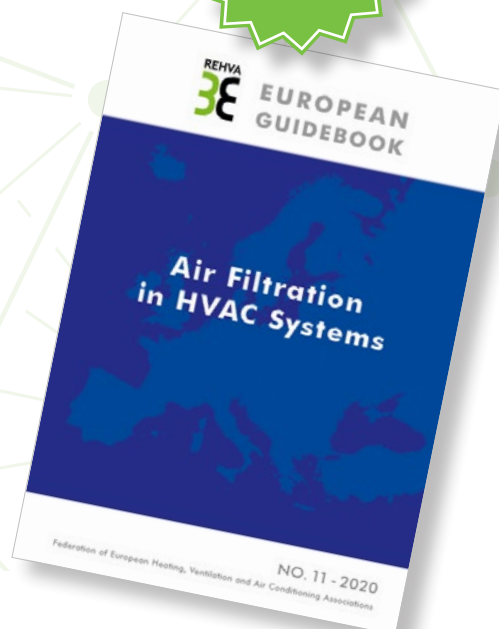
The implementation of smart building control systems, such as those modelled here, has the potential to reduce exposure to indoor pollutants such as PM_{2.5} which could have substantial population health benefits. ■

REHVA EUROPEAN GUIDEBOOKS

Air Filtration in HVAC Systems

No.11

This Guidebook will help the designer and user to understand the background and criteria for air filtration, how to select air filters and avoid problems associated with hygienic and other conditions at operation of air filters. The selection of air filters is based on external conditions such as levels of existing pollutants, indoor air quality and energy efficiency requirements.



REHVA  40 RUE WASHINGTON 1050 BRUSSELS, BELGIUM
 +32-2-5141171  INFO@REHVA.EU  WWW.REHVA.EU

Why a unified IAQ approach is critical to securing public health



MORTEN SCHMELZER

Technical Marketing Director,
Head of Public Affairs,
Systemair Group
morten.schmelzer@systemair.com

Morten Schmelzer, Technical Marketing Director, Head of Public Affairs, Systemair Group, traces the rise and fall of IAQ in the public and political consciousness, the shortfalls of standards and legislation promoting good indoor air, and how addressing the lack of common language and related discussions is critical to achieving a healthier population.

How IAQ has evolved over the years

Over the years, the market's acceptance of Indoor Air Quality (IAQ) has varied. In response to the 1973 and 1979 energy crises, the building industry focused mainly on insulation with limited attention to IAQ. As modern buildings became increasingly tighter to optimise energy usage, ventilation was (re-) discovered to bring fresh air into these tight buildings. Yet, still, there was no genuine interest in the health aspects of indoor air from ventilation. Architects and regulatory committees neglected the topic, and there was little to no concern about IAQ improving the health of occupants.

In time there was a shift in consciousness among architects and building specialists. Since the 1990s, IAQ has gathered momentum, attracting scientific interest, following the development of innovative IAQ equipment within the HVAC industry.

During the early days that IAQ was gaining traction, it was mostly considered an element of building protection, with a strong focus on mould. While it became a consideration for special applications such as operating theatres in hospitals, it remained primarily overlooked in schools, offices, and residential buildings where the only ventilation practice commonly used was opening windows.

There have been positive movements globally, with schemes such as WELL and RESET, initiated around 2010, gaining further traction. These schemes primarily aimed to qualify IAQ in major industrial cities confronted with pollution. Meanwhile, IAQ has become a criterion in LEED and BREEAM certification schemes.

The COVID-19-pandemic has given the correct attention to IAQ worldwide, as everyone had to face the fact that good ventilation is an essential element of public health. It has been at the forefront of discussions related to legislation ever since. Unfortunately, the energy crisis in Europe and rising energy prices are putting the momentum towards IAQ awareness at risk as energy optimisation is becoming a higher priority once again.

Falling short in IAQ standards

Given these global trends, it is critical to take a closer look at the deficits in the standards and regulations that further hamper wider acceptance and adoption of better IAQ practices and the reasons behind them.

Today, there remains no clear framework for IAQ. The approaches to and uptake of IAQ have been different among the EU Member States. In many Member States, IAQ has been added or is being added to the

national transpositions of the Energy Performance of Buildings Directive (EPBD). Depending on the relative strength of local manufacturers, some see a preference for specific solutions in the EPBD transpositions.

Airflow volumes in Member States differ. Between The Netherlands and Germany, for example, the rules are different and typical standards have very high airflow volumes oriented to Scandinavian requirements. The flexibility among the Member States also varies. Some can design lower or higher, and some are more restrained or based on certain factors. In France, for instance, minimum flow is based on mould protection for residential buildings. Even during Covid, there were different interpretations among the Member States on the national level.

Regional standards and guidelines related to IAQ exist. An example is ISO 16890, a series of product standards on air filters for general ventilation. However, its acceptance among Member States deserves to be further improved. There are also standards concerning IEQ classifications available. Examples include:

- EN 16798-1 Energy performance of buildings - Ventilation for buildings - Part 1: Indoor environmental input parameters for design and assessment of energy performance of buildings addressing indoor air quality, thermal environment, lighting and acoustics - Module M1-6.
- ISO 17772-1 Energy performance of buildings — Indoor environmental quality — Part 1: Indoor environmental input parameters for the design and assessment of energy performance of buildings.

These two equivalent standards provide a classification of the IEQ and are the reference for IEQ classification in buildings. The current EPBD revision proposal references EN 16798-1 in Annex 1. This means that the EU Member States must include this information in their national Energy Performance labelling scheme.

Gaps in legislation

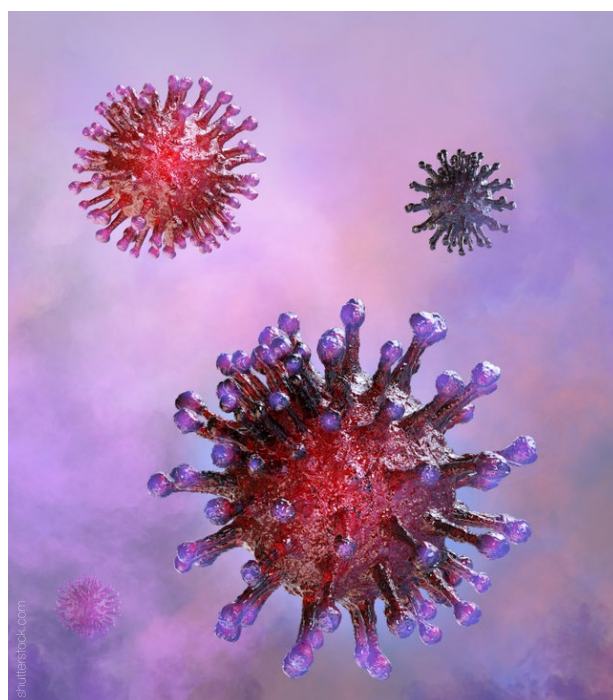
Despite such efforts in standardisation and legislation, the market still falls short as there remain no minimum IAQ standards across Europe. As the IAQ industry is still very dispersed, with few major manufacturers, it has not yet managed to draw sufficient attention to IAQ at the political level to promote and push for inclusion in legislation.

Overall, EU legislation lacks an IAQ focus. The best guess is that real attention towards this issue in Europe

will occur when the new European Commission is in place, and the EPBD is reviewed anew, as it is set for recast. The proposed EPBD recast aims to translate the actions proposed in the Renovation Wave, placing more emphasis on the need for improved IAQ through well-maintained mechanical ventilation systems in new and existing buildings. In the report by the European Parliament Committee on Industry, Research and Energy (ITRE) rapporteur, there is a proposal to address Indoor Environmental Quality (IEQ), not IAQ. The proposal for a new article 11a would require Member States to set minimum IEQ standards. These IEQ standards would have to be according to a methodological framework defined by the Commission. Unfortunately, this framework is not yet available.

Part of the lack of alignment stems from the fact that the industry has not been pushing for voluntary standards at the CEN level, either as a separate Technical Committee or integrated into existing Technical Committees. This may be because many people in the industry now regard standardisation too much as only the development of mandated standards and therefore are no longer developing standards voluntarily, which could be fit for future legislation.

Some industry associations have given up their role in defining state-of-the-art rules and codes of good practice. The latter may be difficult for IAQ because it would also have to liaise with and rely on expertise from the medical and health sector. A risk is that IAQ would be developed separately in different Technical Committees, leading to confusion



and market fragmentation. Due to this complexity, ventilation rates and IAQ may likely have to be developed for specific situations, at home, in the office, and in schools.

An issue of market protection

The lack of alignment in European standards and legislation can also be an offshoot of differing individual company strategies. The inconsistency of IAQ consideration between residential and non-residential provides a clue as to why.

In non-residential applications, the disparity in willingness to invest in IAQ is insignificant. There is a large European market, and products are not linked. Generally, companies and engineers across European countries have aligned principles and understand what constitutes a good solution, with range differences of between 10% more or lower air volumes.

The residential market is more fragmented, with typically smaller ventilation markets, small product ranges and a very simplified market with a wide variety of projects. Companies designed to address local needs may see specific country-wise barriers to protect their market from a larger European supplier. As a result, some companies can be more in favour of having individual specified markets because it gives an element of market protection.

However, a harmonised IAQ approach should not be considered a threat to commercial interests. Not only does this somewhat block innovation, but better IAQ is essentially technology-agnostic. A harmonised approach that will create better IAQ awareness would allow individual solutions locally marketed to grow because they will not have to fight to split a smaller market share due to rising demands.

The root of the problem: A lack of common understanding

Despite the progress of standards and guidelines thus far, much remains to be done. The legal background of EPBD is energy efficiency. Therefore, we still need an IAQ regulation tackling awareness and information on buildings or, perhaps, a building certificate. Hence, the consumer is better informed or would be empowered to choose a facility with better IAQ.

Such a classification would be helpful, but we must consider that today, there is not even a commonly accepted definition of IAQ. If you read the different

standards, there are different approaches. Within the HVAC sector, there is no common understanding of what constitutes a good IAQ.

Typically, benchmarks of IAQ still relate to outdoor air quality. Initially, criteria for IAQ were developed for the elements in the outdoor Ambient Air Quality Directive sulphur dioxide, nitrogen dioxide and oxides of nitrogen, and particulate matter. IAQ was focused on Volatile Organic Compounds (VOCs) emitted from paints, furniture, and other equipment in buildings. CO₂ and VOC are widely accepted indicators because they are measurable and used as common reference points.

Yet, it can happen that if ventilation is weak, even if CO₂ is low, air quality in that building can be bad. This is logical as CO₂ is used as a tracer for human occupancy. If no or minimal persons are in a room, the ventilation system should still run at a level that the building emissions are removed. This factor is also addressed in EN16798-1 and should be considered when designing the ventilation system.

The perceived air quality is a commonly accepted approach in Scandinavia and also addressed in EN 16798-1. While it is a good approach, it is complex and faces challenges related to measurement. Let's not forget that bacteria and viruses are currently not included, and any definition related to IAQ would also be beneficial if this can be considered. (*For reference, we recommend reading the Systemair article on "Why we ventilate"*).

Before any regulation, the industry must work to define what it means to have a good IAQ so the industry has a common language, interpretation and understanding. Addressing this is the key to unlocking better IAQ, allowing us to be better prepared for events such as the COVID-19-pandemic. However, when doing so, we should also not get stuck in details, which tends to be common in Europe. A pragmatic approach is necessary to finally push ahead – rather tomorrow than in 10 years.

To progress, the industry must invest time and resources in people's health first. This would involve advocating IAQ as a prime objective, meaning it would have a priority in line with energy saving and decarbonisation of heating and cooling. While this may be difficult in uncertain times where energy prices are fluctuating, investing now in promoting a better understanding and application of IAQ would lead to a healthier population for the future. ■

Next-Generation Energy Performance Certificates. What novel implementation do we need?



LINA
SEDUIKYTE^a
lina.seduikyte@ktu.lt



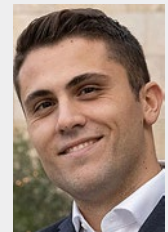
PHOEBE-ZOE
MORSINK-GEORGALI^b



CHRISTIANA
PANTELI^c



PANAGIOTA
CHATZIPANAGIOTIDOU^d



KOLTSIOS
STAVROS^d



DIMOSTHENIS
IOANNIDIS^d



LAURA
STASIULIENĖ^a



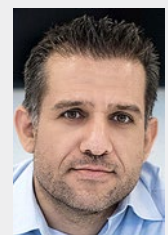
PAULIUS
SPŪDYS^a



DARIUS
PUPEIKIS^a



ANDRIUS
JURELIONIS^a



PARIS
FOKAIDES^b

^a Faculty of Civil Engineering and Architecture, Kaunas University of Technology, Kaunas, Lithuania

^b Frederick Research Center, Frederick University, Nicosia, Cyprus

^c Cleopa GmbH, Hennigsdorf, Germany

^d Centre for Research and Technology Hellas, Information Technologies Institute, Thessaloniki, Greece

Abstract: This study performed under the H2020 project “Next-generation Dynamic Digital EPCs for Enhanced Quality and User Awareness (D²EPC)”, aims to analyse the quality and weaknesses of the current EPC schemes and aspires to identify the technical challenges that currently exist, setting the grounds for the next generation dynamic EPCs.

Keywords: EPC, SRI, LCA, BIM, DT, GIS, human comfort, D²EPC.

The novelty of the dynamic EPC

The aforementioned shortcomings of national EPC schemes urge the development of a holistic framework that will strengthen and improve the quality and application of EPCs. The former can be achieved with the introduction of novel and cost-effective approaches for assessing the energy performance of building envelopes and systems. According to the collected information,

the introduction of novel aspects in the certification process and the simplification thereof, the strengthening of its user-friendliness, as well as the conformity with national and European legislations, can be accomplished using a standard collection of indicators based on a specific methodology. All upgrade needs of EPCs can be met by choosing acceptable output indicators supported their automated estimation.

New indicators

The introduction of novel aspects into the energy performance certification process in our project includes three indicators – the smart-readiness level of the buildings (SRI), human comfort-related indicators, and environmental aspects (LCA).

Smart readiness indicator. The scheme for rating the smartness of buildings was presented in 2018 in a revision of the Energy Performance of Buildings Directive (EPBD). It was established that the smart readiness of buildings should be optionally evaluated by the smart readiness indicator (SRI) [1]. According to the EPBD, this indicator reflects the building's ability to adapt to the needs of its occupants and outdoor energy infrastructure, improving its overall energy performance.

To define the smartness of buildings' services, three main functionalities of smart readiness are introduced in the methodology:

- The ability of the building to adapt its energy consumption based on the needs in an energy-efficient way;
- The ability of the building to adapt its operation to occupant's needs;
- The building's flexibility to its overall electricity demand, as well as its ability to participate in demand-response, in relation to the grid.

Within the H2020 D²EPC project, both SRI and EPC methodologies will be included in the same calculation engine allowing, where possible, to merge these two methodologies to progress the SRI to a higher level.

Human comfort. People in developed countries spend more than 90% of their time in closed environments - buildings and transport [2]. Air quality indoors is 2-5 times lower than outdoors [3]. These values can be even lower if we consider the future effects of climate change (extreme temperatures, heat waves, heavy rainfalls, air pollution). Therefore, significant attention should be paid from researchers, businesses, and standardization organizations to the field of indoor environment quality (IEQ) [4-6].

The main indicators that assess the IEQ of a building and human comfort/wellbeing can be described by an integrated multi-comfort concept that includes indoor air comfort/quality, thermal, visual, and acoustic comfort. The indoor air quality (IAQ) examines how fresh the air is in a building and the concentration in the air of certain pollutants (e.g. CO₂, VOC). Thermal comfort provides a state of satisfaction with the existing thermal environment. Visual comfort ensures that the luminance levels are within acceptable levels. Acoustic comfort creates a comfortable acoustic environment without uncomfortable noise or vibrations.

Within the H2020 D²EPC project, human comfort / wellbeing parameters will be measured and used in the calculation engine allowing dynamic input for dynamic EPCs.

Life cycle assessment. LCA indicators such as “energy savings”, expressed in “embodied energy/m²” and “carbon reductions”, expressed in “carbon dioxide equivalent/m²”, will be included in the dynamic EPCs calculation engine. This will provide to the building design team the option

D²EPC

HORIZON 2020 PROJECT

DYNAMIC
DIGITAL
ENERGY
PERFORMANCE
CERTIFICATES

Next-generation Dynamic Digital EPCs for Enhanced Quality and User Awareness

to improve and optimize the environmental performance of the building, based on changes to be integrated at the initial design stages of the building.

In the D²EPC project, the LCA Indicators for EPCs will allow maximizing energy saving and carbon reduction of the buildings, introducing this way the aspect of building's sustainability as part of the EPC issuance process. This could speed up the transaction into NZEBs as well as control the building's energy demand, reduce carbon emissions, and enhance public awareness.

The D²EPC project will propose additional indicators, which will demonstrate the environmental performance of buildings, for their introduction in the next-generation EPCs.

The Introduction of BIM and Digital Twin Concepts for the Next-Generation EPCs

The use of BIM technology helps to improve the collaboration of stakeholders from the design to asset maintenance phases. While BIM delivers static data, Digital Twin (DT) focuses on linking physical objects to their respective digital replicas using periodically updated (dynamic) data flow. The key features of DT are sensing and monitoring, data linkage, Internet of Things (IoT) implementation, simulation, predictions, and controls.

Figure 1 represents the definition of BIM and DT concept regarding the energy efficiency of the building throughout its life cycle stages: plan and design > produce and construct > use and maintain.

It is evident that BIM and DT overlap in the construction phase since BIM can deliver object-based data utilized for the DT.

Introduction of GIS in EPC

In the D²EPC project and GIS context buildings are described and considered in the concept of BuildingsExtended3D, i.e. with correct geometric dimensions, proportions, scale, but not considering geolocation of a particular building. The use of geo-spatial technologies and accurate data location could improve the processes related to the data needed to assess the energy performance and needs of buildings and urban areas. In addition, the use of geolocation practices can increase decision-making effectiveness by different stakeholders (policymakers, technicians, citizens).

Introduction of financial schemes

Introducing financial schemes in EPC is suggested in this study. Based on the well-established principle of lifecycle costing, a set of financial indicators could be developed to allow the individual elements of buildings' energy efficiency to be interpreted into standardized

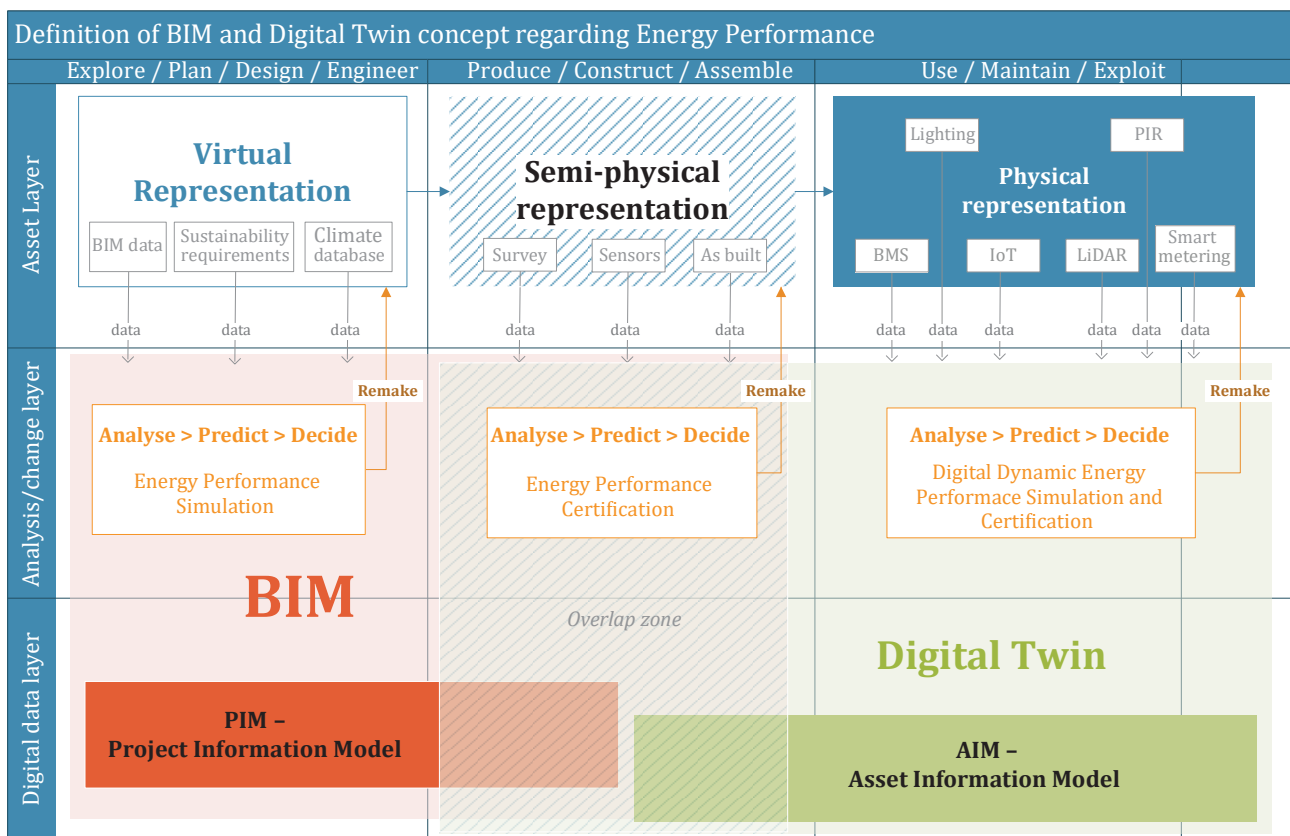


Figure 1. Definition of BIM and DT concept regarding energy performance.

numerical values. The delivery of such indicators could allow the use of EPCs for the financial evaluation of energy upgrading measures for buildings. For example, financial awards (e.g. tax reliefs) should be included if the building owner exceeds new EPC requirements and class. In the opposite case – penalties should be imposed based on the “polluter pays” principle.

D^2EPC System Architecture

A novel methodology for dynamic EPC is being developed within the H2020 D^2EPC project, which introduces the aspects of SRI, occupant comfort, LCA, integration with DT, and GIS systems. Key functionalities of D^2EPC architecture are presented in **Figure 2**.

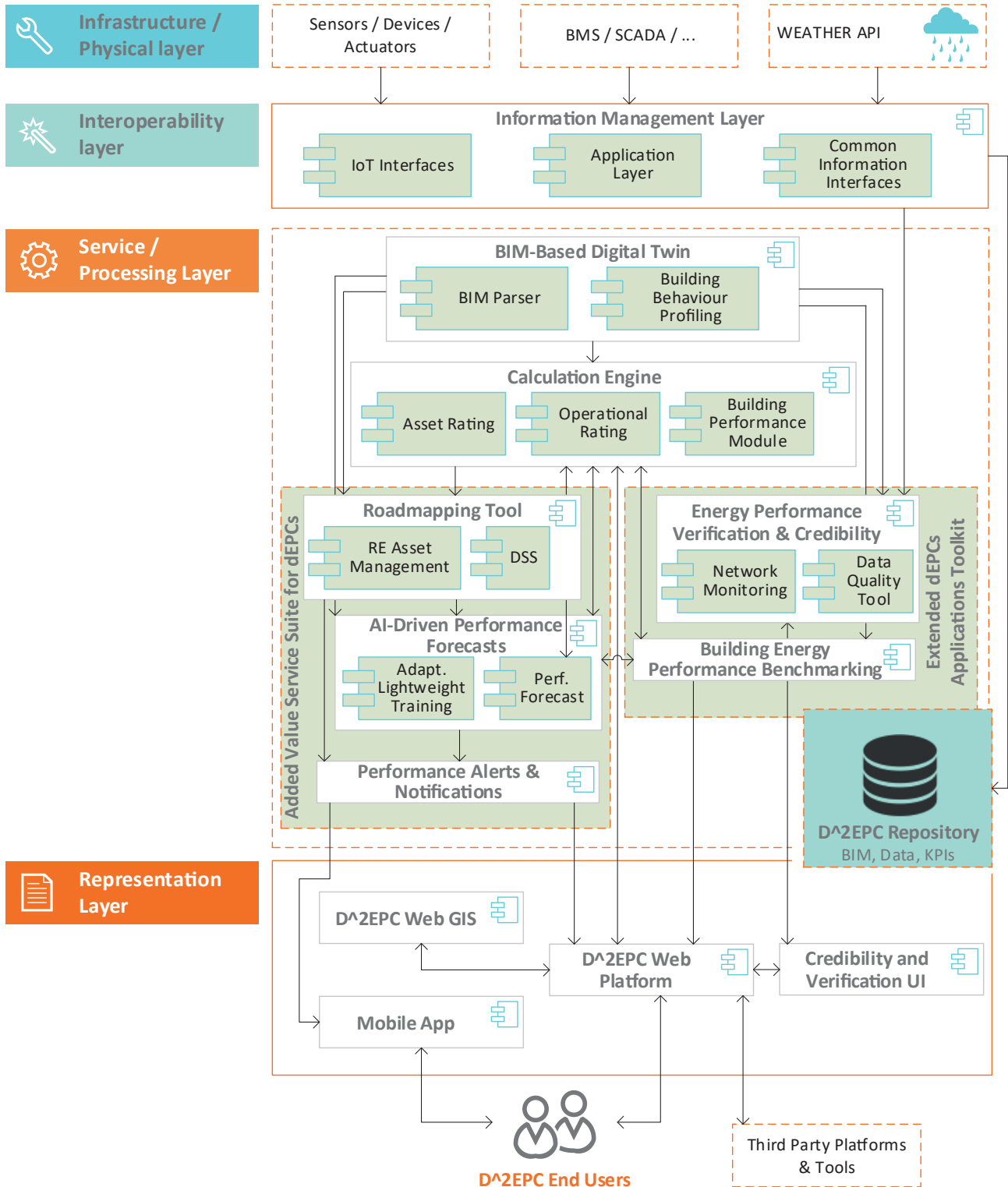


Figure 2. D^2EPC System Architecture. [13]

D²EPC framework consists of four layers:

- Infrastructure/Physical Layer,
- Interoperability Layer,
- Service/Processing Layer, and
- Representation Layer [7].

Conclusions

New technologies that didn't exist at the time when the current EPCs schemes were developed, enable new approaches towards building energy certification. D²EPC platform aims to integrate IoT, AI, and other novel technologies to enhance end-user awareness and facilitate a more sustainable life cycle of buildings. Nevertheless, integrating these technologies into a coherent unified tool is still a challenging task. D²EPC aims to provide a demonstrator platform that will help increase the understanding of European building stock's EPCs. ■

References

- [1] "BPIE of the European Parliament and of the Council of 30 May 2018 on the energy performance of buildings (recast)".
- [2] U.S. Environmental Protection Agency. 1989. Report to Congress on indoor air quality: Volume 2. EPA/400/1-9/001C. Washington, DC.
- [3] U.S. Environmental Protection Agency. 1987. The total exposure assessment methodology (TEAM) study: Summary and analysis. EPA/600/6-87/002a. Washington, DC.
- [4] ASHRAE, "Indoor Air Quality Guide Best Practices for Design, Construction, and Commissioning, Guide", 2012.
- [5] ASRHAE, "Position paper on IEQ", 2015.
- [6] American Society on Heating, Refrigeration and Air-Conditioning Engineers, "Standard 55. (2004) Thermal Environmental Conditions for Human Occupancy", 2004.
- [7] Koltsios S., Tsolakis A.C., Fokaidis P.A., Katsifaraki A., Cebrat G., Jurelionis A., Contopoulos C., Chatzipanagiotidou P., Malavazos C., Ioannidis D., Tzovaras D. D²EPC: Next Generation Digital and Dynamic Energy Performance Certificates. 6th International Conference on Smart and Sustainable Technologies, Bol and Split, Croatia, 2021.

Full article: <https://proceedings.open.tudelft.nl/clima2022/article/view/348>



Healthy Homes Design Competition: “reTHINK living”



CAROLINE REICH

master student, energy efficiency design (e2d), University of Applied Sciences, Augsburg, Germany
caroline.reich@hs-augsburg.de



AMELIE REISER

master student, energy efficiency design (e2d), University of Applied Sciences, Augsburg, Germany

REHVA announced the Healthy Homes Design Competition 2022 with the aim to encourage students in different building disciplines to design a building with increased comfort quality while also tackling the problems of climate and demographic change. The team “re²THINK tank” convinced the international jury with both their space-efficient and user-focused proposal as well as their clean technical approach. The two master students from Augsburg, Germany were able to achieve the third prize.

Keywords: healthy homes, demographics, wellbeing, housing shortage, user-centric design, space-efficiency, communal space, synergies, comfort, daylight simulation, PV generation

The submission of the project “reTHINK living” depicts a radical answer to the question of how we will live together.

Before the implementation of any design idea, a healthy home was defined as a way of life that considers all kinds of wellbeing: social, physical, mental and eudaemonic health, hedonic and subjective wellbeing, productivity, as well as environmental quality and comfort. This groundwork formed the basis of a user-centric design of this building complex in Pernis.

An analysis of the demographics of the Netherlands, of Rotterdam and of Pernis in general gave an idea of the kind of future residents that could be expected. The fact that a household has to wait 5.5 years for an affordable flat on average is just one out of many issues that occur because of the increasing problem of the

alarming high housing shortage in the Netherlands. Therefore, the huge gap between the number of needed accommodation and number of affordable and available ones is calling for new solutions regarding the complex question of how we will live tomorrow.

The concept of “reTHINK living”

The concept of reTHINK living questions the given apartment sizes and suggests a solution that is remarkably more space-efficient and results in a smaller per capita living space than in any form of conventional housing.

The left side of **Figure 1** depicts a conventional building organisation. The coloured area stands for the communal area inside every flat, usually the living room. The concept of “reTHINK living”, as seen on the right side of **Figure 1**, removes this space and

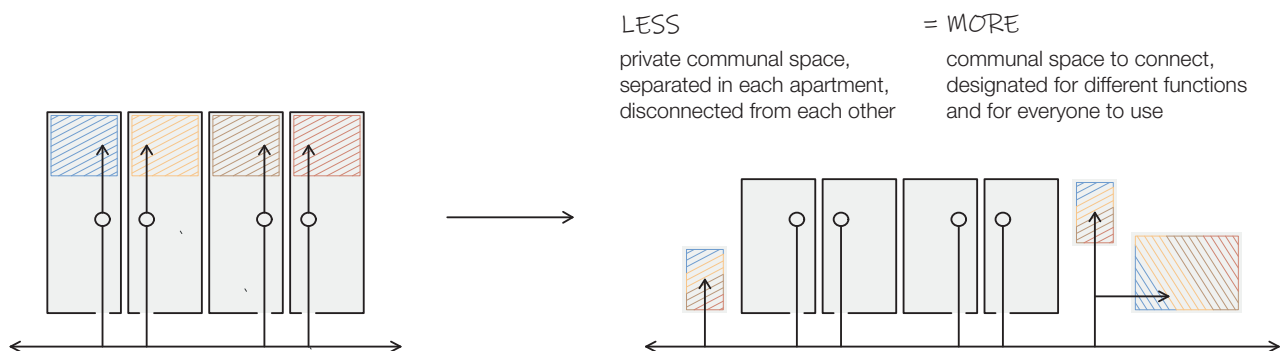


Figure 1. Conventional living becomes reTHINK living.

shares it with all the other residents of the building. The result of less private space and a reduced flat size is compensated by a maximised common area that can be used by every resident in a specific and meaningful way.

Synergies between the future residents

Coming from the demographics and the social infrastructure of Pernis, four different household types have been created: families, friends + couples, seniors, and singles. They all differ in their needs and desires, particularly when it comes to the kinds of communal areas that need to be close to them, be it a communal room for “sports + health” or “silence + rest”, a room for childcare or some shared office spaces.

The organisation of the different kinds of common areas is depicted in **Figure 2**. It depends on the importance of the room for the household. Ultimately, this concept allows to build synergies among the residents throughout the building complex and strengthens the neighbourhood.

Urban design principles

The location of the competition at the Pernis waterfront presented an exciting but challenging site. The weaknesses include constant emissions from the nearby motorway in the west, a continuously present noise level coming from mainly the west as well, the smell of Diesel that is only partly shielded from the existing trees and lastly a poor social and functional mix.

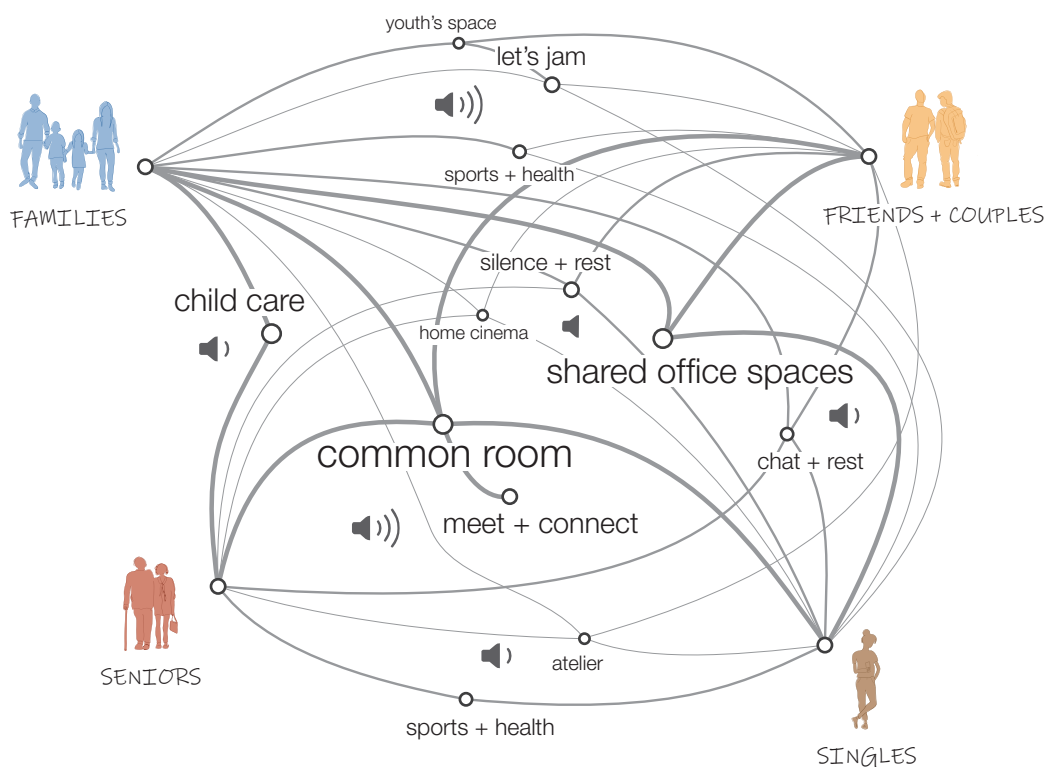


Figure 2. The four household types and the synergies among them.



Figure 3. Perspective views.

An urban analysis led to the following three urban design principles that define the cubature of the building:

1. Blocking the west side of the site to prevent the existing smell and noise.
2. Opening the complex to the east and south and alongside the solar path.
3. Strengthening the sightlines to Pernis as well as those to Rotterdam downtown.

Building organisation and flood concept

The building complex is vertically organised, which means the privacy increases with the floors of the building. The ground floor consists of a communal area for everyone to use, including the non-residents. The previously mentioned communal rooms are located on the first floor. The apartments can be found on the second to fourth floor. The reason why there are no rooms on the ground floor is the flooding concept of the building. As a maximum flooding of the site of one meter had to be considered (a number that is estimated to rise as a result of the climate crisis), the building was elevated by one floor level. This way, the ventilation of the courtyard can be increased, which counteracts the

heat island effect. Small parts of the ground floor area are used for the technical equipment of the building.

Cubature

In order to improve the incidence of daylight, the southern facade is tilted by 70° and the eastern and western facades facing the inner courtyard are tilted by 80°.

The roof is tilted as well. There are five floors on the western side and four floors on the eastern side of the building to strengthen the urban principles.

Access and building organisation

The access to the flats and to the common areas is via a circumferential and completely glazed arcade and two staircases, each of them contains a lift. This makes the building completely barrier-free which marks the simplest way of inclusion. The plans in **Figure 5** also illustrate that each flat gets light from at least two directions, so there is no apartment with an insufficient exposure. In addition to that every flat has at least one loggia which allows each resident to enjoy their own private outdoor space. This creates a connection to the outside space and nature.

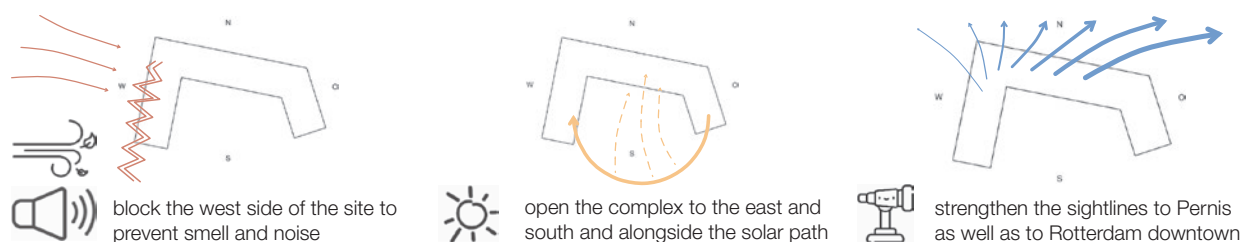


Figure 4. Three urban design principles.



Figure 5. Detailed floor plans of two out of the four household types (seniors and families).

Detailed floor plans

The differences of the four household types result in different floor plans. Two out of the four kinds of floor plans are depicted below.

The seniors' floor plans are primarily located close to staircases and elevators to shorten the access routes within the building. Each of their floor plans are designed to be extra-spacious to allow an independent life regardless of age or inability. Since the relative need for daylight increases with age, the south-facing window areas are relatively larger than in other floor plans.

The families enjoy a spacious entrance situation with the living room as the heart of the apartment referring to both the location and communication inside the apartment. Several loggias designated to different rooms maximise private outdoor areas.

The common features of the floor plans are that all circulation areas have been reduced to a minimum to keep the usable space as generous as possible. In addition, the bathroom is always located next to the entrance area facing the north in order to maximise the southern exposition of living and sleeping rooms in general.

Heating / cooling / ventilation concept

Passive cooling and heating of the building is provided by a water-water heat pump, which uses the heating and cooling energy from the river water. The heat pump delivers the correspondingly cooled or heated medium to a hot water tank and a heating water buffer tank. The hot water is then transferred from the hot water storage tank to all water points in the house. The cooled or heated medium is passed on from the heating water buffer tank to the underfloor heating with concrete core activation. Concrete core activation

brings with it a high storage capacity as well as a high level of comfort due to a uniform heat radiation.

The choice of ventilation concept is a hybrid ventilation. This allows the building to be naturally ventilated in summer, in our case by cross-ventilation. In winter, the mechanical ventilation system with heat recovery is used to ventilate the building sufficiently while only a negligible amount of thermal energy is released into the outside air. The choice of a hybrid ventilation system that draws in air through an air tower in the south with a fine filter also gives the chance to optimise the indoor air quality. Thus, the residents can decide for themselves whether to ventilate via natural ventilation by means of cross-ventilation, which is made possible by the arcade in which the upper part of the glazing can be opened at any time, or whether to use the mechanical ventilation system to ventilate the room.

Winter and summer comfort policy

To improve the thermal comfort in winter on one hand, the building is heated by a water-water heat pump. An underfloor heating system using concrete core activation serves as a radiator which allows the heat to be kept in the building as efficiently as possible. Hybrid ventilation, which ventilates the building mainly in winter, releases as little thermal energy as possible to the outside air, improving thermal comfort in the building in winter.

To avoid overheating in summer on the other hand, the external blinds, which are attached to each exterior window facing south and the inner courtyard, were controlled with a sun sensor. In addition, it is possible to override the control of the external blinds by means of the sun sensor, so that the user can also control the external blinds individually. The building is equipped with

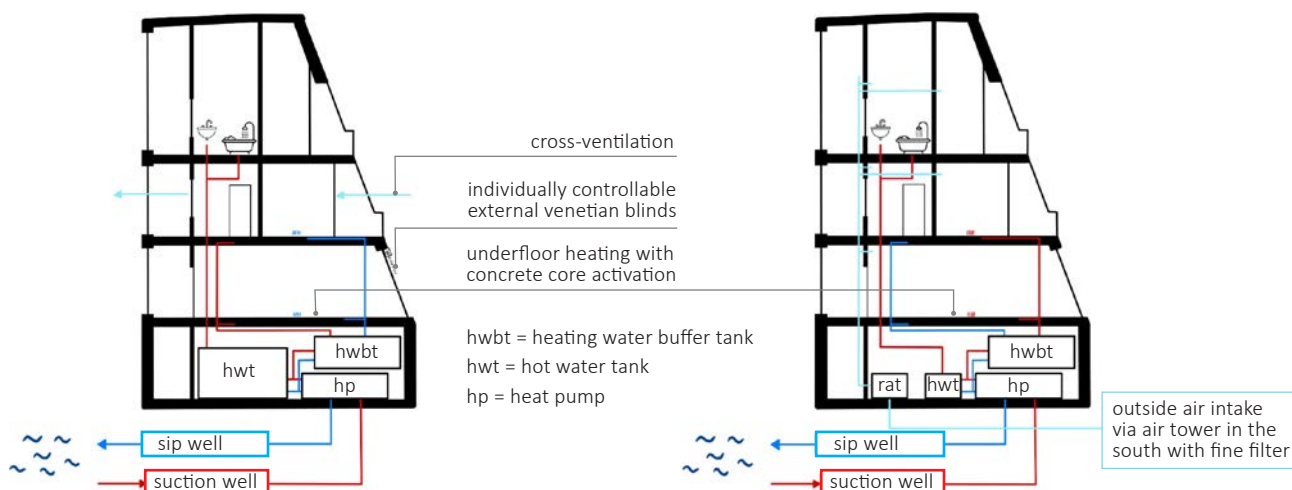


Figure 6. Heating / cooling / ventilation: summer (left) and winter (right) situation.

a water-water heat pump, which extracts the heat or cold from the adjacent river, so that overheating of the building can be avoided by cooling through the underfloor heating with concrete core activation. The river has an average temperature of 18°C in the warm months, which makes it ideal for cooling the building with a water-water heat pump and thus optimising comfort in the summer.

Integrated water systems

In terms of water use, all the rainwater from the roof of the building is collected in a rainwater storage tank. The water is then filtered and transported to the toilets or washing machines via domestic waterworks or a pump, so that the rainwater can be used for these purposes.

Energy concept and on-site energy use

Regarding to the on-site energy use concept, a 370 m² photovoltaic system will be installed on the roof of the building. This photovoltaic system generates a total of roughly 78 430 kWh/a, so that theoretically the entire electricity demand of 61 914 kWh/a (including the electricity demand to supply the heat pump) can be covered by the photovoltaic system through the integration of an electricity storage unit – this creates a plus-energy building.

The electricity generated by the photovoltaic system is first used to cover the current electricity demand in the building (washing machine, PCs, TVs, kitchen, e-mobile charging stations). If the photovoltaic system generates more electricity than is needed in

the building, it is stored in an electricity storage unit for use at a later time. If there is still surplus electricity, it is fed into the power grid.

Overall lighting concept

Floor-to-ceiling windows maximise the visual axes to the south and the inner courtyard. The view to the north and thus towards the water is also improved by a completely glazed arcade which means that depending on preferences the occupants can enjoy the view towards the water or towards nature and neighbourhood.

Strategy to minimize overall energy use

In order to minimize overall energy use of the concept, passive cooling by using a water-water heat pump was applied on the one hand, and the 3E-strategy was purposed on the other hand:

1. **Sufficiency = energy saving**
→ less floor space by removing and reducing the common area from the flats
2. **Efficiency = energy efficiency**
→ use of a heat pump, a hybrid ventilation system and clever energy management throughout the building
3. **Consistency = renewable energy**
→ availability of the required energy as efficiently as possible. In this case, all the energy required on the site is produced on the roof of the building and partly stored in an electricity storage system to be available for use at any time. ■

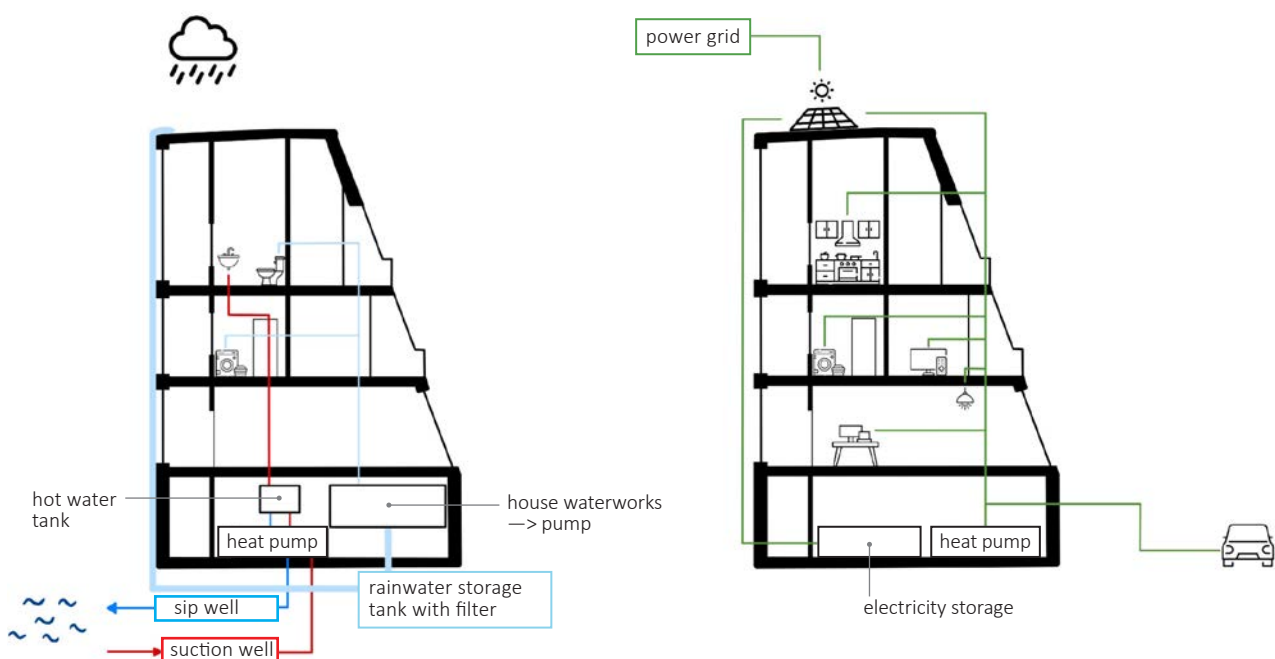


Figure 7. Integrated water systems and energy concept.

Tiny Homes – *A Tiny solution to a big problem*



LAURA DENOYELLE

Ir. Arch.

laura.denoyelle@onetinystep.eu

onetinystep.eu

Master thesis: A Tiny solution to a big problem. How Tiny Homes could benefit you, society and how they could play their part in climate change communication.

The Healthy Homes design competition organized by CLIMA 2022 asked for a design of an innovative apartment building. They asked big, but I decided to hand in a proposal with Tiny Homes of 20-40 m² instead.

Why tiny homes?

Humanity has a big problem on their hands: climate change. It is affecting everyone, and it is everyone's responsibility to do their part. Whether that is eating less meat, revolutionizing solar power, or looking at sustainable industry from the perspective of ... a Tiny Home. Exactly what I looked at in my master thesis.

But why choose to look at Tiny Homes? Put simply: I was living in one myself. Considering the struggle, I encountered to live there legally, my original motivation was to legalize my own house using my thesis research. Somewhere along the road the scope changed drastically, and the research focused more and more on how Tiny Homes can help the transitioning to a sustainable society and what role they could help play in climate change communication, preparedness, and mitigation.

The thesis explored many fields in relation to Tiny Homes, through the methodology of research by design. The practical aspect of the design helped keep all elements connected, and focus on a design that is feasible to build today. As we need these homes ... well, now!

While I did not win the CLIMA 2022 competition, I did impress the jury with my proposal, following is how.

Climate preparedness

The brief of the competition asked for a very specific building: An apartment building that will be unaffected by potential flooding. This is not just an interesting



The Tiny Home Design created in master thesis
'A tiny solution to a big problem'.

design point; it is a reality we face today, and will face more frequently in the future: Rotterdam has depleted its land use within protected dikes. In America certain zones are exempt from insurance as the risks for fire hazard due to a changing climate are deemed too high.

Luckily most of the time we are warned for these disasters – in this case a Tiny Home proves to be an elegant solution: In case of disaster, you can drive it away and wait out the storm at a safe location. A Tiny Home does make you a bit slower and we have seen with the floodings in Belgium and Germany that a warning is not always present. But even if you need to leave your home behind in a rush, the financial repercussions and options are less severe than they would be for a conventional home.

Carbon footprint (= climate mitigation)

Preparedness is not the only way Tiny Homes relate to climate change. The Tiny Home designed has a carbon footprint of 15 000 kg CO₂eq. As the thesis focused on Tiny Homes in a suburb/rural environment the comparison was made to the typical house a two-person household will acquire in this environment. The LCA for this home showed that the average house of a two-person household in Danish suburbs is 150 000 kg CO₂eq. The Tiny Home footprint is no less than ten times smaller!

A demographic mismatch

Thus, Tiny Homes are sustainable housing when it comes to climate change, but who will live in them? Looking at the demographics of Denmark – and they are quite similar in most of Europe - shows that 49% of people live alone or as a couple, with the average household being 2.1 people. If we look at the residential buildings being made. However, we see that about 80% of these are aimed at families. Those numbers do not add up on paper. And in reality, they affect the lives of a whole generation, one that cannot afford to buy a home anymore. Tiny Homes are an affordable option for this target market existing of 50% of the population.

Healthy homes

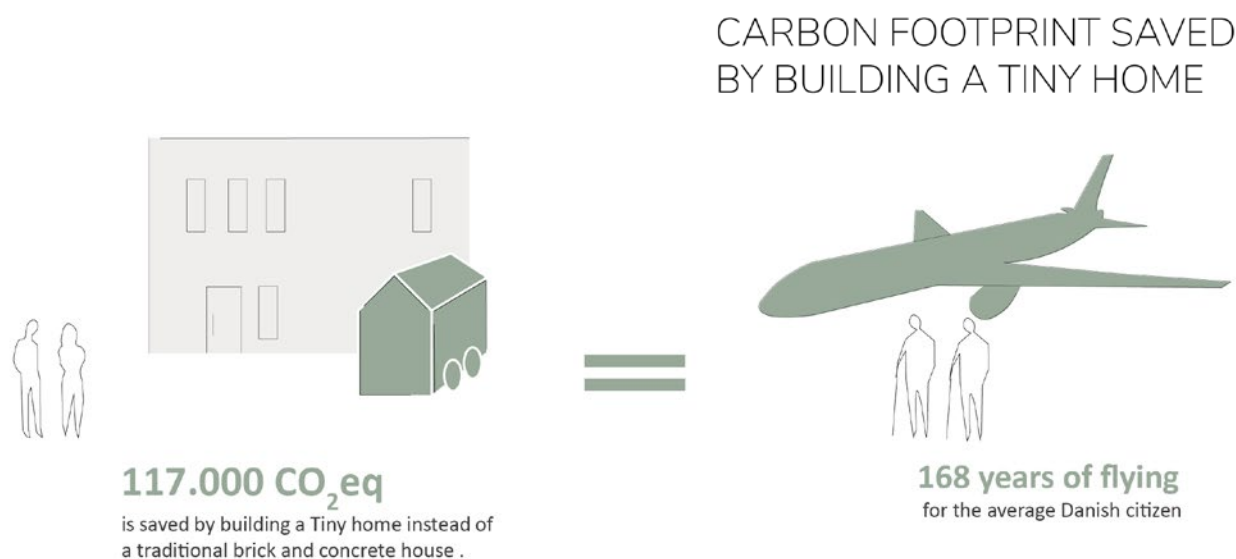
There was a more important reason however, that I chose to submit Tiny Homes into the competition. One that has everything to do with the key word of its title: **Healthy** Homes. The proposed competition

location is near an industrial site. Having been raised in Hoboken in Belgium I have experienced first-hand what that means. An industry scandal 20 years ago showed extreme lead values damaging children's growth and health. Two years back a documentary proved the protection measures taken were actually insufficient. This is not an insulated event. It has been shown on multiple occasions that effects of nearby industrial activity are known too late, and mostly affect children. Thus, an argument is made that the site itself is not suitable for families. Adults however are safe, and the perfect demographic for smaller homes, or Tiny ones.

Zooming in to the level of a building, or a Tiny Home, there are two elements related to Health. The most commonly addressed is the building's influence on the physical health. On the other hand, following the COVID-19 pandemic, a lot of research has been done on buildings' social and mental health.

Buildings' impact on physical health

Tiny Homes provide unique challenges when it comes to Indoor environmental quality, the extremely low volume creates higher pollution levels. Thus, for this article we will focus on air quality. Two factors were considered: materials and ventilation. Volatile organic compounds (VOC's) are so present that, even when we bring clean air into a room, by the time it reaches the occupant it might be polluted again. This is why the first step for the thesis was to design a Tiny Home without VOC's. Again, here I was motivated by own experience of a period with extreme asthma at university. In my Tiny Home that is build VOC free, I had



A carbon footprint comparison, buying the traditional Danish home versus a Tiny Home.

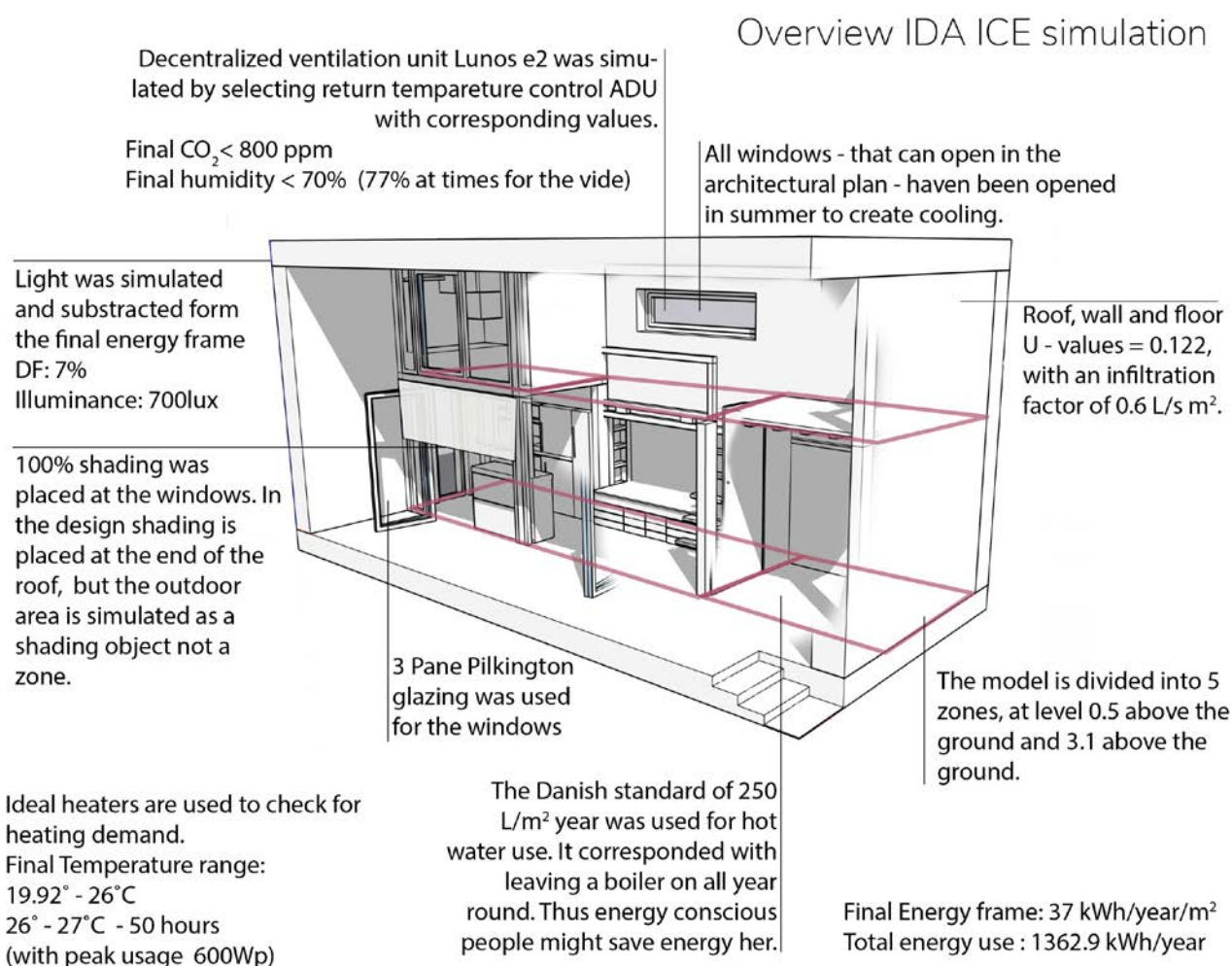
no health problems. But I often had to leave classes early at university, however, as I had no air, despite the ventilation.

To address the ventilation, bringing in a range of pipes in a Tiny Home is not really feasible, space is in short demand in tiny houses after all. After thorough investigation, I ended up working with decentralized ventilation for the design. This has been widely used in Tiny Homes, specifically the Lunos e2. It was even analysed in a research paper studying two Tiny Homes. One of these homes had perfect air quality and humidity control. The second didn't have the same good results, there several cats were also living in the space though and the owners manually choose to use the lowest mode of the equipment.

Simulating the ventilation in my own design proved to be a challenge. I used IDA ICE and decentralized ventilation is just not included yet. Decentralized heating

also regulates humidity differently than traditional systems. And a third obstacle was the size of the Tiny Home. For example, infiltration is calculated using exposed surface/volume ratio, and the size of a Tiny Home completely skews those results. I did manage to speak to some of the PhD-researchers on this topic and got some help to correctly set up a simulation model.

An argument against decentralized heating I often hear is the noise. It is also a main argument I've heard against centralized ventilation. But in all the research I did I have never seen this argument pop up in relation to Tiny Homes. I think an important difference is the owners' involvement in building the tiny home, and their awareness of how the home functions. This makes people more tolerant towards discomfort. Secondly as the Tiny Homes are in such a small volume that serves all the functions of a home, there might be more obstacles between the actual sleeping resident and the ventilation to limit the sound discomfort.



IDA ICE simulation summary.

Buildings' impact on mental health

A subject usually not addressed in the building industry: what influence does a building have on our mental health? A number has been floating around for a while now: we spend 90% of our time indoors. The lockdown probably made this number rise to a solid 99% for many people. Different papers were released following lockdown, investigating tangible parameters that can improve our home designs. Tiny Homes faced similar challenges to lockdown apartments. How do you use a small space as a bedroom, office, bathroom, kitchen. The thesis summarized the research done on these subjects and came to a surprising conclusion: the design principles suggested for Tiny Homes and mental health are largely the same.

Guidelines emphasize a flexible use of space. One room should be able to have multiple functions such as kitchen, workspace etc. Flexible furniture can play a big role in this. What was different from Tiny Home living that usually features open lifts was the emphasis on a closed bedrooms for biorhythm. The importance

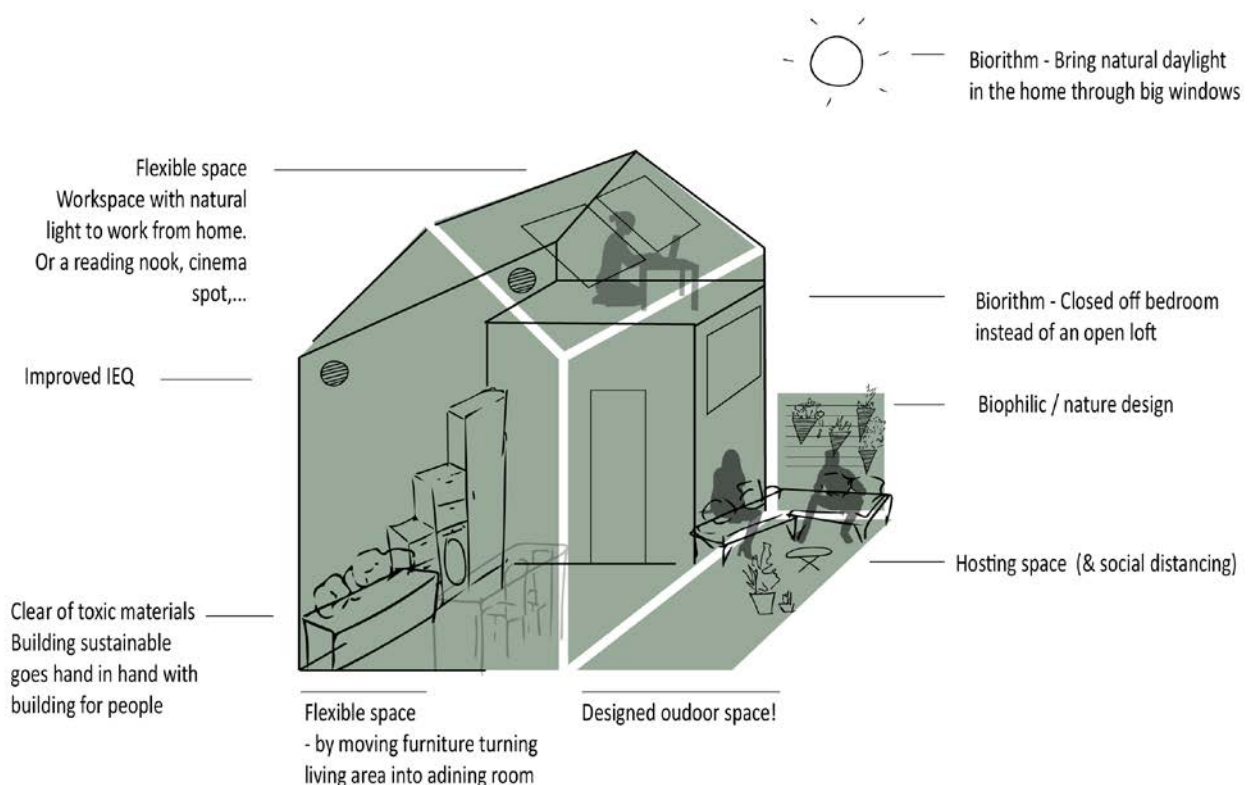
of designed outdoor space and biophilic design was also never mentioned in Tiny Homes. Most of these end up in the countryside however, where nature and outdoor space are plenty.

Back to the original question

Right now, Tiny Homes are largely illegal, or at least not entirely legal. European law however allows a country to implement a different building code for buildings under 50 m². Thus, what if we consider Tiny Homes as a housing typology? They serve 50% of our society and have a carbon footprint that is 10 times lower. They are also fast to build, and cheap compared to large projects. The estimate for the entire building site development of the CLIMA 2022 competition with Tiny Homes was 2.7 million euros compared to the 7.35 million euro's development that the asked for apartment building would cost. Last but not least they have been pioneers in off grid living, and they are the perfect field for optimizing new technologies. ■

SOCIAL HEALTH OF DESIGN

Design principles isolated by post Corona pandemic research



Design guidelines for social/mental health of a home.



Meet the BIM-SPEED Competition Winners & Finalists



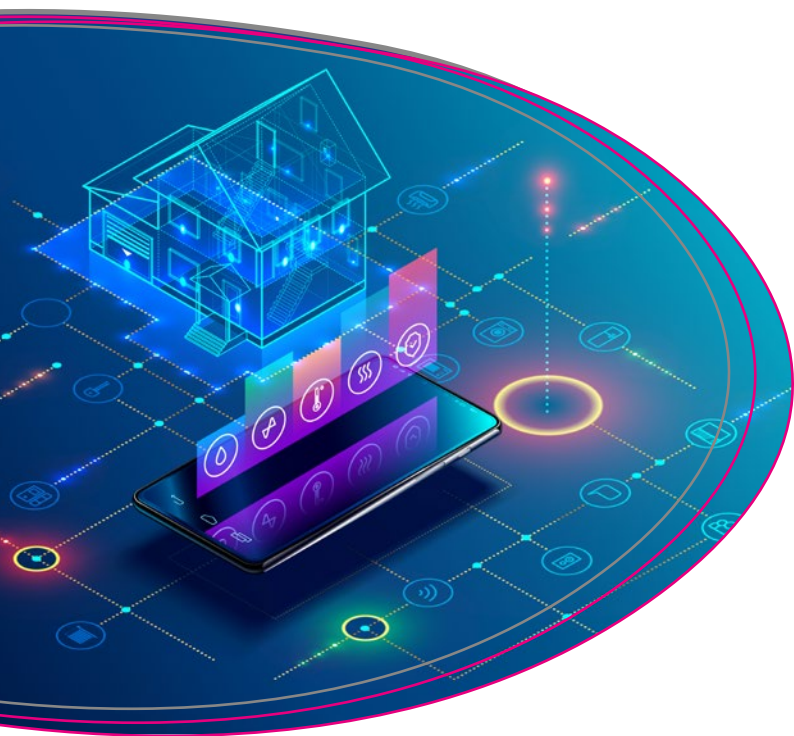
JASPER VERMAUT
Policy & Project Officer
at REHVA

As part of the BIM-SPEED project¹, REHVA co-organised the **EU BIM for Building Renovation Competition** together with other Brussels-based EU associations Architect Council of Europe (ACE), European Builders Confederation (EBC) and the European Construction Industry Federation (FIEC). BIM-SPEED with technical support from other partners in the consortium such as the Technical University of Berlin and Erasmus University Rotterdam.

The Competition took place from June 2021 until April 2022 and aimed to engage professionals and students active in the design and construction industry to present a residential building renovation project that applies the BIM tools and methods developed by the BIM-SPEED consortium². The challenge was to **demonstrate a renovation project**, using BIM-SPEED platform for collaboration, in a way that allows **energy saving for the occupants**, improves their **comfort** while **reducing the time and the cost** of the overall process. The participants had to do this by making use of one or more of the tools developed within the BIM-SPEED project and made available through the project's platform³. After submission the results were assessed by a jury of professionals who have a long experience with BIM from different perspectives:

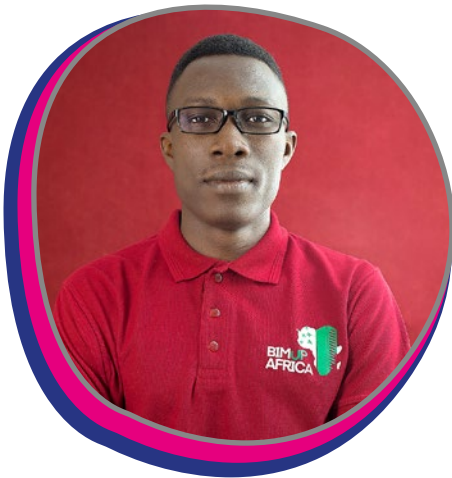
- András Rónai: Mechanical Engineer M.Sc.; HVAC+R and BIM – Óbuda Group – MMK.
- Chiara Dipasquale: Expert in Innovation and Sustainability – Volksbank.
- Olga Venetsianou: Architect PhD, MA in Digital Arts ASFA - Representative from the Technical Chamber of Greece to the Architects' Council of Europe BIM Working Group.

On the following pages we're delighted to present you the winners and finalists of the competition. REHVA interviewed both teams to give the opportunity to present themselves, their experiences with the competition and the BIM-SPEED platform, and what future they see for the digitalization of the construction sector.



¹ <https://www.bim-speed.eu/en> ² <https://www.bim-speed.eu/en/competition> ³ <https://www.bim-speed.eu/en/training-materials>

Interview with the Competition Winners: Team ENSTP from the National Advanced School of Public Works (Yaounde, Cameroon)



Idriss Tchaheu Tchaheu

- Works at Consultation et Project D'Afrique (CPA) in charge of digitalization of the construction of French-speaking Saharan Africa;
- Founding member of the the non-profit association BIMUP AFRICA which aims to create awareness on BIM to students and professionals in French-speaking Sub-Saharan Africa.
- Master's Degree in Civil Engineering at National Advanced School of Public Works (NASPW) in Yaounde (Cameroon) in partnership with the University of Padova (Italy) with the thesis topic "BIM applied to the structural assessment of a multi-story reinforced concrete building;
- Team leader of ENSTP BIM team who the second prize of the student BIM competition by BIM Harambee Africa in 2021;



Charlène Delavictoire Sobgoum Jiogo

- Student in Fifth year of Architecture at National Advanced School of Public Works (NASPW), Yaounde (Cameroon) in partnership with the University of Padova (Italy).
- Founding member of the non-profit association BIMUP AFRICA which aims to create awareness on BIM to students and professionals in French-speaking Sub-Saharan Africa;
- Member of the ENSTP BIM team who won the second prize of the student BIM competition launched by BIM Harambee Africa in 2021;
- Team leader of BIM ENSTP team who won the EU BIM FOR BUILDING RENOVATION COMPETITION launched by BIM SPEED 2022.

Congratulations on winning the EU BIM for Building Renovation Competition! Tell us more about your team, specialization and career

The ENSTP BIM Team that participated in the EU BIM SPEED 2022 competition is a team composed of Idriss Tchaheu Tchaheu and Charlène Delavictoire Sobgoum Jiogo from the National Advanced School of Public Works (NASPW) of Yaoundé (Cameroon) in partnership with the University of Padova in Italy. We are passionate about digital technologies that are revolutionizing the construction industry and helping to improve productivity. We are determined to contribute to the technological transition process of the construction sector in Africa.

Idriss is a civil engineer graduated from (NASPW); he works at the consulting firm Consultation et Projects D'Afrique (CPA) which operates for the digitization of the construction sector in Saharan Francophone Africa. Charlène Delavictoire SOBGOU M JIOGO is a student in fifth year of architecture at (NASPW).

In 2021, we were members of the team that won the second prize in the student BIM competition launched by BIM Harambee Africa. We are also members of the team that created in 2022 the non-profit association BIMUP AFRICA in order to raise awareness about BIM among students and professionals in French-speaking sub-Saharan Africa.

Can you briefly describe the project that you worked for the Competition and how you used the BIM-SPEED tools available?

The project submitted to our study is located in France in the municipality Massy precisely at 15 Avenue de la Republique, the building is a basement, R + 10 storey for residential purpose. The objective of the study was to renovate the building while using the BIM Speeds tools integrated to the collaborative platform kroqi. The BIM Speed tools used in our project are the Mereen Weather Service and the file naming convention service which was respectively used to collect historical climate data and to define naming convention standard across project files to ensure standardization.

How does the BIM-SPEED platform contribute to this? Can you tell us more about your experiences with the platform?

The platform allowed us to collaborate smoothly and efficiently throughout our project by deploying a common data environment and workspace, allowing us to work in a hierarchical manner. In addition, the naming convention defined for the files allowed us to discern with precision the discipline, phase and version of the software used for the model. All the data was stored in a hierarchical and easily accessible way inside BIM-SPEED platform that is available through Kroqi.

The Mereen Weather Service that is available through the platform allowed us to collect free of charge historical climate data from 1999 to 2021 in EPW format. This collected climate data was used in Graitec Archiwizard software to simulate the daylighting analysis as well as the energy analysis through which we managed to get the cost savings.

Another available tool in the platform allowed us to increase time efficiency, which is the File Naming Convention Service that uses an automate workflow which consisted on creating; managing and applying a naming standard across project files to ensure standardization.

Interview with finalists of the BIM-SPEED Competition: Team from the Federal University of São Carlos (São Paulo, Brazil)



Clélia Mendonça de Moraes

- Postdoctoral Researcher at the Federal University of São Carlos (2018 – ongoing), Postdoctoral Researcher at Institute for Technological Research (IPT) (2013 – 2018);
- Ph.D. Degree in Mechanical Engineering (UNICAMP), thesis on “Thermal comfort in the classroom in Brazil: experimental analysis and numeric” in collaboration with the Indoor Environment & Energy Department in DTU;
- Architect and Urban Planner for the Department of Transportation and Urban Mobility in the Araraquara Prefecture;
- Publications: <https://bv.fapesp.br/pt/pesquisador/54287/clelia-mendonca-de-moraes> & <https://lattes.cnpq.br/4970119616148506>



Everson de Castro Rodrigues

- Graduate Civil Engineering at *Faculdade Estácio de Belém* (2020);
- Graduate student BIM Manager at Unyleya (2022);
- Designer in architecture, structures, hydraulics and electrical;
- Publications at scientific national events: <https://www.linkedin.com/in/engcivileverson/>



Anderson André Lima de Souza

- Graduate Civil Engineering at *Faculdade Estácio de Belém* (2020);
- Graduate student BIM Manager at Unyleya (2022);
- Designer in architecture, structures, hydraulics and electrical;
- Publications at scientific national events: <https://www.linkedin.com/in/engcivileverson/>

Congratulations on winning the EU BIM for Building Renovation Competition! Tell us more about your team, specialization and career

Clélia: I'm a researcher at the Federal University of São Carlos in Brazil at the department of Urban Engineering and work as an architect on smart buildings and urban mobility for the municipality of Araraquara, in São Paulo state. My specialisation is in sustainable design, environmental and thermal comfort, BIM management and the integration of renewable energy in buildings, airplane and cities. I was also part of the scientific committee of the CLIMA: REHVA HVAC World Congress in 2013 and 2019.

Everson: I've graduated in civil engineering, during college I started working with BIM and specialised in it further since my graduation in 2020. As a BIM manager I've contributed to research articles related to civil engineering and how BIM can be used for different types of buildings.

Anderson: Similar to Everson, I've graduated from civil engineering and working on BIM management but with a focus on industrial design and concrete structures.

Can you tell us more about the project that you worked on that was submitted in the competition and your experiences with the BIM-SPEED platform?

Clélia: Our project was a residential building for a family in a sustainable urban neighbourhood in Araraquara, São Paulo state. The aim of the project was to lower energy consumption and costs while improving the IAQ and comfort levels of the building. The BIM-SPEED platform made it a lot easier for us to work with each other on this project in the same digital workspace, even if we live in different regions (Clélia lives in São Paulo while Everson and Anderson live on the other side of Brazil in Belém).

Everson: We used different tools that were made available through the platform. First there's the File Name Convention tool which allowed us to more efficiently have control over the different documents that we used within the project. We also used the Merein Weather Service on the platform, which allowed us to assess the climate and meteorological data in the region by inputting the latitude and longitude. From there we used BIM to better analyse the surroundings of the building and the amount of solar exposure.

Anderson: To a certain extend we've also used the BIMSpeed Library, or at least the concept of it, as the data on the platform was adapted to different European regions. We've used the software and adapted it with data from our own region. Through this we could examine

different parameters in our model for the sustainable use of materials for different element in the buildings, for example of the roof.

Clélia: As last we've also made use of the GIS Data Provider to do a study of the terrain while using active and passive technologies to make the building an active generator which contributes to the local grid.

From your perspective, what do you see as the main opportunities & challenges for the uptake of BIM within the building industry in Brazil?

Anderson: It can be challenging in Brazil to work with as it takes time to get to know new software and platforms that are related to BIM. Many platforms in Brazil that work with BIM can only be used in quite isolated cases, while the BIM-SPEED platform is more universal, which is a key element for the uptake of BIM in our country.

Everson: The platform and the available tools don't just focus on one element but consider the full life-cycle of a building, from design to the post-construction phase, which makes it very useful to analyse the full impact of a building.

Clélia: The BIM-Speed platform is universal and allows specialists from different fields to work together. For me it's not just important to look at individual buildings but also look at city-level, which is what I focus on for my work for the local government in Araraquara (São Paulo). By looking at the wider level we can see the wider impact that buildings have on the environment around them, which is made a lot easier through digital technologies. We look which neighbourhoods are less energy efficient and how we can better tackle this at a district level. This is why I've been advocating for a long time already to increase the uptake of digital technologies, such as BIM, at the local government. ■

Acknowledgement

This article is prepared within the scope of the BIM-SPEED project, which has received funding from the European Union's Horizon 2020 research and innovation programme under the grant agreement number 820553. The European Union is not liable for any use that may be made of the information contained in this document, which is merely representing the authors' views.



Smart Industrial Thermal Imaging Device PX1 – A Building HVAC Protection Tool – Escorts the Heating Season

Application Background

As an efficient, scientific, and intuitive detection tool for detecting building HVAC faults, the thermal camera has been widely received by the market for its “nondestructive testing” performance. **Thermal Imaging** is widely used in the building HVAC field for its competitiveness such as visualization of temperature data, which can detect problems before hidden dangers occur, and also quickly determine the fault location in case of failure.

When the heating season comes, problems such as heating failure, water seepage at welds or joints, floor heating leakage, and surface deformation, and aging are the most common. **Thermal Imaging** can detect these problems to help engineers efficiently complete daily maintenance work, ensuring warmth for citizens throughout the winter.

HVAC Fault Detection

As a nondestructive testing tool that visualizes temperature data, **Thermal Imaging** can visualize the heat distribution on the ground, making it clear to see the temperature of the pipeline from the floor heating to the ground, and can scan the area of the leaks, which is conducive to accurate and rapid positioning of the underground leaks, facilitating maintenance, reducing energy loss and ensuring normal heating in winter.

Air Tightness Test for Houses

The air tightness of the house is crucial in the cold winter. If there are gaps in the windows, doors, or walls, the chill wind will blow into the house along the gaps, plummeting indoor temperatures. **Thermal Imaging** can quickly locate the gaps in the walls, doors, or windows to figure out where the chill wind comes from, thus solving the problem of wind

leakage and wind pouring in of the house caused by poor sealing, and blocking the cold wind outside promptly to ensure the warmth inside.

Hollow External Wall Detection

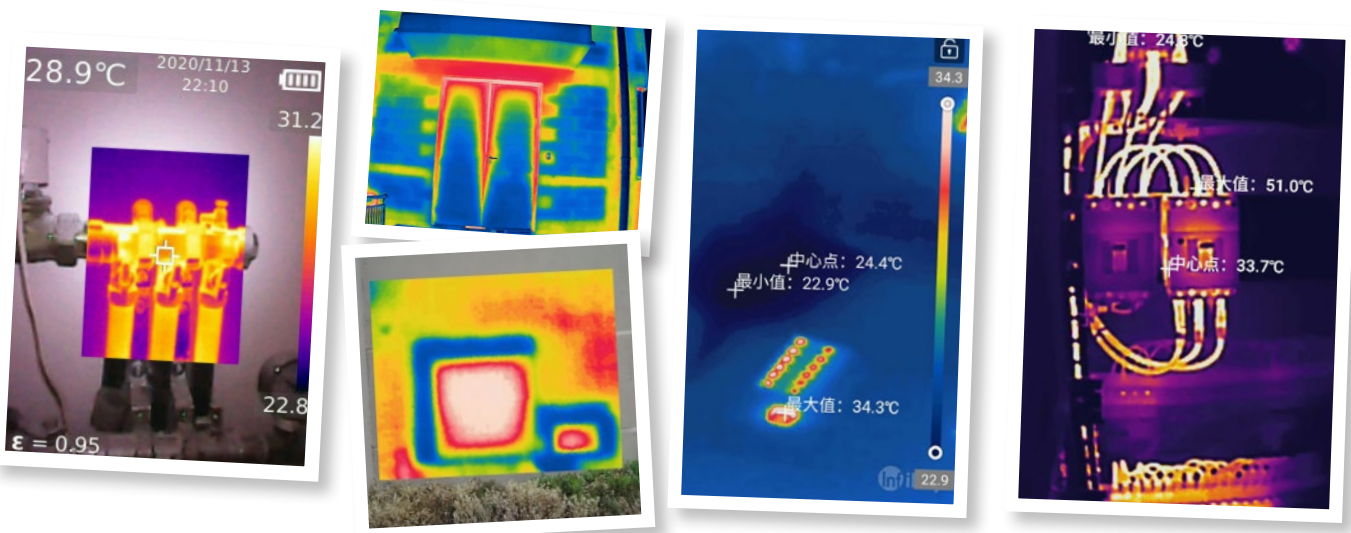
Due to different thermal conductivity coefficient, the temperature transfer will be hindered when there are hollows or cavities on the walls of a building. Therefore, a non-uniform temperature field will be formed on the surface during temperature rise or fall. For example, when the indoor temperature is low and the outdoor temperature is high by sunlight, heat will accumulate at the hollow spot. Compared with the traditional hand-knocking method, **Thermal Imaging** does not need to erect scaffolds for detection and can shoot in a large area. And the area and extent of damage can be clearly distinguished through infrared images.

Water Leakage Detection for Buildings

Leakage in building roof, window wall corners, top and bottom slab is a common quality common problem. With excellent thermal sensitivity, **Thermal Imaging** can quickly and clearly display subtle temperature differences, search and locate the leakage point, and help routine inspectors efficiently troubleshoot the wall faults so as to formulate effective maintenance plans to improve building quality.

Electrical Device Security Monitoring

As temperature drops, there will be an increase in electricity consumption in both enterprises and communities. Whether power supply devices and electrical devices in the distribution stations work properly affects the production operations of the park and the livelihood of the community residents. In the event of a malfunction, power



failure, voltage instability, and other electrical accidents may ensue. **Thermal Imaging** can timely discover a thermal defect and hidden thermal danger of electrical devices, thus preventing line thermal accidents, and ensuring the security of electricity in winter.

Introduction to Smart Industrial Thermal Imaging Device PX1

PX1 is built with an InfiRay self-developed 12 μm high performance 256×192 infrared detector, a dual night vision system and a 48-megapixel main camera, which can support routine inspection **Thermal Imaging** in any light. High IP grade and large-capacity battery can meet the requirements of engineers for long outdoor inspection in harsh environment.

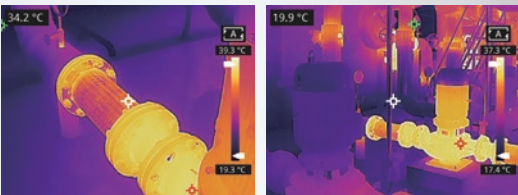
- Three-spectrum sensing of **Thermal Imaging**, visible light, and low light night vision is available to support engineers for routine inspections at any time without any blind spots
- The minimum temperature difference of 0.04°C can be distinguished, and the measurement accuracy can reach ±2°C, with the frame rate up to 25Hz
- Professional SDK and technical support can be provided to help customers develop their own apps
- Professional APP for analysis on infrared temperature measurement is built in, analyzing while shooting to quickly get accurate data

- IP68/IP69K protection rank is reached, complying with MIL-STD-810H standard
- 1.5 m-drop protection, as well as water and dust resistance, makes it solid and durable
- 5500 mA ultra-large capacity battery supports long outdoor use

Application Value of Smart Industrial Thermal Imaging Device PX1

- Non-contact measurement can be realized, which allows for remote measuring without changing the structure of the measured target, thus ensuring inspectors' safety
- Professional measurement tools are provided to freely monitor the areas selected and automatically obtain the highest temperature point to implement intelligent photographing and fault diagnosis of devices
- Photographing and video recording are supported to transmit inspection data to the background, which is helpful for secondary analysis and remote diagnosis of on-site faults
- App development is supported to help customers enhance the level of intelligent inspection for efficiency improvement and cost savings
- Lightweight structure makes it easy to carry, and enables an all-in-one design, which lightens the burden of inspectors carrying many devices ■

InfiRay | Sense Difference



Iray Technology Co., Ltd.

www.infiray.com
 Contact: Mr. Charles Lee
 Position: Regional Sales Manager
 Email : xrl@iraytek.com
 Tel/Whatsapp : +86-15063823603

New Arrival

Innovative systems for better performance



Let's create the systems that take indoor climate comfort further

By delivering complete solutions rather than just components, we can offer indoor climate comfort that takes multiple aspects of performance optimisation into account. This includes supporting our customers with advice and guidance to make sure our solutions match their needs exactly. At the same time, our solution approach enables us to better deliver higher energy efficiency. For example, by combining low temperature heat emitters with underfloor heating, we can deliver an optimal balance between swift changes in room temperatures and energy efficiency. Our configuration software is very useful at product selection and system design stages. Product information can be easily forwarded to BIM design systems and from there, support the entire process from planning to installation.

Discover more at www.purmogroup.com

PURMO
GROUP

Exhibitions, Conferences and Seminars in 2022 & 2023

Conferences and fairs 2022

November-December

3 Nov 2022	Climatization Days	Lisbon, Portugal
14-15 Nov 2022	Brussels Summit 2022 (rehva.eu)	Brussels, Belgium
30 Nov - 2 Dec 2022	53rd International HVAC&R Congress and Exhibition (kgh-kongres.rs)	Belgrade, Serbia
8-10 Dec 2022	REFCOLD India 2022 (refcoldindia.com)	Mahatma Mandir, Gandhinagar, Ahmedaba, India

Conferences and fairs 2023

February

4-8 Feb 2023	2023 ASHRAE Winter Conference (ashrae.org)	Atlanta, Georgia, USA
28 Feb - 3 Mar 2023	World Sustainable Energy days (wsed.at)	Wels, Austria

March

6-8 Mar 2023	HVAC Cold Climate Conference 2023 (ashrae.org)	Anchorage, Alaska
13-17 Mar 2023	ISH 2023 (ish.messefrankfurt.com)	Frankfurt am Main, Germany
14-16 Mar 2023	ACREX 2023 (acrex.in)	Mumbai, India
20-23 May 2023	IAQVEC 2023 (iaqvec2023.org)	Tokyo, Japan

Due to the COVID-19 circumstances, the dates of events might change. Please follow the event's official website



ATIC vzw—asbl – Belgium
www.atic.be



BAOVK – Bulgaria
www.baovk.bg



STP – Czech Republic
www.stpcr.cz



DANVAK – Denmark
www.danvak.dk



EKVÜ – Estonia
www.ekvy.ee



FINVAC – Finland
www.finvac.org



AICVF – France
www.aicvf.org



VDI-e.V. – Germany
www.vdi.de



ÉTÉ – Hungary
www.eptud.org



MMK – Hungary
www.mmk.hu



AiCARR – Italy
www.aicarr.org



LATVIJAS SILTUMA, GĀZES UN ŪDENS
 TEHNOLOĢIJAS INŽENIERU SAVIENĪBA

AHGWTEL/LATVAC – Latvia
www.lsgutis.lv



LITES – Lithuania
www.listia.lt



AIIRM – Republic of Moldova
www.aiirm.md



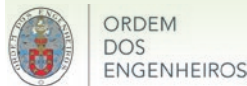
TVVL – The Netherlands
www.tvvl.nl



NEMITEK – Norway
www.nemitek.no



PZITS – Poland
www.pzits.pl



ORDEM DOS ENGENHEIROS – Portugal
www.ordemengenheiros.pt



AFCR – Romania
www.criofrig.ro



AGFR – Romania
www.agfro.ro



AIIR – Romania
www.aiiro.ro



KGH c/o SMEITS – Serbia
www.smeits.rs



SSTP – Slovakia
www.sstp.sk



SITHOK – Slovenia
<https://web.fs.uni-lj.si/sithok/>



ATECYR – Spain
www.atecyr.org



SWEDVAC – Sweden
www.energi-miljo.se



DIE PLANER – Switzerland
www.die-planer.ch



TTMD – Turkey
www.ttmd.org.tr



CIBSE – United Kingdom
www.cibse.org

SUPPORTERS

Leaders in Building Services



Daikin Europe – Belgium
www.daikin.eu



EPEE – Belgium
www.epeeglobal.org



EVIA – Belgium
www.evia.eu



Velux – Denmark
www.velux.com



Granlund – Finland
www.granlund.fi



Halton – Finland
www.halton.com



Uponor – Finland
www.uponor.com



Eurovent Certita Certification –
 France
www.eurovent-certification.com



LG Electronics – France
www.lgeaircon.com



Viega – Germany
www.viega.com



Aermec – Italy
www.aermec.com



Evapco Europe – Italy
www.evapco.eu



Rhoss – Italy
www.rhoss.com



Purmo Group – The Netherlands
www.purmogroup.com



Royal Haskoning DHV –
 The Netherlands
www.royalhaskoningdhv.com



SMAY – Poland
www.smay.eu



E.E.B.C. – Romania
www.eebc.ro



Dosetimpex – Romania
www.dosetimpex.ro



Testo – Romania
www.testo.com



Camfil – Sweden
www.camfil.com



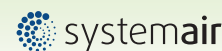
Fläkt Group – Sweden
www.flaktgroup.com



Lindab – Sweden
www.lindab.com



Swegon – Sweden
www.swegon.com



Systemair – Sweden
www.systemair.com



Belimo Automation – Switzerland
www.belimo.com



Arçelik – Turkey
www.arcelikglobal.com



Friterm Termik Cihazlar
 Sanayi ve Ticaret – Turkey
www.friterm.com



Zoonex – United Kingdom
www.zoonexsystems.com

REHVA Associate Organisations:



Enerbrain srl – Italia
www.enerbrain.com



Enviomech – United Kingdom
www.enviomech.co.uk



ISIB – Turkey
www.isib.org.tr



ECI – Belgium
copperalliance.org



OAER – Romania
www.oaer.ro

Network of 26 European HVAC Associations joining 120 000 professionals

REHVA Office: Rue Washington 40, 1050 Brussels - Belgium • Tel: + 32 2 514 11 71 - info@rehva.eu - www.rehva.eu

welcome to the

REHVA

3 BRUSSELS SUMMIT

14-15 November 2022

